ISTANBUL TECHNICAL UNIVERSITY ★ GRADUATE SCHOOL OF SCIENCE ENGINEERING AND TECHNOLOGY

INTEGRATED ONSHORE OFFSHORE TECTONIC AND MORPHOLOGICAL ANALYSIS OF THE ZAGROS SIMPLY FOLDED ZONE, SW IRAN

M.Sc. THESIS

Hasan Özge GEZGİN

Department of Geological Engineering

Geological Engineering Programme

APRIL 2019

ISTANBUL TECHNICAL UNIVERSITY ★ GRADUATE SCHOOL OF SCIENCE ENGINEERING AND TECHNOLOGY

INTEGRATED ONSHORE OFFSHORE TECTONIC AND MORPHOLOGICAL ANALYSIS OF THE ZAGROS SIMPLY FOLDED ZONE, SW IRAN

M.Sc. THESIS

Hasan Özge GEZGİN
(505111313)

Department of Geological Engineering

Geological Engineering Programme

Thesis Advisor: Prof. Dr. H. Serdar AKYÜZ

APRIL 2019

ISTANBUL TEKNİK ÜNİVERSİTESİ ★ FEN BİLİMLERİ ENSTİTÜSÜ

INTEGRATED ONSHORE OFFSHORE TECTONIC AND MORPHOLOGICAL ANALYSIS OF THE ZAGROS SIMPLY FOLDED ZONE, SW IRAN

YÜKSEK LİSANS TEZİ

Hasan Özge GEZGİN
(505111313)

Jeoloji Mühendisliği Anabilim Dalı

Jeoloji Mühendisliği Programı

Tez Danışmanı: Prof. Dr. H. Serdar AKYÜZ

APRIL 2019

Hasan Özge Gezgin, a M.Sc. student of İTU Graduate School of Science Engineering and Technology student ID 505111313, successfully defended the thesis/dissertation entitled "INTEGRATED ONSHORE OFFSHORE TECTONIC AND MORPHOLOGICAL ANALYSIS OF THE ZAGROS SIMPLY FOLDED ZONE, SW IRAN", which he prepared after fulfilling the requirements specified in the associated legislations, before the jury whose signatures are below.

Thesis Advisor:	**Prof. Dr. H. Serdar AKYÜZ** İstanbul Technical University	.....
Jury Members:	**Prof. Dr. Ziyadin ÇAKIR** Istanbul Techical University	.....
	Prof. Dr. Hayrettin KORAL Istanbul University	.....

Date of Submission : 12 March 2019
Date of Defense : 05 April 2019

To my family,

FOREWORD

Before I composed the thesis, I had started to have an interest in the remote sensing technology. I learned how to use the Google Earth and the ArcGIS programs. Furthermore, I have specialised in the Kingdom and the Move programs. Then, I came up with an idea studying in an active tectonic area with using these programs. After, I have focused on studying in the Zagros Simply Folded Belt (ZSFB), SW Iran. This master thesis covers tectonic and geomorphologic studies in the ZSFB.

First and foremost, I would like to thank my thesis advisor, Professor H. Serdar Akyüz, from the Department of Geological Engineering Program at Istanbul Technical University. Without his contribution and involvement in every stage throughout the process, this thesis would have never been composed and accomplished. Therefore, I owe him a great debt of gratitude.

Besides my advisor, I would like to thank to Professor Stefan Back from the Institute of Geology, Energy & Mineral Resources Group at RWTH Aachen University, and Professor Klaus Reicherter from the Institute of Geology, Neotectonics and Natural Hazards Group at RWTH Aachen University. Their additional help and lectures provided many insights and served as sources of inspiration and knowledge that I was able to include in the master thesis. My sincere thanks goes to Mrs. Kathrin Heinzmann who is coordinator of the department of Geoscience & Geography, Geology Institute, RWTH Aachen University. In general, I am grateful to my friends and fellow researchers from Energy & Mineral Resources Group, RWTH Aachen, especially for creating such a pleasant working environment.

Finally, I would also express my deep gratitude to my parents for providing me with infinite support and continuous encouragement throughout my years of education and through the duration of writing this thesis. This success would not have been possible without them.

April 2019

Hasan Özge GEZGİN
(Geological Engineer)

TABLE OF CONTENTS

Page

ABBREVIATIONS

2D : Two-dimensional
3D : Three-dimensional
a.s.l : Above Sea Level
b.s.l : Below Sea Level
BPM : Bitlis-Pötürge Massif
ca : Circa
DEM : Digital Elevation Model
E : East
EAAC : East Anatolian Accretionary Complex
et al : Et Alii (and others)
etc : Et Cetera
GCS : Geographic Coordinate System
GIS : Geographic Information System
GPS : Global Positioning System
H1 : Horizon 1
H2 : Horizon 2
H3 : Horizon 3
H4 : Horizon 4
H5 : Horizon 5
H6 : Horizon 6
H7 : Horizon 7
H8 : Horizon 8
H9 : Horizon 9
H10 : Horizon 10
H11 : Horizon 11
H12 : Horizon 12
H13 : Horizon 13
HZF : High Zagros Fault
i.e : Id Est (that is)
Ma : Mega-annum (million years)
MFF : Mountain Frontal Fault
MZRF : Main Zagros Reverse Fault
N : North
NE : North-East
NIOC : National Iranian Oil Company
NNW : North North-West
NW : North-West
PNG : Portable Network Graphics
RPA : Rhodope-Pontite Arc
S : South
SE : South-East
SSE : South South-East

SSZ : Sanandaj-Sirdjan Zone
STWT : Second Two-way Time
SW : South-West
TIF : Tagged Image File Format
TWT : Two-way Time
UDMA : Urumieh-Dokhtar Magmatic Arc
USGS : United States Geological Survey
UTM : Universal Transverse Mercator
W : West
WGS : World Geodetic System
XYZ : Three Dimensional Cartesian Coordinate System
ZFF : Zagros Foredeep Fault
ZFTB : Zagros Fold and Thrust Belt
ZSFB : The Zagros Simply Folded Belt

SYMBOLS

> **:** Modifier Letter Right Arrowhead
% **:** Percent Sign
***** **:** Asterisk (times)
~ **:** Tilde
® **:** Registered Sign
° **:** Degree Sign
A3 **:** Standard Paper Size Format (29.7 x 42.0cm)
km **:** Kilometre
km^2 **:** Square Kilometre
m **:** Metre
mm **:** Millimetre
ms **:** Millisecond
Pb **:** Lead
s **:** Second
U **:** Uranium

LIST OF TABLES

Page

LIST OF FIGURES

Page

INTEGRATED ONSHORE OFFSHORE TECTONIC AND MORPHOLOGICAL ANALYSIS OF THE ZAGROS SIMPLY FOLDED ZONE, SW IRAN

SUMMARY

This study includes tectonic and morphological studies of the Zagros fold and thrust belt, including the western shore of the Simply Folded Belt section and a part of the Persian Gulf. In addition, it is aimed to reveal the structural features of the region through modeling.

The technological developments in the last 20 years have allowed the use of the data obtained from 2D seismic reflection studies in 3D researches and these technological innovations have been used in the bay area of the study area. The raw seismic data acquired by seismic research vessels. Relevant seismic data were interpreted in the Kingdom program. Grids and thickness maps were included in the study. In the onshore part of the study area, the existing geological maps were used, and in the first place, the maps were combined in the ArcGIS program and a 1: 600.000 scale geological map was drawn. Then, four geological sections were drawn from this geological map and these profiles were rearranged by using previous studies. Seismic interpretations and geological sections covering the whole study area were digitized in the Move program and 3D modeling was performed.

The 2D seismic research line selected from the Persian Gulf was combined with the A-A' geological cross section taken from its continuation, and the shortening and thickening of the formations under the influence of the tectonism in the region were shown in two-dimensions. The effect of the reverse faults and right-lateral strike-slip faults in the region were analyzed in two-dimensions while using the Simple and Complex Approach methods.

Previous studies in the region indicate that the Zagros Fold and Thrust Belt is formed as a result of collision between the Arabian plates in the northeast and Eurasia plates in the southwest. However, the formation thickness maps found within the study area

showed the extension and thickness of depocenters. The depocenters have not developed in the same direction and showed variations over time in the Persian Gulf.

With the obtained surface and thickness maps, the depths and distributions of the formations in the onshore and offshore parts of the study area were determined by using the models. Modeling in the study will also shed light on the location of future potential oil / gas fields. In addition, under the influence of tectonism, the formation of the structures in the region to the present day, forward tectonic and geomorphological work in terms of perspective will provide a direction.

“ZAGROS SIMPLY FOLDED BELT”İN BATI KIYI KESİMİNİN SİSMİK YANSIMA VERİLERİ YARDIMIYLA MORFOTEKTONİK ANALİZİ, GB İRAN

ÖZET

Bu çalışma Zagros kıvrım ve bindirme kuşağının, “Simply Folded Belt” bölümünün batı kıyı kesimi ile Basra körfezinin bir bölümünü içine alan tektonik ve morfolojik araştırmaları içermektedir. Ek olarak, yapılan çalışma ile bölgenin yapısal özelliklerinin, modellemeler vasıtası ile ortaya çıkarılması amaçlanmıştır.

Son 20 yıl içindeki teknolojik gelişmeler, 2 boyutlu sismik yansıma çalışmalarından elde edilen verilerin, 3 boyutlu araştırmalarda da kullanımına izin vermiş ve bu teknolojik yenilikler çalışma alanının körfez bölümünde kullanılmıştır. Sismik araştırma gemileri ile elde edilen ham/işlenmemiş sismik data, yaklaşık 2600 km^2 lik bir alanı kapsamaktadır. Araştırma hatlarının iç ve çapraz hat uzunlukları takribi 2km*2km’dir. İlgili sismik veri, Kingdom programı vasıtası ile yorumlama çalışmalarında kullanılmıştır.

Çalışma alanının Basra Körfezi tarafında yapılan 2 boyutlu ve 3 boyutlu çalışmalar kapsamında, ilk olarak araştırma hatları içersinde yer alan sismik yansıma verileri sırası ile horizon-1, horizon-2, horizon-3, horizon-4, horizon-5, horizon-6 ve horizon-7 olmak üzere zonlara ayrılmıştır. Ek olarak ilgili derinliklerdeki zon haritaları oluşturulmuştur. Daha sonra oluşturulan ilgili zonlardan yararlanılarak, gridler (3 boyutlu tabakalar/yüzeyler) elde edilmiştir. Bu yüzeyler grid-1, grid-2, grid-3, grid-4, grid-5, grid-6 ve grid-7 olarak tanımlanmıştır. Aynı şekilde ilgili zonlardan faydalanılarak, horizonlar arası kalınlık haritaları olusturulmuştur. Bu kalınlık haritaları sırası ile; deniz tabanı/horizon-1, horizon-1/horizon-2, horizon-2/horizon-3, horizon-3/horizon-4, horizon-4/horizon-5, horizon-5/horizon-6 ve horizon-6/horizon-7 olarak isimlendirilmiştir.

Çalışma alanının kara bölümümde ise mevcut jeolojik haritalardan yararlanılmış, ilk etapta ilgili haritalar ArcMap programında birleştirilerek 1:600.000 ölçekli jeolojik harita çizilmiştir. Kingdom programındaki sismik yansıma verilerinden elde edilen

tüm horizon haritaları, gridler ve kalınlık haritaları ArcMap programına yüklenerek, çalışma alanının Basra Körfezimdeki kapsamı tespit edilmiş ve karada yer alan 1:600.000 ölçekli jeolojik harita ile birlikte düşünülerek, calışma alanının daha büyük ölçekteki ön morfotektonik yorumlama çalışmaları yapılmıştır. Daha sonra bu jeolojik haritada yer alan antiklinal ve senklinal yapılarının, eksenlerini yaklaşık olarak dik kesen, A-A', B-B', C-C' ve D-D' isimli jeolojik kesitler çizilmiş ve bu profiller önceki çalışmalardan da faydalanılarak yeniden düzenlenmiştir.

Tüm çalışma alanını kapsayan sismik yorumlamalar ve jeolojik kesitlerin birer örnekleri ilgili programlardan alınarak Move programında dijitalleştirilmiştir. Basra körfezi tarafından seçilen 2 boyutlu sismik araştırma hattı (Line X), karadaki devamından alınan A-A' jeolojik kesiti ile birleştirilmiş ve bölgedeki tektonizmanın etkisi altında bulunan formasyonlardaki kısalmalar ve kalınlaşmalar 2 boyutta gösterilmiştir. "Basit" ve "Kompleks Yaklaşım" metotları ile bölgedeki bulunan ters fayların ve sağ yönlü doğrultu atımlı fayların, bu kesitlerin kapsamı içerisinde bulunan formasyonlar üzerindeki etkisi, 2 boyutta analiz edilmiştir. Ayrıca, sismik yorumlamalar sonucu elde edilen gridler ve karadan alınan jeolojik kesitlerin tamamından yaralanılarak 3 boyutlu yüzey modellemeleri yapılmıştır. Bu yüzeyler; yüzey-1, yüzey-2, yüzey-3, yüzey-4, yüzey-5, yüzey-6 ve yüzey-7 olarak tanımlanmıştır. Bu yüzeyler bölgede yer alan jeolojik formasyon sınırlarını göstermektedir. Örneklemek gerekirse; yüzey-1: Bakhtyari Formasyonunun tabanı ile Agha Jari Formasyonunun Lahbari üyesinin yüzeyini; yüzey-2: Agha Jari Formasyonunun Lahbari üyesinin tabanı ile Agha Jari Formasyonunu yüzeyini; yüzey-3: Agha Jari Formasyonunun tabanı ile Mishan Formasyonunun yüzeyini; yüzey-4: Mishan Formasyonunun tabanı ile Gachsaran Formasyonunun Guri üyesinin yüzeyini; yüzey-5: Gachsaran Formasyonunun Guri üyesinin tabanı ile Gachsaran Formasyonunun yüzeyini; yüzey-6: Gachsaran Formasyonunun tabanı ile Asmari Jahrum Formasyonunun yüzeyini ve yüzey-7: Asmari Jahrum Formasyonunun tabanı ile Pabdeh Gurpi Formasyonunun yüzeyinin görüntüsüdür.

Bölgede yapılan önceki çalışmalar, Arap levhasının Avrasya levhası ile KD yönünde çarpışması sonucu Zagros kuşağının oluştuğunu belirtir. Çalışma alanının Basra Körfezi bölümünde yer alan formasyon kalınlık haritaları, sediman depolanma alanlarının yayılımlarını ve kalınlıklarını göstermektedir. Kalınlık haritaları ile ortaya çıkan 3 farklı yön, zaman içersinde Zagros Foredeep Fayı ile Borazjan Fayının

sediman depolanma alanlarının yönlendirilmesinde rol oynayabilecegi sonucunu ortaya çıkarmıstır.

Elde edilen yüzey ve kalınlık haritaları ile çalışma alanının kara ve deniz bölümlerinde yer alan formasyonların derinlikleri ve dağılımları, modellemeler kullanılarak ortaya konmuştur. Çalışmada yer alan modellemeler, potansiyel petrol/gaz sahalarının yer belirleme çalışmalarına ışık tutacaktır. Buna ek olarak, tektonizma etkisi altında, bölgede yer alan yapıların oluşumundan günümüze değişimleri, tektonik ve jeomorfolojik çalışmalar açısından yön verici bir bakış açısı sunacaktır.

1. INTRODUCTION

1.1 General

1.1.1 The Study Area and Topographic Features

The study presents a geomorphological and geological interpretation of onshore and offshore areas in the western part of the Zagros Simply Folded Belt (ZSFB), southwest Iran. The study area extends between ~28°N and 29°N: 50°E and ~52°E in Geographic Coordinate System (GCS) WGS 1984. The offshore-onshore study area covers roughly 12500 km^2.

The drainage system of the study area is chracterised by several rivers and streams. The major rivers, which are the Dalaki River in the NW and the Mand (Mond) River in the SSW, flow into the Persian Gulf.

Iran geographically comprises two branches of the Alpine-Himalayan Orogenic Belt that are the Zagros Orogen (Figure 1) with a NW-SE trend and the Alborz Mountains with an E-W trend. The Zagros Orogen stretches from Eastern Turkey (Bitlis Province) and through the NW Iran to Oman. (Alavi 1994; Agard et al. 2005). The highest point of the Zagros Mountains is the Mount Zardkuh, with an elevation of 4,548 metres. The study area consists of some mountains and hills. Well-known mountains for the local resident are the Mand Mountain (Kuh-e Mond) (585m) and Khurmuj Mountain (Kuh-i- Khurmuj) (1616m).

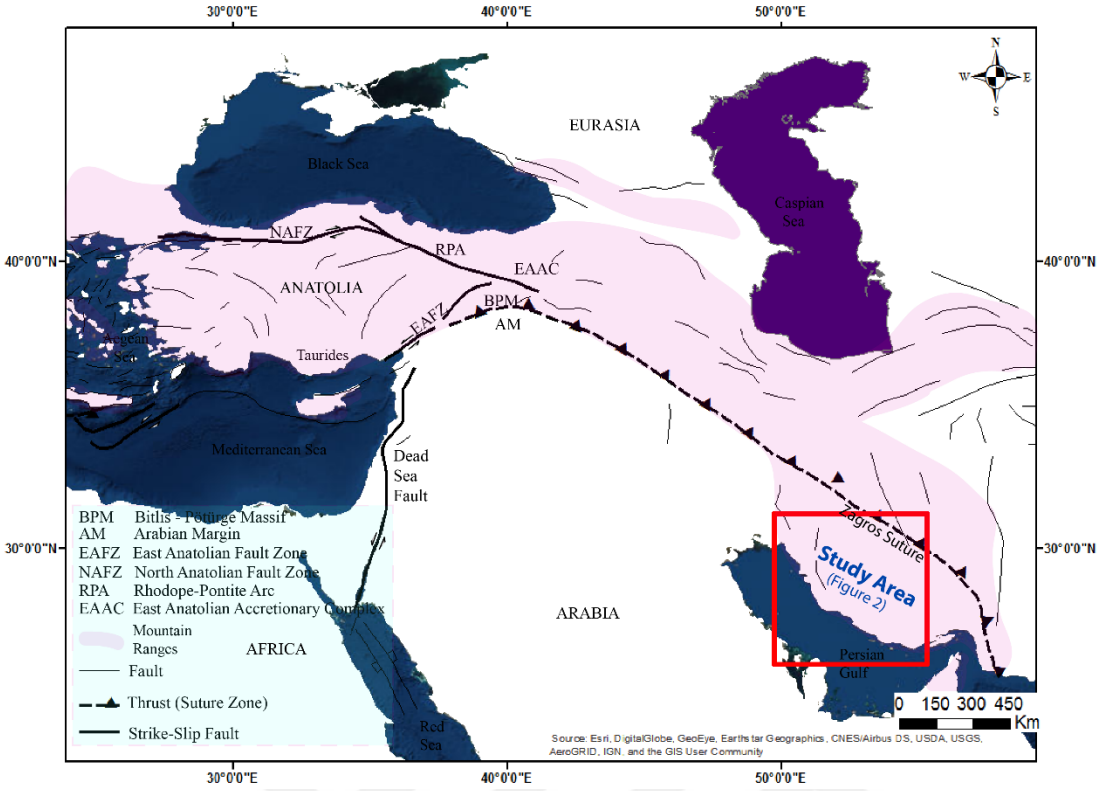

Figure 1 : Tectonic Map of the Tethys Foreland (Husing et al., 2009).

1.1.2 Residential, Life and Transportation

The study area is located in the Bushehr Province of Iran. The province has ten counties that are Asaluyeh, Bushehr, Dashtestan, Dashti, Deyr, Deylam, Jam, Kangan, Ganaveh and Tangestan. Main settlement areas around the study area are called; Bushehr (Bandar Bushehr), which is the capital of Bushehr Province, Borazjan, which is the capital city of Dashtestan County, and Ahram, which is the capital city of Tangestan. Less populated residential areas are Khormoj (Khurmuj) in Dashti County, Kaki in Dashti County and Shif in Bushehr County. The population of these counties differ between 34,828 (Deylam) and 298,594 (Bushehr) (2016 census). The province has altogether a population of 1,163,400 people (revised from http://www.hamshahrionline.ir/news/263382 and https://www.citypopulation.de/php/iran-admin.php).

Roads, ferries and flights can be used to reach the study area. The Bushehr Province has two international airports that are Bushehr Airport and Persian Gulf International Airport. Additionally, there is an airport in the Khark Island that is called Khark.

Moreover, a seaport, which is named port of Bushehr, may also be used for the transportation.

The Bushehr Province has a hot semi-arid climate. The weather is hot, sometimes extremely hot in the summer season and warm to cool winters, with a precipitation model corresponding a mediterranean climate (revised from https://en.wikipedia.org/wiki/Bushehr#cite_note-records-3).

1.2 The Aim of the Study

This study focuses on the geomorphological and tectonic evolution of the offshore and onshore parts of west ZSFB, SW Iran. As a result of active tectonics, a large amount of younger stratigraphic units exactly around the anticline structures may have been eroded. One of the reason for this inference is prominent discontinuities in the stratigraphic record, which documented on geological cross sections and three-dimensional (3D) models in the interpretation and results of the study.

The overall purpose of this study is to:

- ✓ Interpret depositional environments by applying seismic stratigraphic principles for horizon and surface interpretations, and the interpretation of thickness maps.
- ✓ Show the propagation of stratigraphic units in 3D.
- ✓ Find out and document the structural features of the region, setting of faults and anticline/syncline geometries in relation with stratigraphic units.
- ✓ Add a new geological perspective into the study area by applying a 3D subsurface prediction study.
- ✓ Calculate the shortening rate in the foreland of the Zagros Mountains.
- ✓ Assist in the research of potential hydrocarbon fields.
- ✓ Contribute the further academic studies around the study area.

1.3 Previous Studies Around the Study Area

Early significant studies related to the evolution of the Zagros Mountain Belt were made by Stocklin (1968), Ricou (1971), Hassanzadeh et al. (1974), and Berberian and King (1981). Premature orogenic movements resulted of a consolidation in the Precambrian basement. During the preorogenic time, in spite of the prevailing platform character, the influences of the entire stages of the Alpine orogeny can be seen in Iran (Stocklin, 1968). The Precambrian basement, which is broadly exposed in Iran, is mainly concealed underneath of the Zagros Mountains (Hassanzadeh et al., 1974). In the early Cretaceous, the base of the High-Zagros Alpine Ocean began to subduct underneath southern Central Iran and seemingly disappeared between the Late Mesozoic and the Early Cenozoic (ca. 65 Ma) (Berberian and King, 1981).

The NW part of the Zagros Mountains, which covers the eastern part of Turkey, the NNE part of Iraq and NW Iran was well-studied and the tectonic evolution of the region and the Mesozoic-Cenezoic plate tectonics were investigated with field studies by Sengör and Yilmaz (1980). The Bitlis-Zagros suture zone was researched by Husing et al. (2009). These authors mainly focused on the closure of the eastern Tethys gateway and the geodynamic evolution of the Arabian-Eurasian convergence zone.

The Zagros is mosly known for its active collisional belts named the Zagros Fold and Thrust Belt (ZFTB). Folding and thrusting is the result of the Arabian-Eurasian convergence. The ZFTB can be broadly subdivided into the Sanandaj-Sirdjan Zone (SSZ) in the North, and the Imbricate Zone and the Zagros Simply Folded Belt (ZSFB) in the South (Stocklin,1968; Paul et al., 2010). The study area is located in the ZSFB in SW Iran.

1:250000 scale geological maps, which are the Kharg-Ganaveh-Kazerun geological quadrangle map (1975), the Bushehr geological quadrangle map (1980) and the Khormoj (Khurmuj) geological quadrangle map (1980), were published by National Iranian Oil Company (NIOC). Recent studies have mapped active faults of Iran (Hessami et al., 2003), provided a morphotectonic map of Bushehr region and resulted in a geological map (on DEM) showing the major structural features of the ZFTB (S. Jahani et al., 2017).

2. GEOLOGICAL SETTING

The section provides an overview of the geological framework of the Zagros Simply Folded Belt (ZSFB) that is situated in the south-west Eurasian Plate between the Persian Gulf in the west and south-west, the Taurus Mountains in the north-west and the Zagros Orogeny in the east and north-east (Figure 1).

2.1 Tectonic Settings

Primordial fragments of the Arabian plate took shape in the Late Proterozoic while micro-continental parts and sequences of island arcs joined against the northeastern wing of Gondwana (Nehlig et al., 2002; Johnson and Stern, 2010). This collisional situation caused NE trending structural framework, while persisted throughout the Late Proterozoic and the Cambrian. At this time, the area was acting as a sub-basin that controlled accumulation of Hormoz evaporitic sequences in the north of the Arabian Plate (Talbot and Alavi, 1996). The basin displayed a residue of the old passive margin between the late Paleozoic and the beginning of Mesozoic while the surface of the Arabian Plate immersed in northeastern and eastern ways (Konyuhov and Maleki 2005).

In the Middle Triassic, while Gondwana subdivided into an eastern and a western part, the Neo-Tethys Ocean was opened. In the Jurassic and in the Cretaceous, widely spread sedimentary accumulations were deposited in the northern and eastern parts of the Arabian platform. The closure of the Tethys Ocean began in the Turonian in the Late Cretaceous (Ziegler, 2001).

After subduction of the Tethys Ocean, collision between the Eurasian and the Arabian platforms initiated in the Zagros Thrust Belt. First compressional tectonism probably occurred between the late Eocene and the early Oligocene (Jolivet and Faccenna, 2000; Agard et al., 2005; Mouthereau et al., 2012). There are also other suggestions regarding the timing of the Zagros initiation, which propose a variable

time range between the late Cretaceous and Pliocene (Stocklin, 1968; Stoneley, 1981; Berberian and King, 1981). This issue is still uncertain and controversial.

Due to the Eurasia-Arabia collision, the eastern Anatolia was subdivided into: the Bitlis-Pötürge Massif (BPM) (Figure 1), the East Anatolian Accretionary Complex (EAAC) and the eastern Rhodope-Pontite Arc (RPA) that were overlaid the north margin of the Arabian plate (Sengor and Yilmaz, 1981).

The Zagros Orogeny is one of the youngest continental collisional belts and is mainly caused by the convergence between the Eurasian and the Arabian plates. This continent-continent collision is defined as one of the last collision sequences which took part in the extensive Alpine-Himalayan orogenic system. Recent kinematic studies related to convergence rate of these plates measured 22 ± 2 mm/year (Vernant et al., 2004). The orogeny expands approximately 2000km from the Makran subduction zone in SW Iran to the East Anatolian Fault in the NW (Mouthereau et al., 2012). In addition to the Makran domain, previous kinematics indications illustrated tha the Makran oceanic subduction is still active (Ellouz-Zimmermann et al., 2007).

The Zagros Fold and Thrust Belt (ZFTB) is bordered in the north by the Main Zagros Reverse Fault (MZRF), which represents the suture zone of the Neo-Tethys Ocean (Ricou, 1971). From NW to SE, the Zagros Mountains are subdivided into different tectonostratigraphic domains that are from NW to SE: the western Zagros or the Lurestan Arc, the central Zagros or the Dezful Embayment, the Izeh zone and the eastern Zagros or the Fars arc (Motiei, 1994, 1995). The Fars arc extends for approximately 300km, surrounded by the Zagros Foredeep Fault (ZFF) to the westernmost, the Kazerun Strike Slip Fault to the west, the Mountain Frontal Fault (MFF) (Berberian, 1995) to the south and the Minab-Zendan Fault system to the SE (Regard et al. 2004, 2010). The main Zagros Trust Belt can be divided into: the Imbricated Zone and the Zagros Simply Folded Belt from the Interior Zagros; the Urumieh-Dokhtar Magmatic Arc (UDMA) and the Sanandaj-Sirdjan Zone (SSZ) (Figure 2) (Stocklin,1968; Paul et al., 2010). During Eocene, magmatic activity in the crush zone reasoned temporal shift of magmatism from the SSZ to the UDMA, and large-scale magmatism occurred much of Iran (Agard et al, 2011).

The study area contains one of the primary segments of the Zagros Belt in the Fars region, which is named the Zagros Simply Folded Belt (Alavi, 1974; Hessami et al., 2001). The ZSFB is flanked from the northwest to the southeast by the Persian Gulf, and is characterized by quite steady fold wavelength and a displacement over hundreds of kilometers (Sepehr and Cosgrove, 2004; Mouthereau, et al., 2006).

Total shortening in the ZSFB has been previously estimated at 70-100km, which covers the entire fold-belt since the initiated collision (Edgell, 1996; Bahroudi and Koyi, 2003).

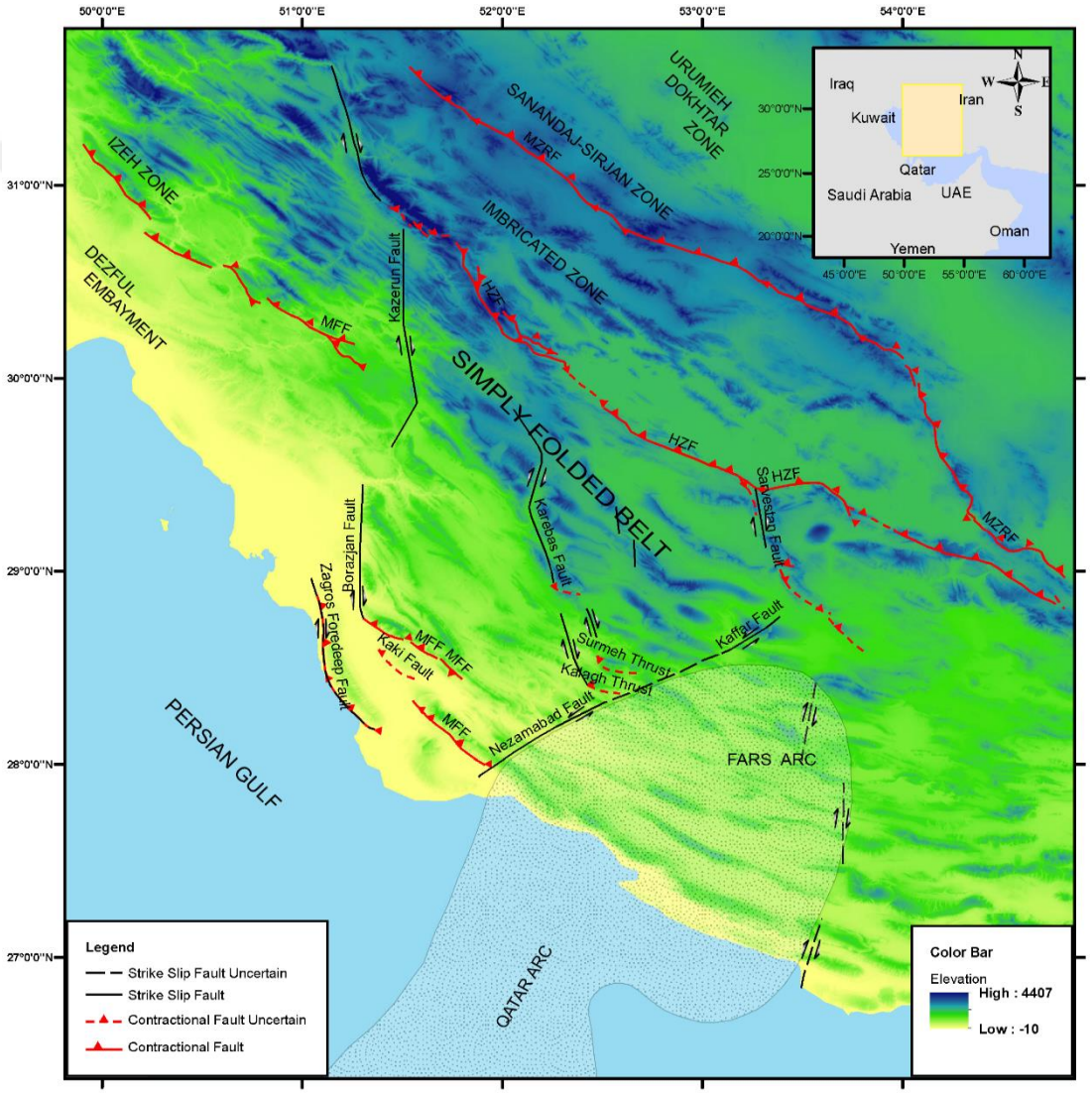

Figure 2: Main structural features of the Zagros fold-thrust belt on DEM representing tectonostratigraphic units from SW to NE: The Simply Folded Belt, the Imbricated Zone, the Sanandaj-Sirdjan Zone and the Urumieh-Dokhtar Magmatic Arc. Contractional Faults are the High Zagros Fault (HZF), the Main Zagros Reverse Fault (MZRF) and the Mountain Frontal Fault (MFF) (adapted from Ruh et al, 2014, Elliott et al., 2015 and Jahani et al., 2017).

2.2 Geology of the Zagros Simply Folded Belt

The sedimentary rocks of the ZSFB are placed on a Panafrican basement in the western part of the Arabian Plate (Husseini 1988; Konert et al., 2001). No evidence is found for basement outcrops in the Iranian Zagros, but the basement location is constrained by seismic studies and aeromagnetic surveys (Kent, 1970). All areas in Iran contain an approximately 3km thick cores of carbonate and salt deposits that formed between the infra-Cambrian to the mid-Triassic, overlying the late Precambrian (Hassanzadeh et al., 2008).

The Hormoz Formation is the basal decollement level in the High Zagros area and the Fars Region. It is not seen on the surface in The Izeh Zone and the Dezful Embayment. According to the various researchers, this basal decollement is cut by late basement faults (Sherkati et al., 2004; Molinaro et al., 2005; Sherkati et al., 2005).

At the beginning of the Mesozoic, a Triassic evaporate formation (Dashtak Fm), consisting of mainly anhydrite and marl that occur in the Fars region, served as intermediate decollement level in the coastal areas. A middle Cretaceous shale (Kazhdumi Fm) also described as another intermediate decollement level within the sedimentary pile in various regions of the ZSFB (Sherkati et al., 2006).

During the Paleogene, related to continental collision, sediments were accumulated in the flexural basin, consisting of Eocene dolomitic limestones (Jahrum Fm) and Oligo-Miocene shallow marine limestones (Asmari Formation). In the Miocene, in the central Fars, evaporites (Gachsaran Formation) and marls (Mishan Formation) overlapped on the Asmari Formation.

In the Bandar Abbas area of the south Fars Region, the Mishan Formation represents the upper decollement (Molinaro et al., 2005). Massive reefal limestones are existing at the base of the Mishan Formation (Guri Member) (Pirouz et al., 2011). At the boundary between the Miocene - Pliocene, sandstones and red marl (Agha Jari Formation) are deposited in the area. Over time, these fluvial river materials were eroded from part of the Zagros Mountains. Lastly, conglomerates and cross-bedded gravels (Bakhtyari Formation) settled between the Pliocene and the Quaternary (Motiei, 1993). The lowest part of the Bakhtyari conglomerates, in many domains, is represented by a major angular discordance (Hessami et al., 2001).

Table 1 summarize the entire lithological succession found in the ZSFB.

Table 1. Generalized Stratigraphical Column of the Study Area (compiled after Bordenave, 2004; Oveisi et al, 2007).

Era	Period	Formation	Lithology	Time (Ma)
CENOZOIC	Quaternary	Quaternary Deposit	Alluvium and Recent Deposits, Unconsolidated Soils, Clays, Sand and Gravels	2,5
	Upper Pliocene	Bakhtyari	Conglomerate, Sandy Marly Conglomerate	3,6
	Pliocene	Lahbari Member	Red Marl	5,3
		Agha Jari	Sandstone and Red Marl	
	Miocene	Mishan Fm	Gray Marl	
		Guri Member	Limestone	
		Gachsaran	Marl, Anhydrite and Salt	
		Razak	Sandstone, Marl and Sandy Limestone	
		Champeh Member	Thin Bedded Marly Limestone	
	Oligocene	Asmari	Limestone	23,0
	Eocene	Asmari - Jahrum	Limestone and Dolomitic Limestone	33,9
		Pabdeh	Calcareous Marl	66,0
		Pabdeh - Gurpi	Calcareous Shale and Gray Marl	
MESOZOIC	Cretaceous	Gurpi	Gray Pelagic Marls and Marlstones	
		Ilam - Sarvak, Kazhdumi	Bituminous Shale and Limestone	
		Dariyan - Gadvan - Fahliyan - Hith -Surmeh	Limestone, Shale, Dolomitic Limestone, Anhydrite	
		Dariyan - Gadvan - Fahliyan	Limestone, Shale, Dolomitic Limestone	
		Dariyan - Gadvan	Limestone, Shale	145,0
		Hith - Surmeh	Anhydrite, Dolomitic Limestone and Dolomite	
		Fahliyan - Surmeh	Limestone, Dolomitic Limestone	
	Jurassic	Hith	Anhydrite	
		Surmeh	Dolomitic Limestone and Dolomite	
		Neyriz	Thin Bedded Shaly Sandy Limestone	201,3
	Triassic	Dashtak	Anhydrite and Marl Thin Dolomites	252,0
	Permian	Dalan	Limestone, Dolomitic Limestone including Nar Member Anhydrite	
PALAEOZOIC	Ordovician	Faragun	Shales, Sandstone, Conglomerates and Olive Shales	
	Lower Palaeozoic	Lower Palaeozoic	Shales, Olive Bituminous Shales and Sandstones	500,0
	Early Palaeozoic	Hormoz Series	Salt Diapirs and Glaciers with Paleozoic Sediments and Igneous Rocks	

The 1:250,000 scale geological maps were published by the National Iranian Oil Company (1975, 1980). Involved other maps were created by Hessami et al. (2003). Figure 3 contains the 1:600000 scale geological map of south west of Iran and additional features of the area.

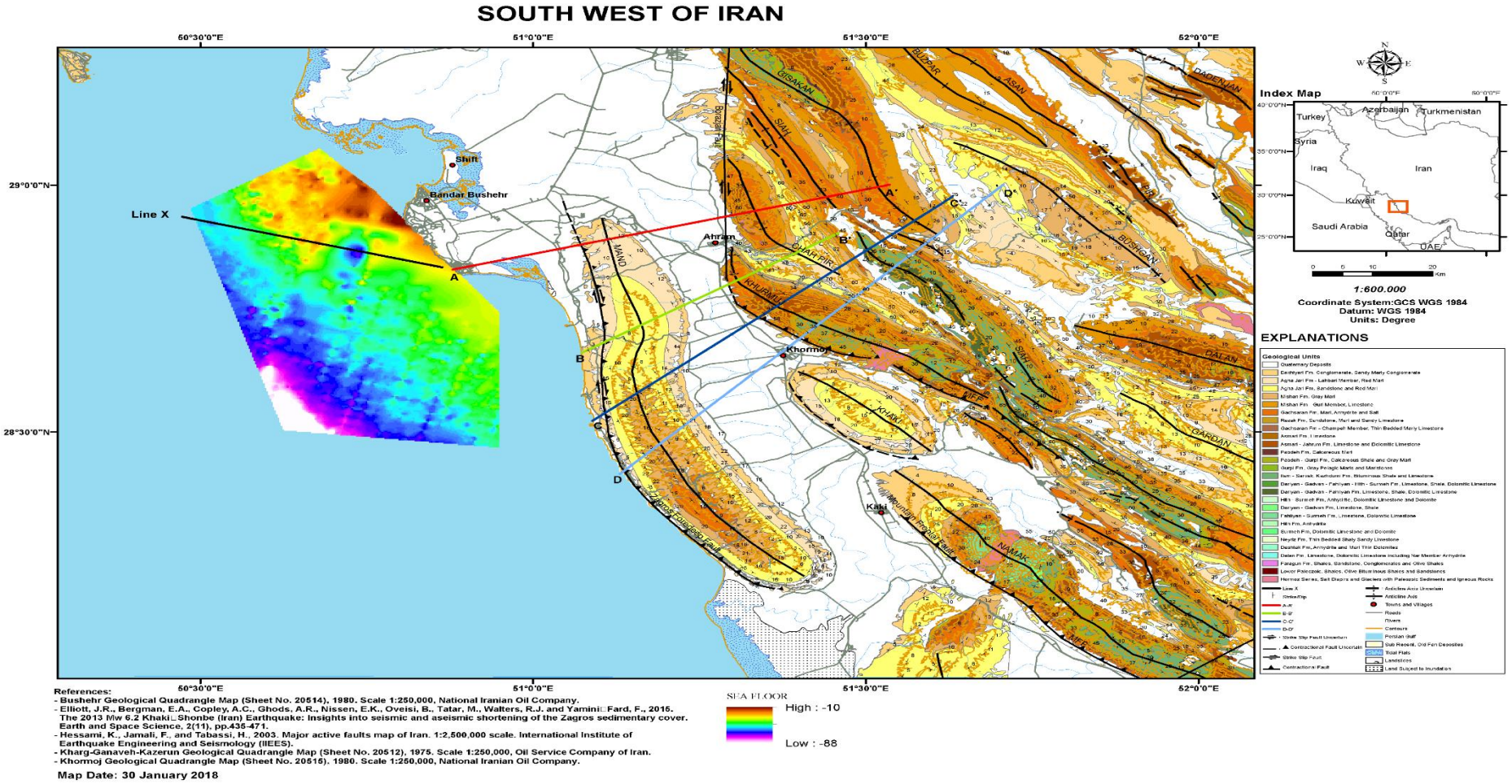

Figure 3 : Grid-Seafloor (Back et al. in preparation) and Geological Map of SW Iran (revised from NIOC, 1975, 1980; Hessami et al., 2003; Elliott et al., 2015).

3. DATASET & METHODOLOGY

3.1 Type and Source of Data

3.1.1 Onshore Data

The onshore study area is located in the costal part of the Simply Folded Belt, SW Iran. It is stretched between ~28°N and 29°N: 51°E and ~52°E in Geographic Coordinate System (GCS) WGS 1984, and includes several villages, towns and cities (Shif, Khormoj, Kaki, Ahram and Bandar Bushehr).

The Digital Elevation Model (DEM) dataset illustrates the elevation details of the area. The picked DEM datasets were downloaded from the United States Geological Survey (USGS) EarthExploration website. The DEM datasets are consist of 6 parts and covers the entire study area.

The ArcGIS 10.4.1 is short of a digital drawing program, supplies Geographic Information System (GIS) dataset, which is a primary application that is called ArcMap. ArcMap provides analysis, mapping, editing, data management options, et cetera (etc.).

While the geological map of study area (Figure 3) was prepared in ArcMap, previous studies and maps were used for drawings and symbols. Thematic maps included, are the Khormoj geological quadrangle map (National Iranian Oil Company, 1980), the Bushehr geological quadrangle map (National Iranian Oil Company, 1980) and Kharg-Ganaveh-Kazerun geological quadrangle map (Oil Company of Iran, 1975). The latest studies are the Major Active Faults Map of Iran (Hessami et al., 2003) and the Morphotectonic Map of Bushehr region.

The study area map in GCS was sized 1:600.000, illustrating the index map, geological units, main faults, strike and dips, cross section lines, rivers, roods and contours. Closely studied and focused geological structures are named Bushehr, Mand, Khurmuj, Chah Pir, Siah and Gisikan anticlines, which are in the costal part of the ZSFB (Figure 3).

Move 2016.1 program, the core application of the Move suite, was used for 3D structure modelling and analysis, cross section construction and 2D-3D kinematic/geomechanical model building. This surface was also applied for the integration of onshore and offshore data in the study area. Furthermore, the Move is also ensured fault restorations and unfolding options.

3.1.2 Offshore Data

The major source of the study is a set of 2D reflection seismic data (Back et al. in preparation). It was used for the geological structures offshore and displays fluctuation differences of land formations in the coastal area of Persian Gulf. The distances of shot lines in the survey are approximately 2 km (Figure 4). The area covered by this data is roughly 2600 km^2 and the entire area was taken into account to explicate 3D movement of the structure. The survey is in two way time (TWT), involves seismic reflectivity and anomalies in 3D view.

The seismic reflection survey is situated on the costal part of the Simply Folded Belt, west Iran. The data type of the survey is offshore and the survey type is three-dimensional (3D). The coordinate sytems were chosen the Universal Transverse Mercator (UTM) and the Geographic Coordinate System (GCS). The pure seismic data was taken in UTM format. The GCS was selected for the further drawings.

All seismic interpretations were gradually executed by the seismic explication program which is entitled IHS^{TM} Kingdom® V 8.8. Additionally, Ultraedit 32 program was run to edit Z axis values from positive to negative. Furthermore, GlobalMapper 6 program was utilized for the conversion of the coordinate system from the UTM to the GCS, and these converted data were used for the advanced program use.

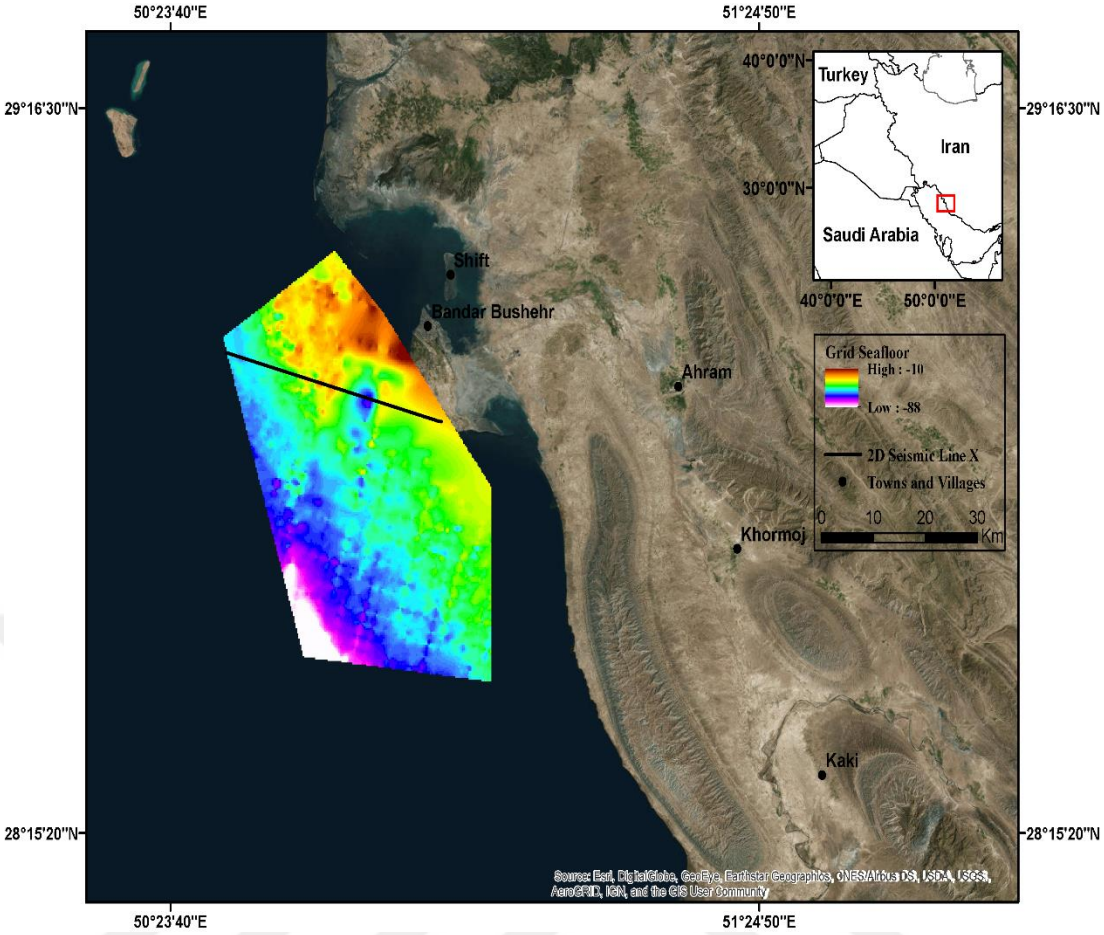

Figure 4 : Location of the Seismic Survey.

3.2 Interpretation Workflow

3.2.1 Land Data

- First, the 1:250,000-scaled geological maps (National Iranian Oil Company, 1975, 1980) and involved other maps (Hessami et al., 2003) were uploaded in the ArcGIS program. For this application, the add date function were picked from the standard menu in the Toolbars.

- Second of all, the GCS WGS 1984, was selected as a projection system. After that, study area maps were georeferenced incrementally according to coordinate systems of the existing maps.

- Furthermore, all geological units on the maps were detected and the polygon feature were used giving shape to them. Additionally, the same method were also picked for the Persian Gulf, sub recent-old fan deposits, tidal flats, landslides and land subject to inundation in order to give form to them.

- The line feature in new feature class was selected to generate cross section lines, contractional faults, strike slip faults, anticline axises, rivers, roads and contours.

- The point feature was picked to create strikes/dips and towns/villages.

- The 1:600000 scaled geological map of south west of Iran was drawn in ArcGIS (Figure 3), adjusted in the layout view for A3 format.

- A Digital Elevation Model (DEM) was used forming the contours. The Aster Global DEM's in Tagged Image File Format (TIF-Datei) was downloaded from USGS EarthExplore website and uploaded into related folders in ArcGIS. Furthermore, the DEM were also turned to account in order to entrench the elevation lines on the concerned cross section.

- 4 different domains on the study area in the land part, almost perpendicular to principle axis of anticlines, were determined related to connected offshore areas to make geological cross sections. Then, picked elevation profiles were denominated as A-A', B-B', C-C' and D-D'.

- The two-dimensional (2D) geological cross-sections were not enabled by ArcGIS program. Involved 2D geological profiles were drawn by hand, moreover, scanned copies were saved in Portable Network Graphics (PNG) format.

- 2D geological cross-sections were adjusted in accordance with some published compressive articles (Sherkati et al., 2006; Oveisi et al., 2007, 2008).

- Finally, all the data were exported corresponding to the further drawing program formats and recorded systematically in a file.

3.2.2 Offshore Data

- First of all, 3D seismic reflection data was loaded into the Kingdom Program.

- According to previous land seismic and well studies (Sherkati et al., 2006; Oveisi et al., 2007, 2008), eight different horizons were detected for the interpretation. These horizons were entitled seafloor, horizon 1 (H1), horizon 2 (H2), horizon 3 (H3), horizon 4 (H4), horizon 5 (H5), horizon 6 (H6) and horizon 7 (H7).

- The selected horizons were generated throughout northwest to southeast and southeast to northwest directions with respect to the 2D sections and covered whole the study area.

- Due to lack of the available data in some part of the 2D sections, the drawn horizon lines were not continued in every meters of the study area. The lines were created according to persistence/continuation of the recorded seismic data and the manual interpretation options were used for the interpretation.

- Grids were constructed in compliance with constituted horizons and were named grid - seafloor, grid 1, grid 2, grid 3, grid 4, grid 5, grid 6 and grid 8. While they were creating the flex gridding algorithm method were picked and 500m X cell * 500m Y cell distance were chosen in accordance with the data usage for further program drawings.

- Thickness maps (Isochron maps) were composed between the created horizons that displayed accommodation development along time and space in the recorded seismic data.

- The math on two maps calculator method were picked to form thickness maps that subtracted the second horizon elevation from the first horizon elevation wherever the calculation were required.

- Created isochron maps were denominated; thickness between Seafloor and H1, thickness between H1 and H2, thickness between H2 and H3, thickness between H3 and H4, thickness between H4 and H5, thickness between H5 and H6 and thickness between H6 and H7.

- Lastly, entire interpreted horizons, grids and thickness maps were saved and exported as dat format to utilize them in illustration programs that are called ArcGIS 10.4 and Move 2016.

3.2.3 Onshore - Offshore Intersection

- First, 2D geological cross sections in PNG format were uploaded according to its X, Y and Z coordinates in the Move 2016.1 program.

- Create lines section, under model building part, was used for entire line drawings. 2D elevation framework and formation boundaries were gradually drawn with attention to perspective, and drawn lines were constituted with respect to the offshore seismic interpretation horizon names and numbers.

- The 2D move-on-fault option in the 2D kinematic modelling under the Modules was selected to make fault restoration. The related faults in A-A' cross section was reconstructed and the fault parallel flow method was picked to detect better results.

- The 2D unfolding option from the 2D kinematic modelling section was applied to unfold focused anticlines and the simple share method was carried out gradually.

- The seismic Line X was exported from the Kingdom Program, uploaded into the Move, matched with cross section A-A'. In addition to this, remaining gaps between onshore and offshore parts were intersected with the following lines.

- The surfaces and volumes section in the model building part was picked and create surface tool was activated to compose surfaces. The ordinary kriging method was selected while surfaces were being created.

- Created surfaced were cut each other in some places. In order to solve the problem, reshape feature in modify data section was selected.

- Lastly, covered area DEM dataset was added on the 3D surfaces.

4. INTERPRETATION & RESULTS

4.1 Geological Cross Sections

The onshore fragment of the study area comprised four diverse cross sections that were drawn close, partly directly connecting to the seismic data in the offshore domain. These cross sections were assigned in alphabetic order A-A', B-B', C-C' and D-D'. The cross-section lines were selected perpendicular to the axes of anticlines around the study area. Line A-A' is the base cross section to match with the offshore study area. Line X from the seaside intersectes with cross section A-A'. In cross section D-D', directions and inclinations of contractional faults were selected in accordance with previous studies (Sherkatia & Letouzey, 2004, Sherkati et al., 2006; Oveisi et al., 2007, 2008). In the study, strikes, dips, faults and entire structural features on the geological maps considered to construct the cross sections if there was no available subsurface data or related studies.

The seafloor horizon is indicated offshore as top horizon. Geological units and all other horizons are correlated in Table 2. The first table column displays the horizons, and second column assigns formations for both onshore and offshore domains. Geological units and horizons were assigned based on the Sherkati et al. (2006) and Ovesi (2007).

Table 2. Selected Formation Boundaries and Geological Units.

Horizon Name		Formations
Horizon-1	-------	Bakhtyari
Horizon-2	-------	Lahbari Member
Horizon-3	-------	Agha Jari
Horizon-4	-------	Mishan
Horizon-5	-------	Guri Member
Horizon-6	-------	Gachsaran
Horizon-7	-------	Asmari-Jahrum
Horizon-8	-------	Pabdeh-Gurpi
Horizon-9	-------	Ilam-Sarvak-Kazhdumi
Horizon-10	-------	Dariyan-Gadvan-Fahliyan
Horizon-11	-------	Hith-Surmeh
Horizon-12	-------	Neyriz-Dashtak
Horizon-13	-------	Dalan-Faragun
		Lower Palaeozoic

4.1.1 A-A’ Profile

Onshore cross section A-A’ (Figure 5) starts at 50, 879° E - 28,829° W and its end is located at 51, 535° N - 29, 000° W. The length of the section is ca. 66743 m. The minimum altitude is 5,44m (a.s.l.), and the highest elevation is 1138, 84m (a.s.l.) in the cross section area.

There are 5 different anticlines along cross section A-A’, which are the Bushehr Anticline, the Mand Anticline, the Chah Pir Anticline, the Siah Anticline and the Gisakan Anticline (Figure 5).

The contractional faults in the cross section are the Zagros Foredeep Fault (ZFF) and the Mountain Frontal Fault (MFF). Additionally, the Borazjan right lateral strike slip fault was placed between the salt plug and the Mand Anticline (Sherkati et al., 2006).

The offshore horizon lines were picked and based on offshore seismic data. Horizons deeper than H7 cannot be correlated to the onshore section. Due to distorted seismic data after 2,7ms TWT, these horizons could not be matched with our seismic data. Outcrops of unmatched drawn horizons were identified on the geological map (Figure 3) and they were drawn in accordance with their placements in the map.

Cross section A-A’ properly demonstrates the wavelengths of the anticlines. It is clear that the contractional faults are one of the indicator shaping of anticline lengths. It is also obvious that the folding shortening is increased landwards.

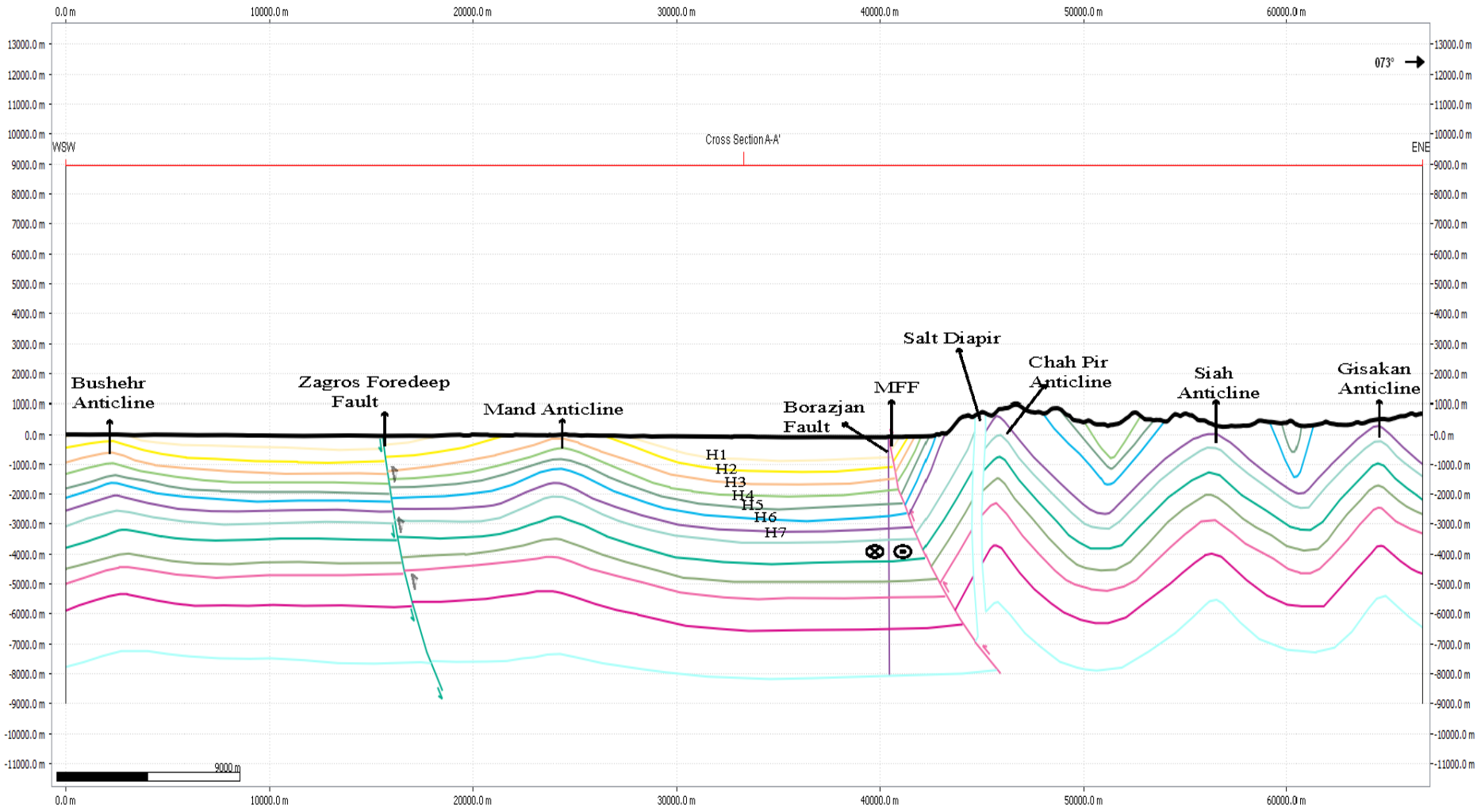

Figure 5 : Cross Section A-A’ line is shown in Figure 3.

4.1.2 B-B' Profile

Onshore cross section B-B' (Figure 7) is between 51,073° E - 28,660° W and 51,458° N - 28,904° W. The lowest height is 5,11m (a.s.l), and the highest altitude is 928,86m (a.s.l). The distance of the profile is ca. 46110m. The Mand Anticline part of the cross section was constructed model of the surveyed terrace sites (Ovesi et al, 2007) (Figure 6).

The cross section illustrates 3 anticlines that are the Chah Pir, the Khurmoj and the Mand Anticlines. The contractional faults are the ZFF and the MFF. Furthermore, the Brozjan Fault crosscutting from the west limb of Khurmuj Anticline, is shown.

Several horizons were picked in the cross section that are named H1, H2, H3, H4, H5, H6 and H7. Below the H7, there is one more drawn horizon which is H8, was adopted from the geological map, and it was created in accordance with outcrop information. Unfortunally, it does not match with the seismic survey lines due to the absence of any discontinuity in the offshore horizons, and was kept for further evaluations.

In the study area, major erosion was active from H1 to H6. It is clear that these horizons are non-continuous in some part of the cross section. Moreover, H1 and H2 were almost completely eroded along the section B-B'. It is apparent in the cross section that horizon thicknesses are directly proportional with depth.

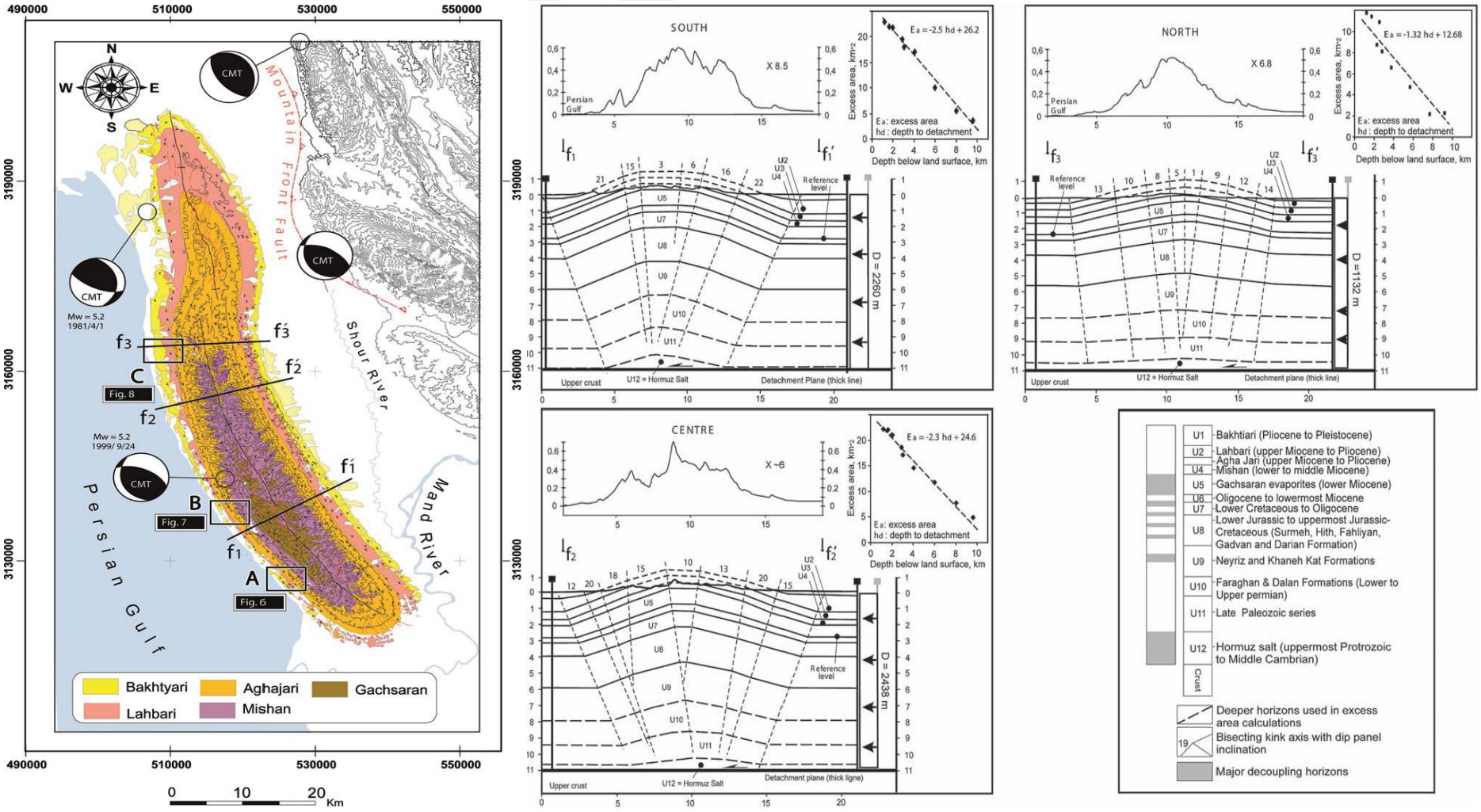

Figure 6 : Geological map and cross Sections on the Mand Anticline were taken from Ovesi et al, 2007.

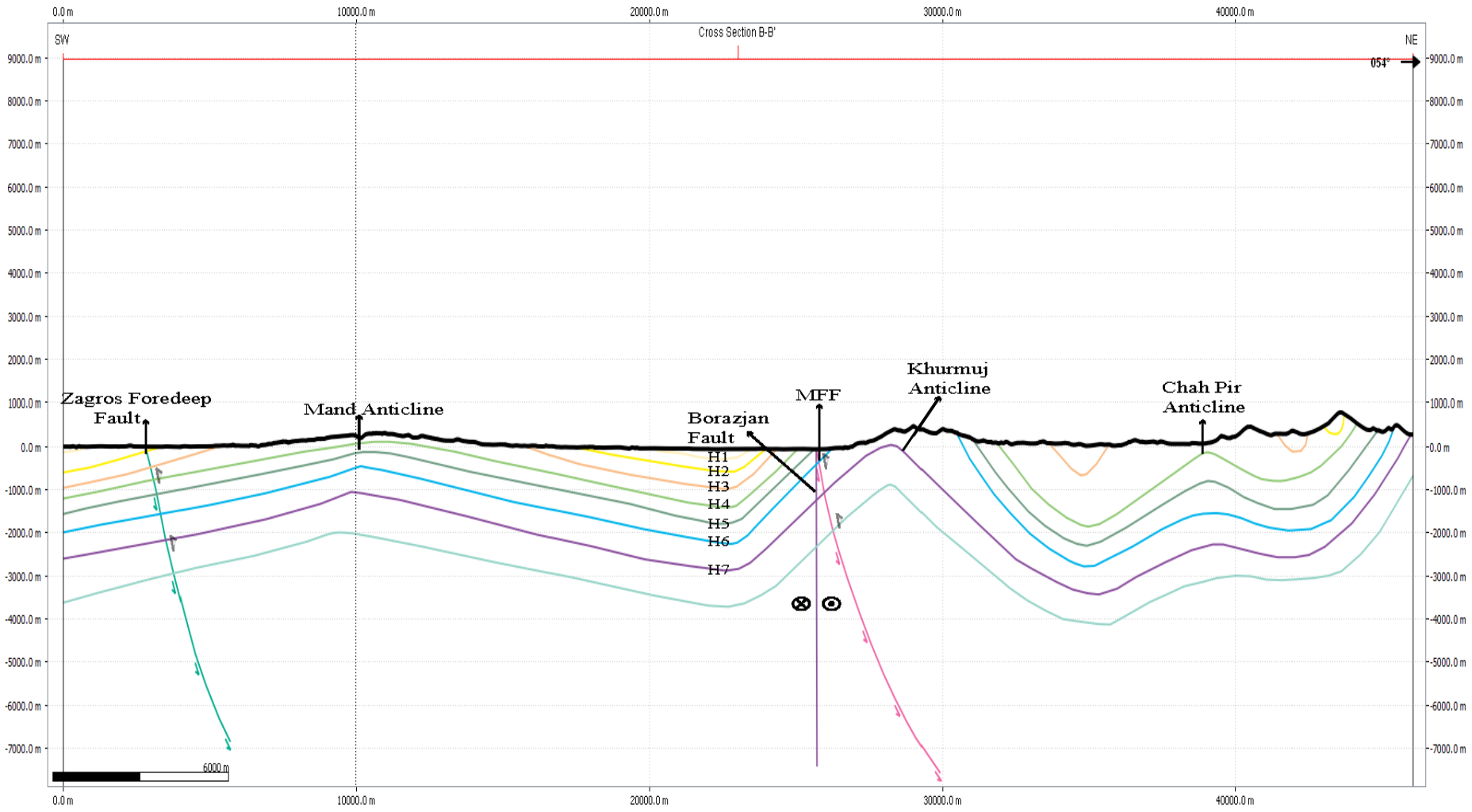

Figure 7 : Cross Section B-B’ line is shown in Figure 3.

4.1.3 C-C' Profile

Onshore cross section C-C' (Figure 8) is between 51,089° E - 28,522° W and 51,629° N - 28,975° W. The length of the profile is ca. 72870m. In the section, sea level is the lowest altitude and 1080, 98m is the highest elevation. The Mand Anticline part was constructed from Ovesi et al, (2007) (Figure 6).

Main horizons for the research are presented in the profile. H1 to H7 intersect with the other cross sections of study area.

Faults MFF and ZFF are displayed in the profile. The dip angles of contractinal faults were estimated from geological structure of the region.

The cross section illustrates that the Chah Pir anticline is plunged. The amplitude of the anticline is decreased in this part of the study area, in comparison for section A-A' (Figure 5) and B-B' (Figure 7). H6 does not continue along cross section C-C'.

Erosion was particularly active in the landward part of the cross section. The amount of erosion increases from the frontal part of the ZSFB in landward direction.

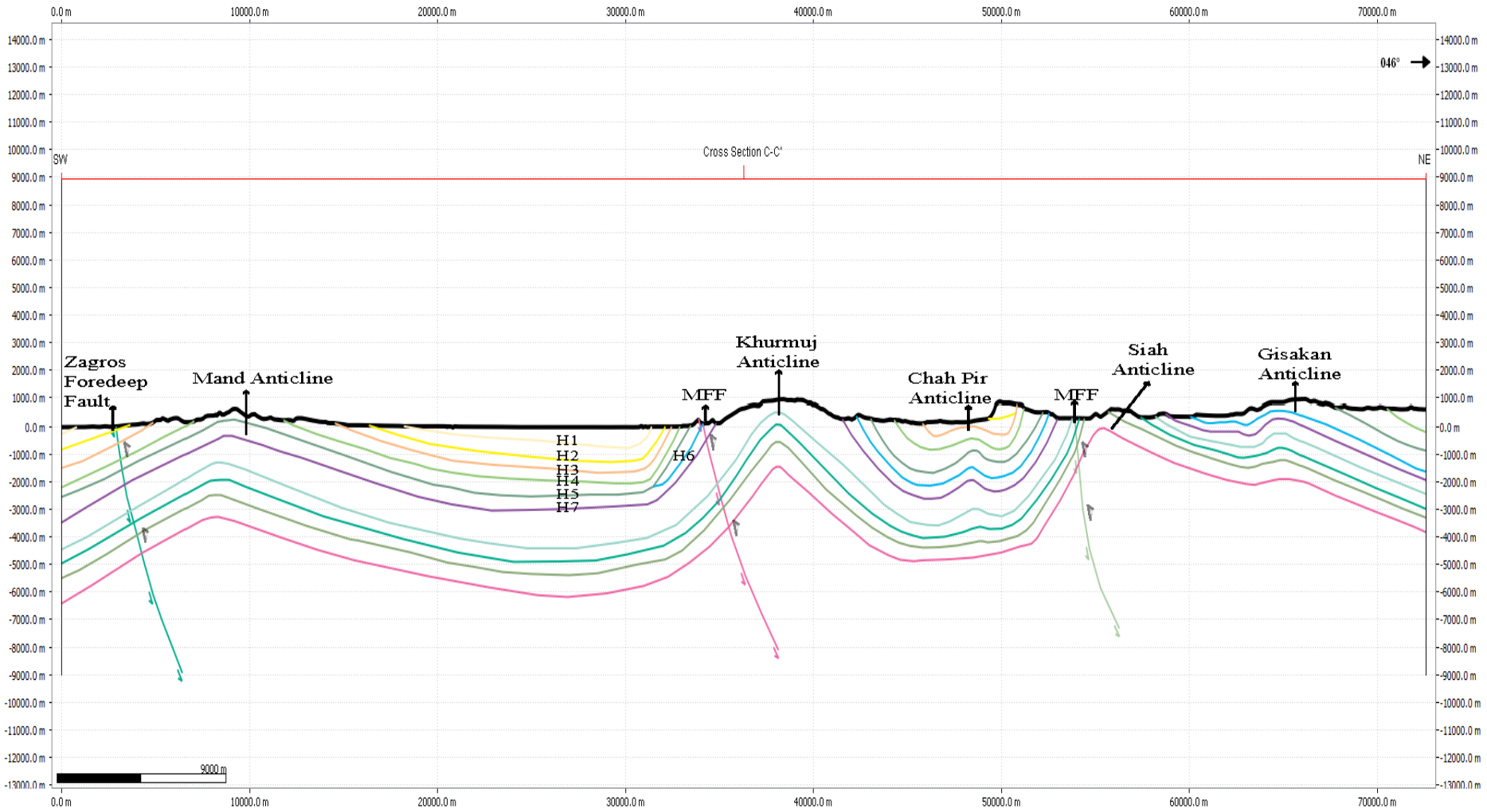

Figure 8 : Cross Section C-C’ line is shown in Figure 3.

4.1.4 D-D’ Profile

Onshore cross section D-D’ is between 51,130° E - 28, 414° W and 51,706° N - 29, 000° W. The minimum altitude is sea level and the highest elevation is 1778, 61m (a.s.l). The maximum topographic steepness is located at the Khurmuj anticline (Figure 10). The length of the profile is ca. 85930m.

The cross section built in comparison with previous studies (Figure 9) (Sherkati & Letouzey, 2004, Sherkati et al., 2006; Oveisi et al., 2007, 2008). According to these studies, the cross section takes into account seismic surveys and geological data.

The section trends from SW to NE. It shows the Mand, Khaki, Khurmuj, Siah and Gisakan Anticlines. The MFF and ZFF contractional faults are also present. Thirteen horizons were constructed, and seven of these were considered for further analysis.

The H5 is a discontinuity on the west part of the cross section. In addition, H1, H2 and H3 either show poor continuity or lack of continuity in the eastern part of the cross section.

It is obvious that the structure is more complex in the profile, if compared for A-A’, B-B’ and C-C’. Due to significant compression, contractional faults are present within almost every anticline. The coastal part of the ZSFB shows less-folded amplitudes than the inner part of the ZSFB.

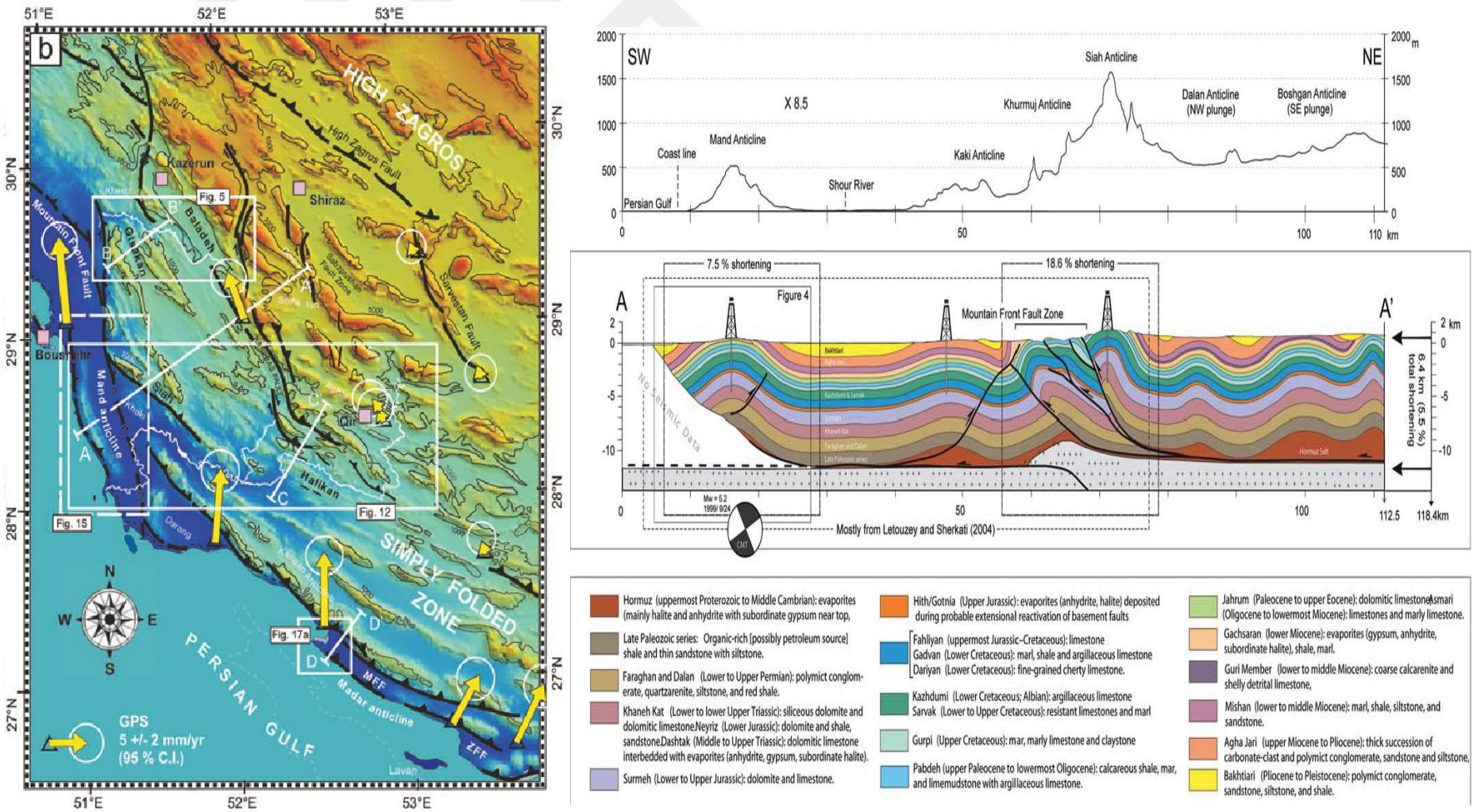

Figure 9 : Cross section and inset map is taken from Sherkati & Letouzey, (2004), Sherkati, (2006) and Ovesi et al, (2007, 2008).

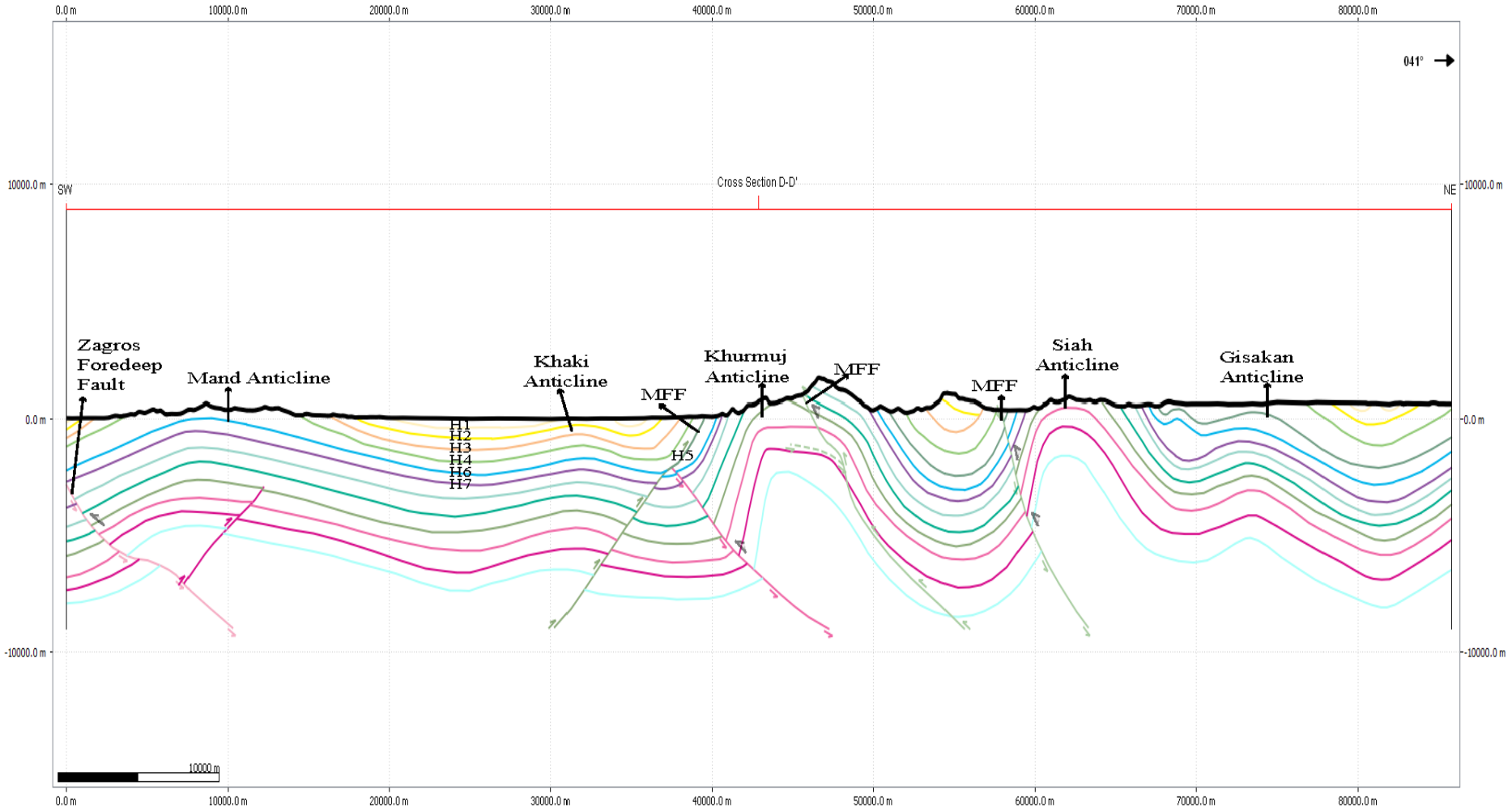

Figure 10 : Cross section D-D’ line is shown in Figure 3.

4.2 Horizons

2D seismic survey lines were progressively interpreted. First line on the top of the 2D seismic view was selected as a baseline (Sealevel). The seismic horizons were assigned and named from the seafloor (young) to depth (old). The data were interpreted into depth of 2.7s (TWT).

For horizon selection, all seismic line images were scanned in order to find a maximum of data continuity. Interrupted or discontinuous line fragments were not taken into account.

The first horizon was entitled sea level and the interpretation process was gradually continued to designate; seafloor, horizon 1 (H1), horizon 2 (H2), horizon 3 (H3), horizon 4 (H4), horizon 5 (H5), horizon 6 (H6) and horizon 7 (H7) (Table 3) (Figure 11). There is an interpreted line which is line X serves as intersection line with the onshore cross section A-A' and is fully presented in figure 11.

The seismic data was interpreted in time format. A default time-depth conversion assuming a constant subsurface velocity of 2000 m/s (i.e. 1s TWT = 1000 m) was used for all subsequent work with the seismic interpretations.

Table 3. Selected Interpreted Seismic Horizons in X.

Name	Time Scale (s)	Color
Sea Level (Baseline)	0	Blue
Seafloor	0,03 - 0,06	Red
Horizon-1	0,15 - 0,25	Violet
Horizon-2	0,90 - 1,14	Burly wood
Horizon-3	1,26 - 1,54	Light Goldenrod
Horizon-4	1,47 - 1,76	Dark Green
Horizon-5	2,11 - 2,44	Black
Horizon-6	2,56 - 2,87	Spring Green
Horizon-7	2,88 - 3,24	Yellow

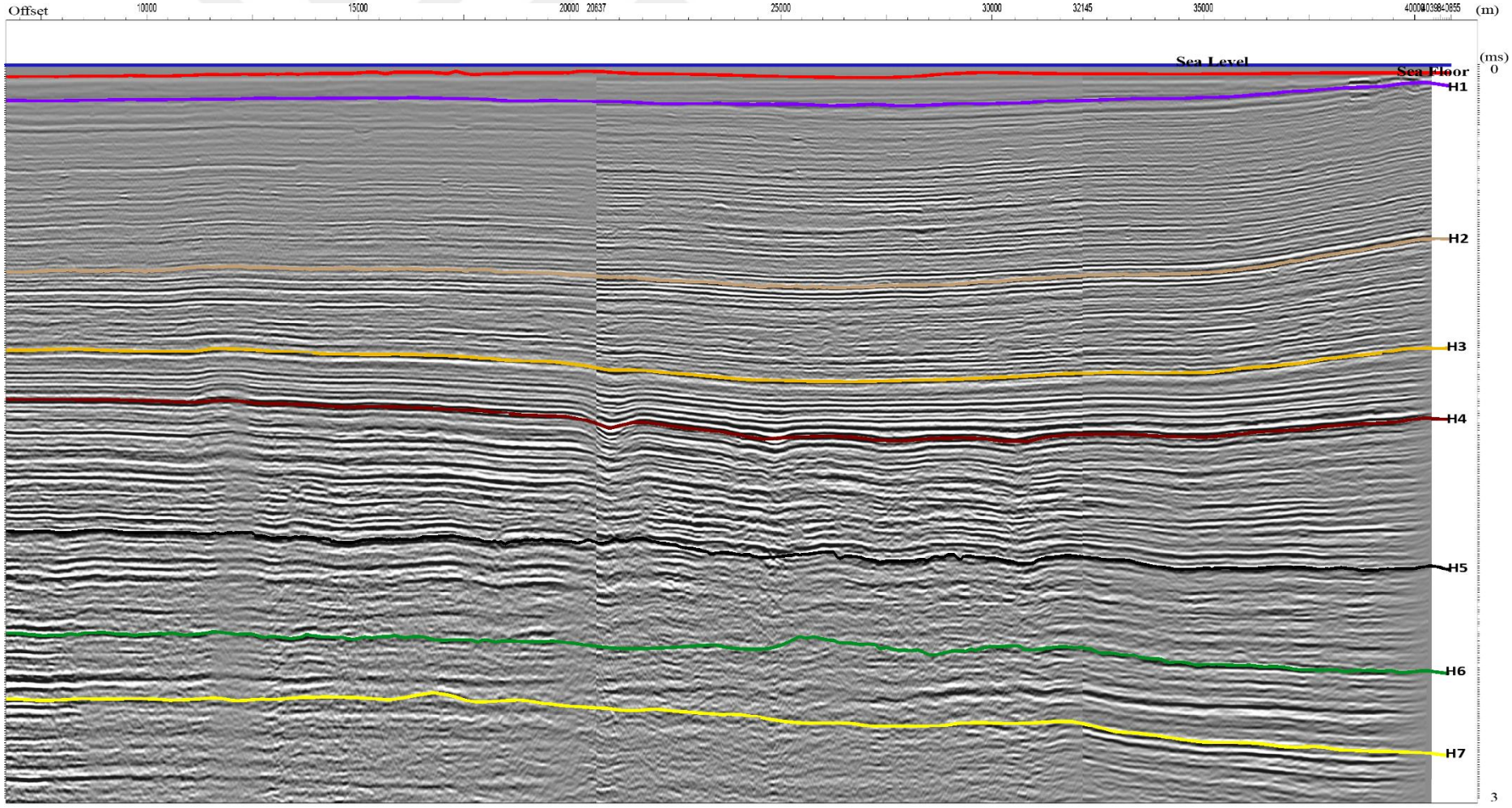

Figure 11 : Interpreted 2D survey line X from the offshore domain.

4.2.1 Horizon - Seafloor

The seafloor horizon was selected in accordance with the apparent seismic line in the upper part of the 2D survey.

The interpreted seafloor horizon lines show depth values in time (STWT) (Figure 12). The reflections show depth differences from the coast towards to Persian Gulf.

The color chart in the Figure 12 illustrates morphological variations. On the right side of the color bar, relevant two-way time numbers are displayed. Reddish colors indicate higher altitude areas, and blue colors show low relief areas.

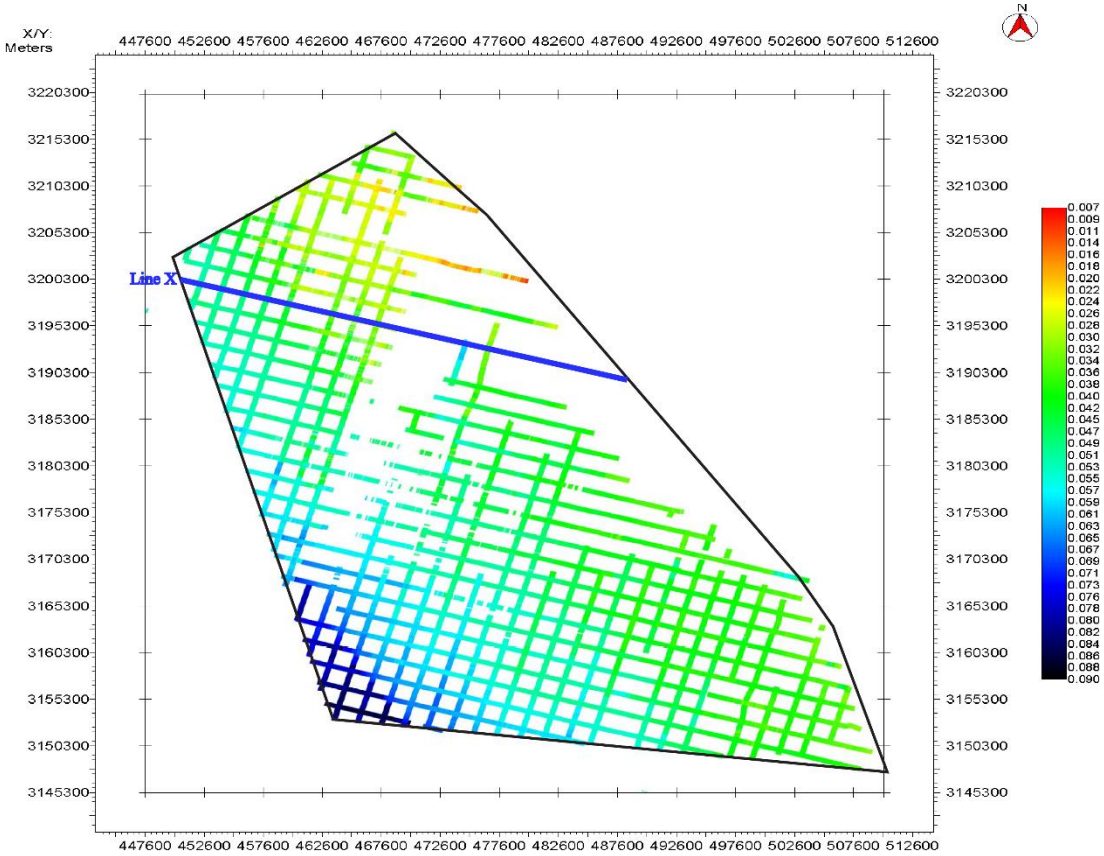

Figure 12 : Horizon - Seafloor Map.

4.3 Grids

All grids (interpreted horizon interpretations in a regular sampling interval) were created from picked horizons in the offshore part of the study area. Selected horizons were mostly mapped on 2km inline and cross line distances. Gridding filled the gaps that occurred between individual inline/crossline squares. All grids were calculated within the convex hull of the data.

Depths are displayed in positive values on all figures. The Kingdom program assigns positive values for depth. Yellow, yellowish, red or reddish colors at the top of the charts indicate higher elevation, and blue to dark colors represent deeper areas.

In total, seven grids, which were generated in the study area, are shown in the following part of the section.

4.3.1 Grid - Seafloor

Arrow one, which is an area of 0,010 to 0,024s TWT, illustrates a higher elevation in the grid-seafloor (Figure 13). The area is also an indicator of the Bushehr Anticline, which is located at the seaside of the ZSFB. From the center to the north, arrow two indicates low elevation. However, it is probably not true and the place may be indicated inaccurate date coverage. The area indicated by arrow 3, shows depths between 0,044s and 0,057s TWT, demonstrates depth changes from middle to deep. Arrow 4 in the southwest shows the regions deepest seafloor.

It is obvious that the depth, below the sea level, increases towards to the inner side of the Persian Gulf from northeast to southwest direction.

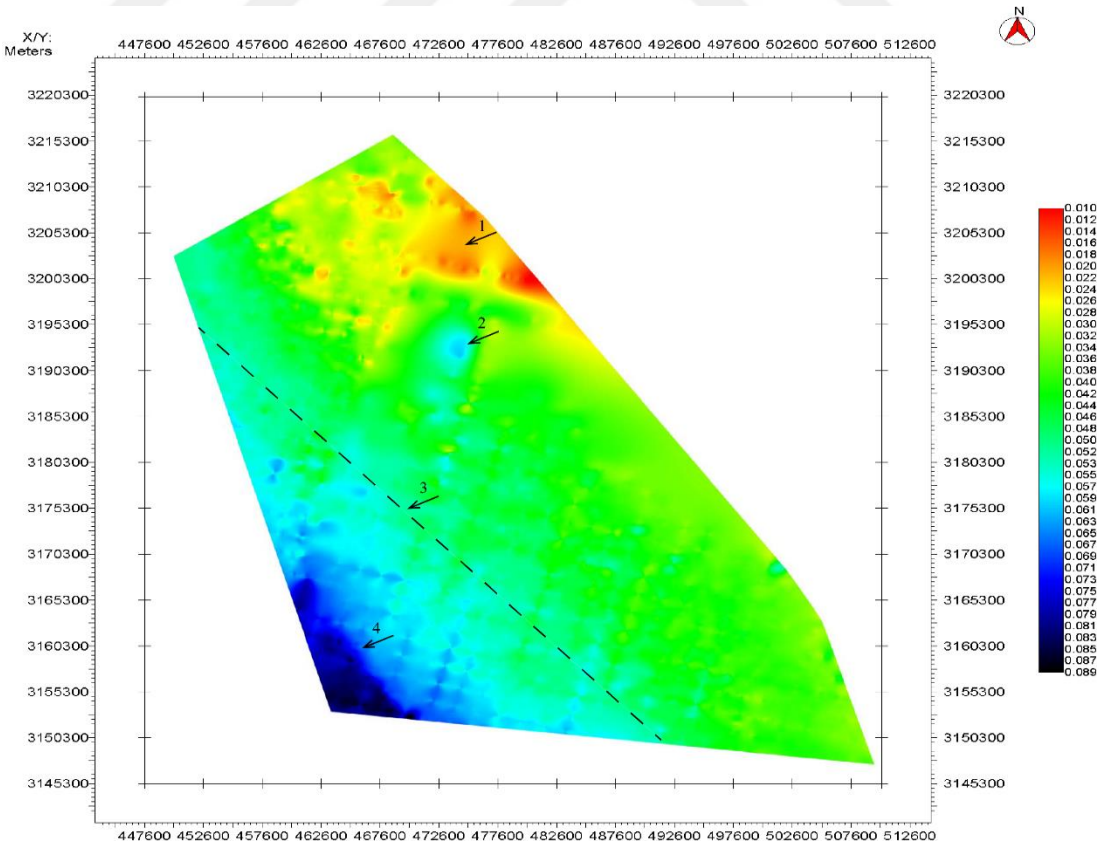

Figure 13 : Grid-Seafloor, constructed by interpretation of Horizon-Seafloor.

4.3.2 Grid-1

Fields marked with different colors in the grid-1 (Figure 14) indicate elevation differences. Arrow 1 shows higher elevations. Arrow 2 shows a deeper area. There are some fields in the grid-1 which display light blue colors (Arrow 3) that may show incorrect data interpretation.

Arrow 1, structured high, shows seaward continuation of the Bushehr anticline, which occurs close to the shore in the Persian Gulf. Arrow 2 is a syncline situated west of the Mand Anticline.

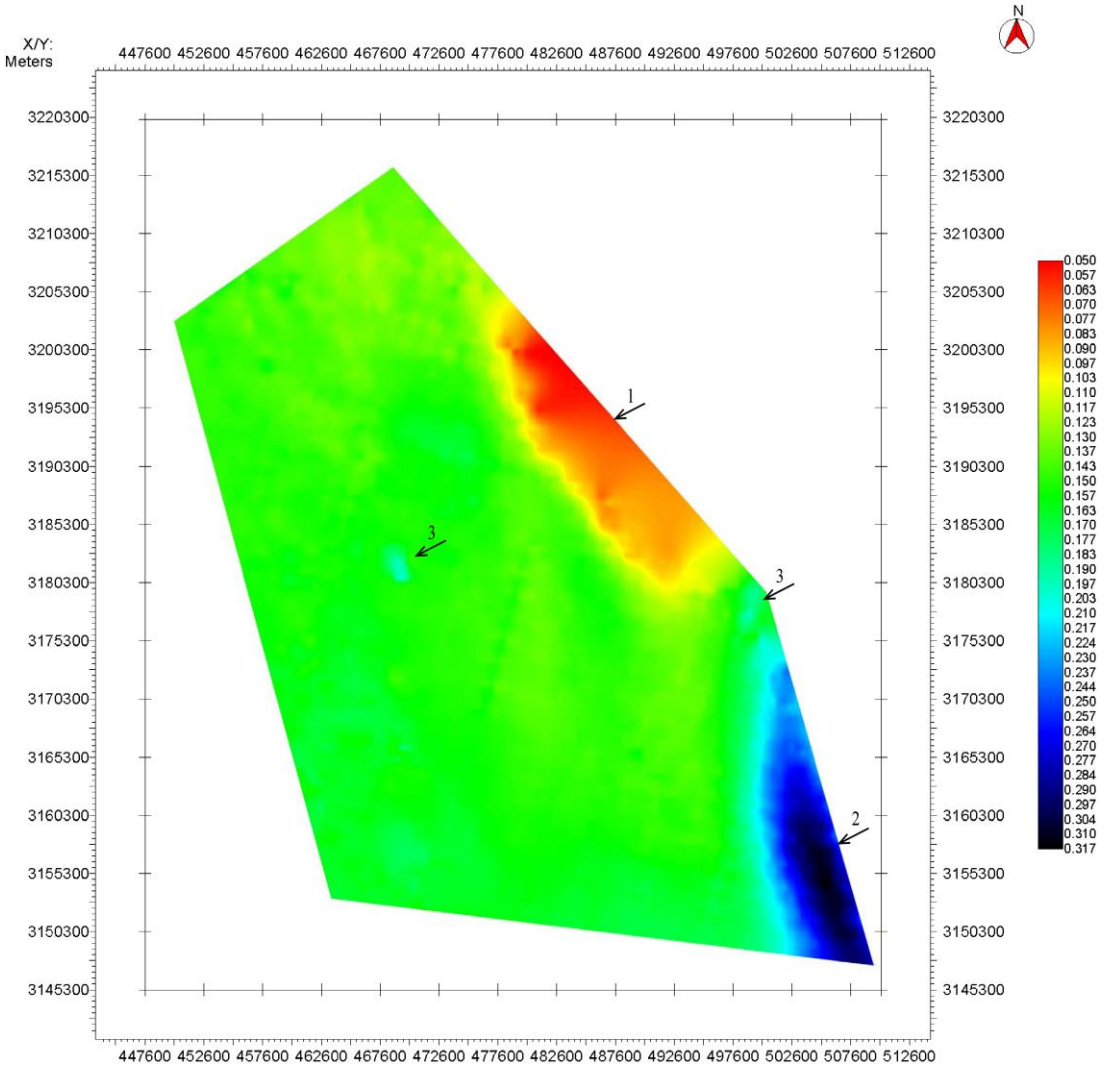

Figure 14 : Grid-1, constructed by interpretation of Horizon-1.

4.3.3 Grid-2

Arrow 1 displays a morphological high in the grid-2 (Figure 15). The high indicates the Bushehr Anticline, but its size has slightly decreased in comparison with grid-1.

The area marked by arrow 2 displays the syncline west of the Mand anticline. It is obvious that wavelength of the syncline is bigger in comparison with grid-1.

Arrow 3 and same colored areas illustrate intermediate depths. Reflection of colors indicate some synclines that could be took shape around the anticline.

Plain areas (green) covers ca 60% of the grid. Additionally, the grid-2 shows much more light blue and light green areas if compared to grid-1. Therefore, grid-2 shows a more diverse morphology than grid-1.

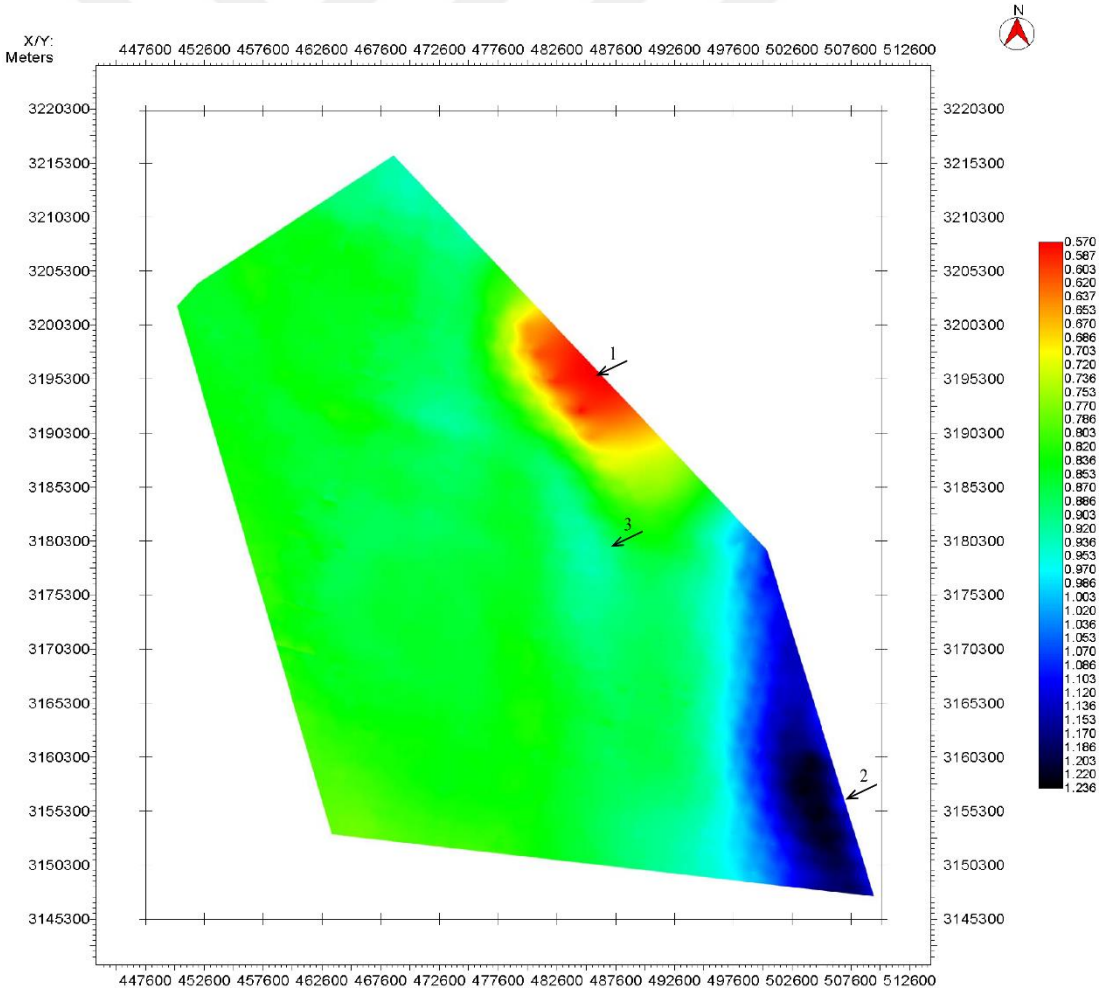

Figure 15 : Grid-2, constructed by interpretation of Horizon-2.

4.3.4 Grid-3

The high illustrated with arrow 1, is colored orange to red in the grid-3 (Figure 16). The high's dimensions are shallower than on the previous grids. This indicates that the Bushehr anticline is probably a symmetrical anticline (in comparison with grid-1 and grid-2).

The area signed with arrow four demonstrates new anticline in the northwest cost of the grid. The axial length of the anticline is ca. 52 km. The anticline may be continuing northwest and southeast directions outside the grid coverage area.

The syncline marked with arrow 3, formed in the north margin of the grid. Arrow 2 illustrates the position of the southern syncline.

Arrow 5 and places of same color show intermediate depth. Light blue regions surround the Bushehr anticline.

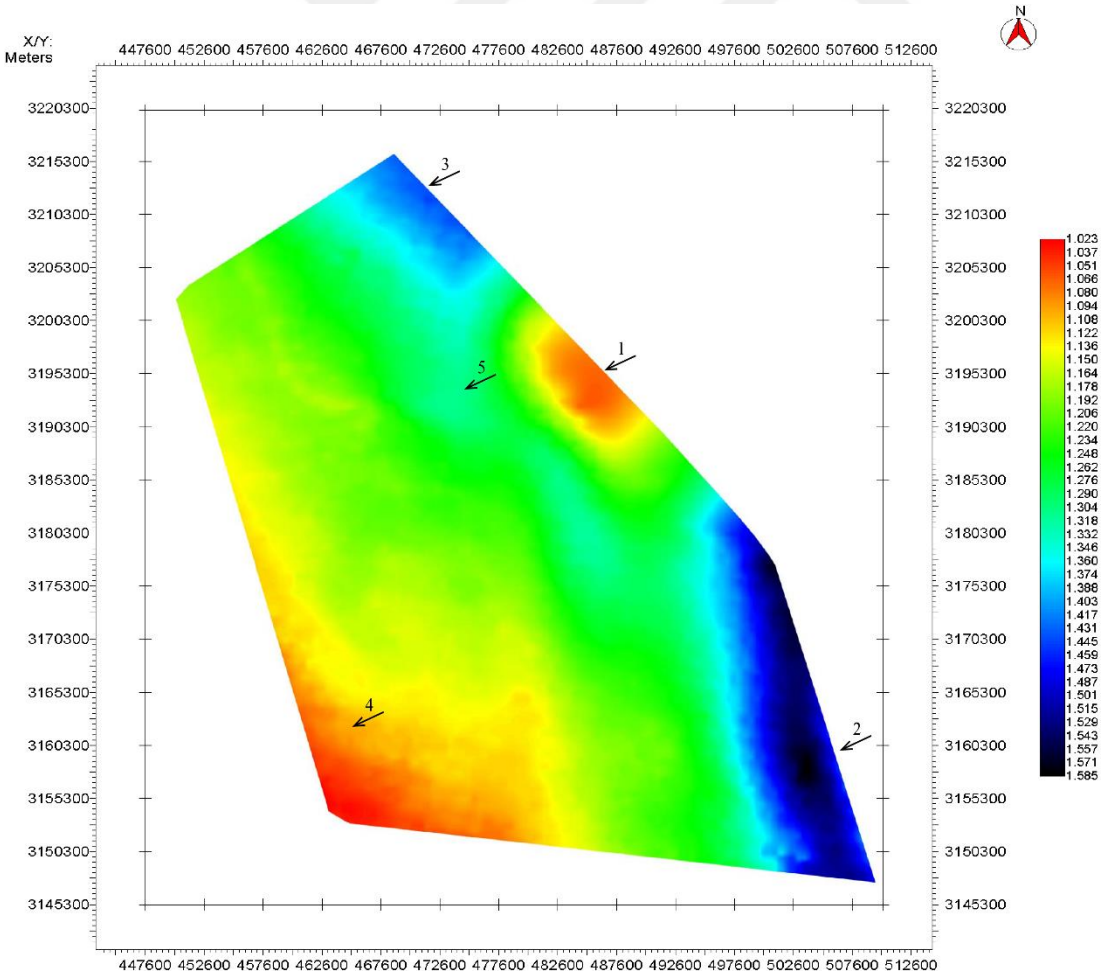

Figure 16 : Grid-3, constructed by interpretation of Horizon-3.

4.3.5 Grid-4

The Bushehr anticline area, signed with arrow 1, shows a slightly curved surface in this depth in grid-4 (Figure 17). Red to reddish area at the southwest part of the grid demonstrate another anticline (arrow 5).

Blue and light blue covered areas, indicated with arrows 2 and 3, show synclines. In the northwest of the grid, the syncline coverage is slightly larger than grid-3. According to grid-3 and grid-4, it seems that the syncline is symmetrical. Apart from that, the hinge point of the second numbered anticline in grid-4 moves northwest direction in comparison with grid-3.

Light blue colors, marked by arrow 4, are determine of the inflection points of the synclines and the Bushehr anticline.

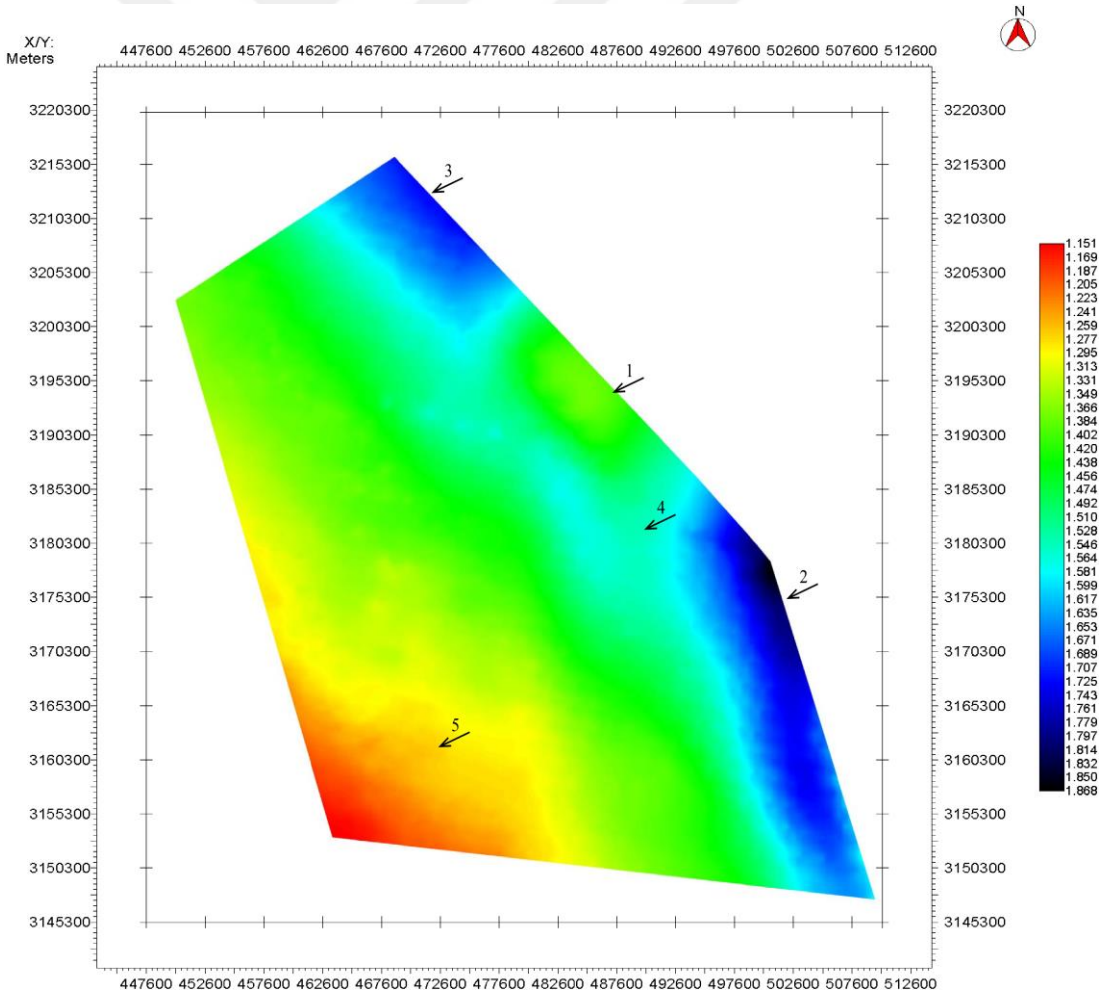

Figure 17 : Grid-4, constructed by interpretation of Horizon-4.

4.3.6 Grid-5

Blue and light blue areas (arrow 1) are still located at east and southeast part of the offshore region. The grid-5 (Figure 18) show the syncline that appears and plunges to northwest direction in comparison with previous grids. The lowest depth is indicated by areas with dark colors in grid-2 and grid-3, which are in the southeast part of the grid. The structure is shifted toward to northwest.

Another syncline in northern part of the grid (arrow 2) however, does not show the syncline due to lack of seismic data coverage. The data is also distorted in this depth of the grid. Nevertheless, it still illustrates a slightly curved area which supposed to be part of the syncline.

Third marked and red to reddish colored areas of the grid illustrates an anticline. The northeastern limb of the anticline is covered over large areas in the dataset.

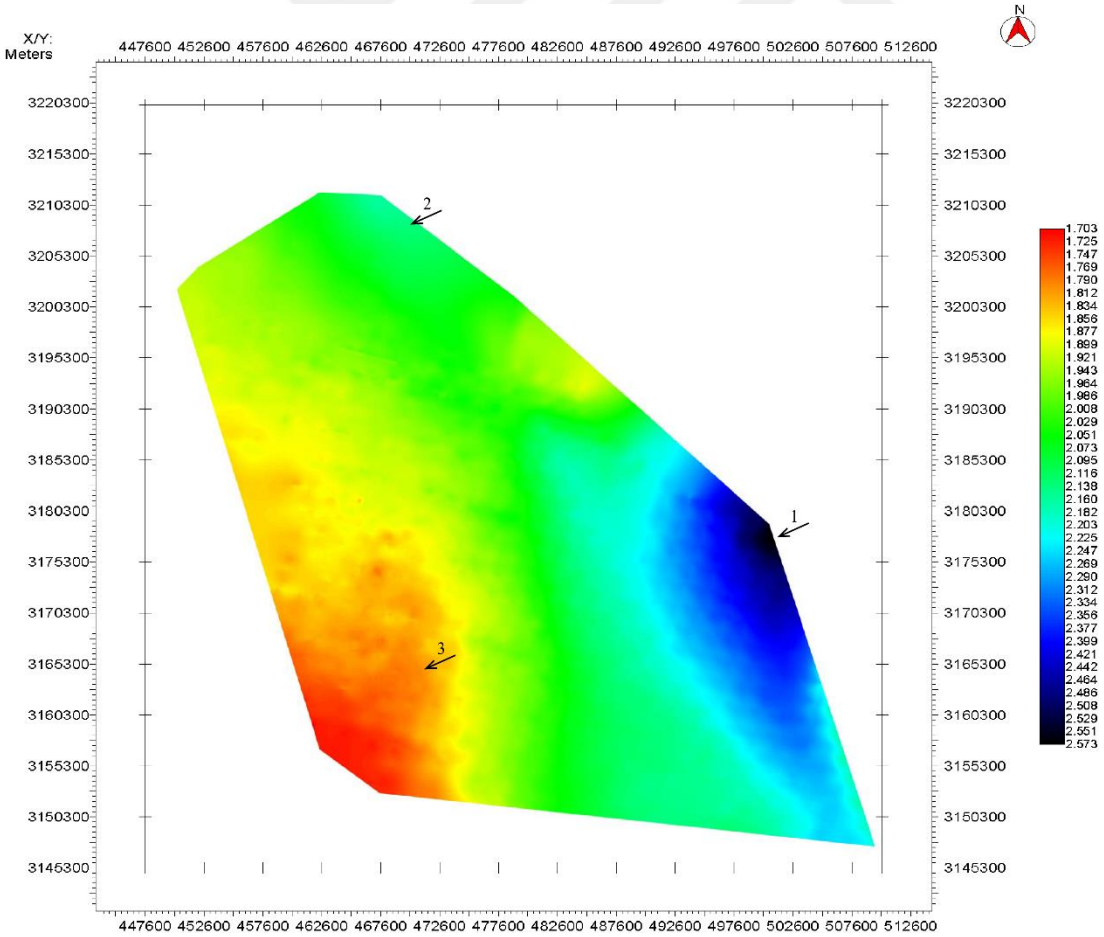

Figure 18 : Grid-5, constructed by interpretation of Horizon-5.

4.3.7 Grid-6

Syncline structures are shown within light blue, blue and dark domains. It is clear that deepest point of syncline 1 in grid-6 (Figure 19) relocates towards depth direction of the offshore part of the study area. Additionally, a frontal fault might have shaped the syncline structure, which was situated at the west part of the Mand anticline in the onshore areas. At the northwestern side of the grid, another syncline (arrow 3) is observable and its extent is significantly reduced in accordance with grid-4.

The Bushehr anticline is still visible between the synclines (arrows 1 and 3). Arrow 2 indicates an anticline that shows less areal coverage in comparison with grid-5. The anticline extension is slightly declined.

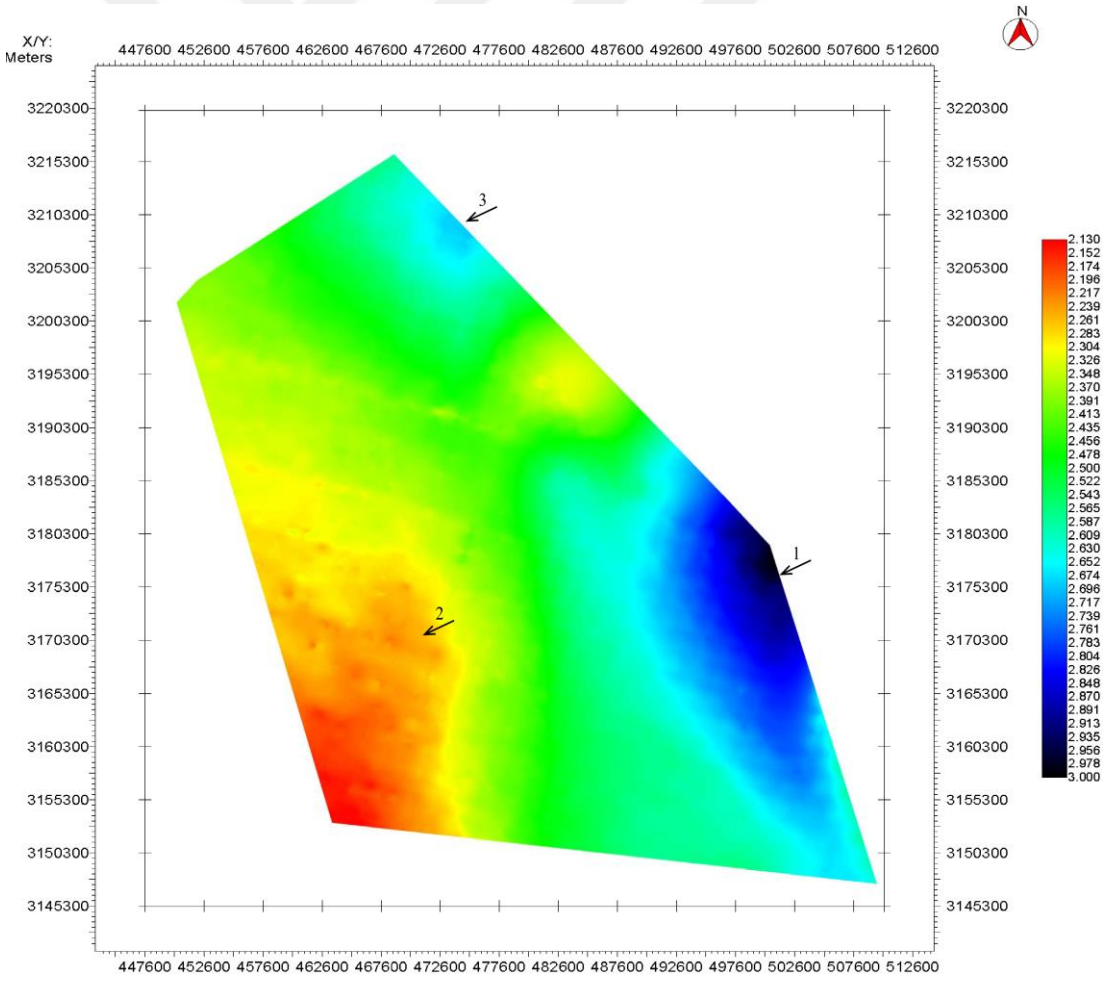

Figure 19 : Grid-6, constructed by interpretation of Horizon-6.

4.3.8 Grid-7

Grid-7 (Figure 20) shows almost same morphological features with grid-6.

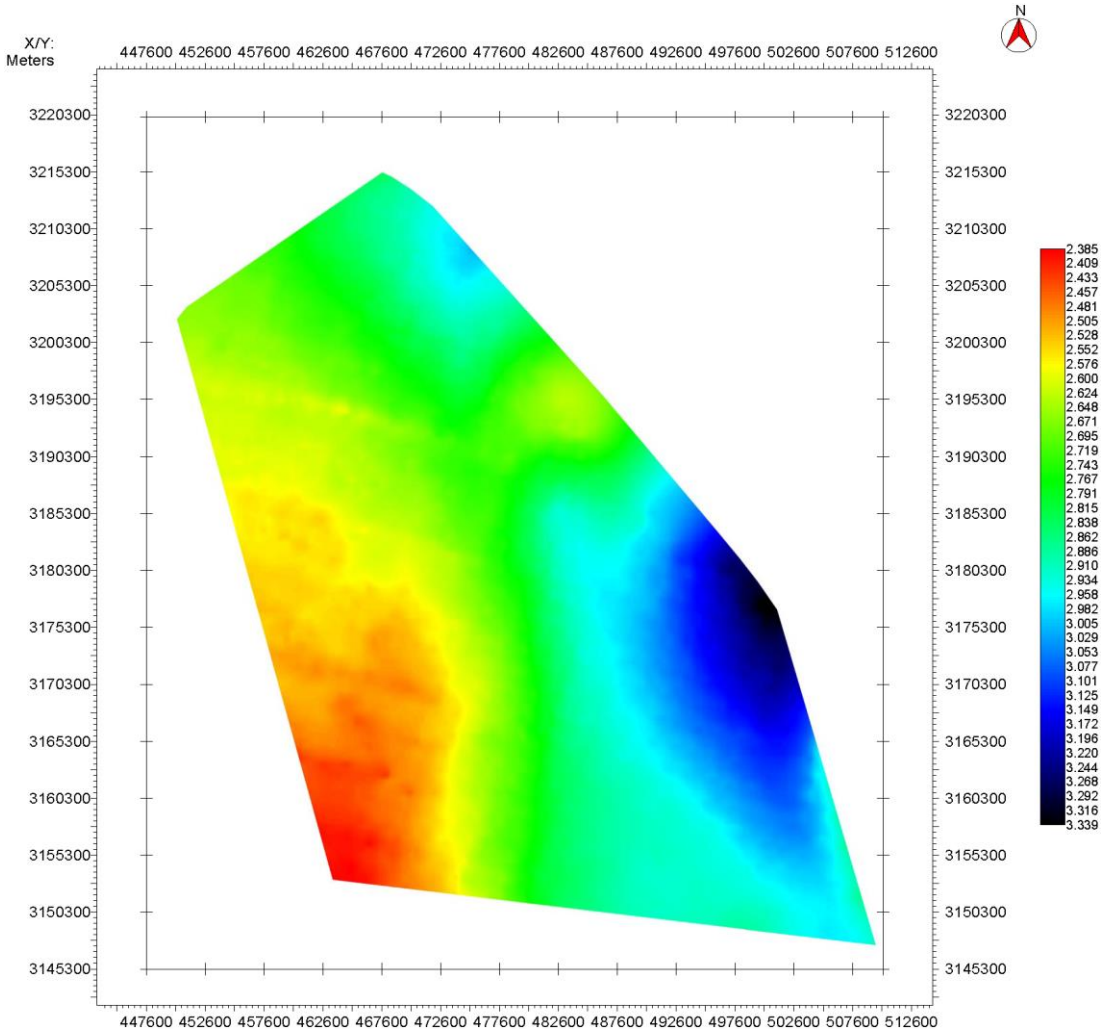

Figure 20 : Grid-7, constructed by interpretation of Horizon-7.

4.4 Thickness Maps

4.4.1 The Thickness Map Between Seafloor and Horizon-1

Thickness maps (Figures 21 to 27) depict thickness differences. Figure 21 shows the thickness differences between seafloor-horizon and horizon-1. In corporison for the onshore geological information, the Geological Unit is assigned as Bakhtyari formation.

It can be seen from the thickness map that areas with green to greenish colors illustrate medium thickness. Excluding areas marked by arrow 1 and 2, medium thicknesses largely covers the grid. Thinner places are demonstrated with red and orange colors and corresponding to anticlinal areas. Blue to dark colors are showed thickest parts of the thickness map that correspond to syncline areas. The thinnest area is 0.027 km and the thickest area is 0.28 km.

The Bakhtyari formation thickness is nearly constant towards to the interior part of the Persian Gulf. Close to the shore around the syncline and the Bushsehr anticline, the unit thickness is significantly changed. The reason of the thinning may be wave erosion. While the study area was uplifting, recent depositional units could be loaded into the syncline.

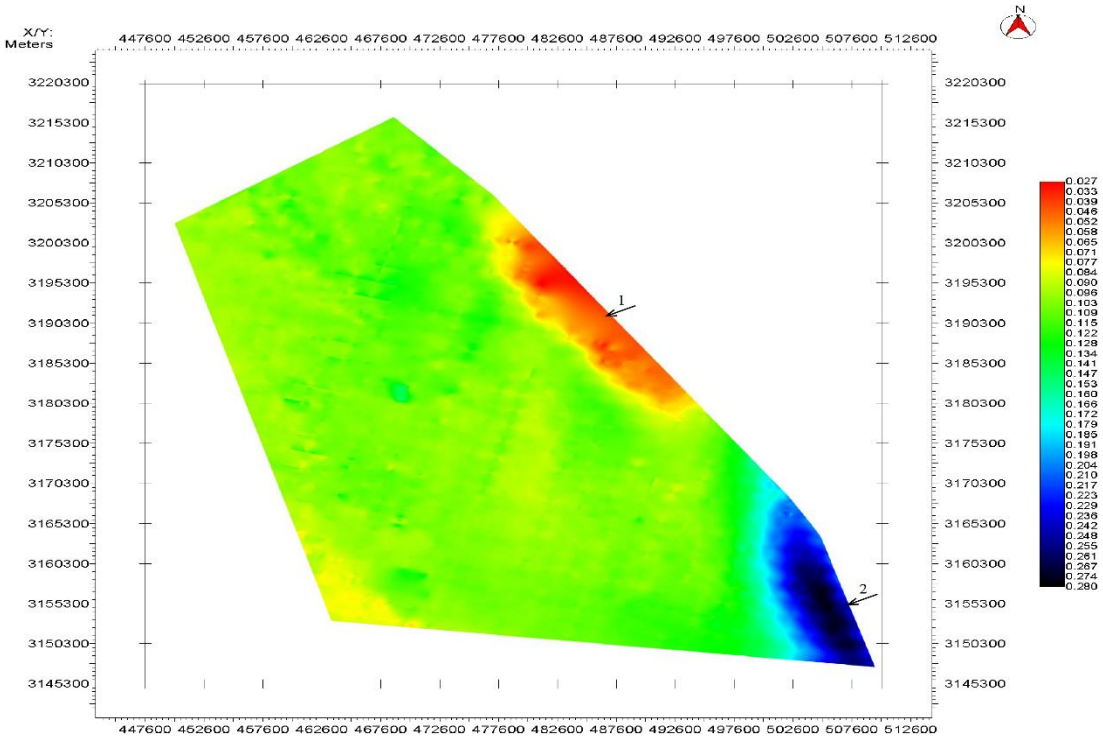

Figure 21 : The Thickness Map Between Seafloor and Horizon-1.

4.4.2 The Thickness Map Between Horizon-1 and Horizon-2

Thickness changes between horizon-1 and horizon-2 are illustrated in Figure 22. This unit can be correlated to the geological unit “Lahbari Member”, and it is a smallest recognizable stratigraphic unit of the Agha Jari Formation.

As can be seen from the thickness map that areas with green to greenish colors illustrate medium thickness. Excluding light blue places and the areas marked by arrow 1 and 2, middle thick areas considerably covers the grid. Blue to dark colors are showed the thickest parts of the thickness map which are marked with first arrow. Thinner places are demonstrated with red and orange colors, and second arrow also marks the area. The thinnest area is 0.51 km and the thickest area is 0.94 km.

Thickness of the Lahbari member is homogenous towards the Persian Gulf. The unit thickness is fairly different around the syncline, the Bushsehr anticline and light blue covered areas. Additionally, it is obvious that thick places of Lahbari member are largely distributed in the syncline in comparison with Baktyari formation.

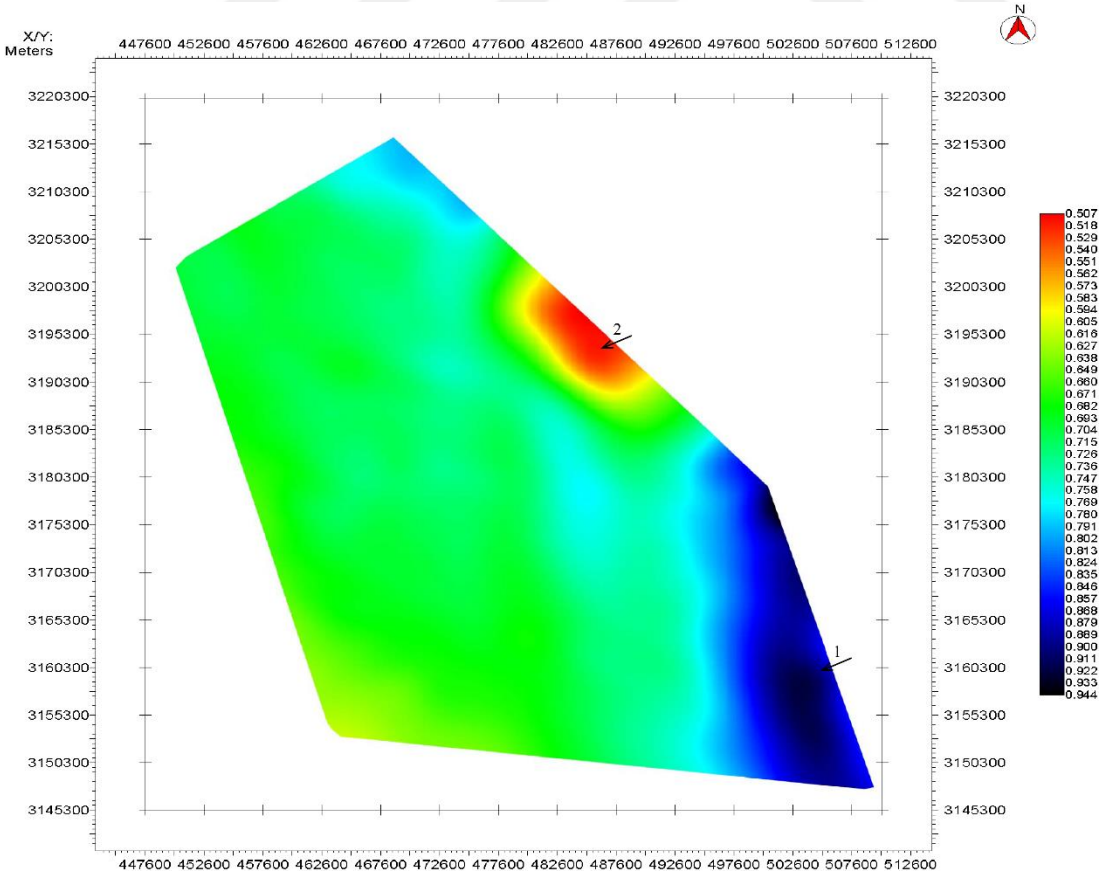

Figure 22 : The Thickness Map Between Horizon-1 and Horizon-2.

4.4.3 The Thickness Map Between Horizon-2 and Horizon-3

The thickness map (Figure 23) shows thickness differences between horizon-2 and horizon-3. The Geological Unit is assigned as the lower part of the Agha Jari Formation.

The thickness map shows that areas, are from light blue to dark colors, are marked as number one and elliptical, indicate high thicknesses. Regions with green to greenish colors illustrate medium thickness. The thinnest area is 0.24 km and the thickest area is 0.53 km. The thinnest part of the formation marked with arrow 2 and an ellipse, is in the south west and displayed with orange and red colors.

It is obvious that thickness wanes from northeast to southwest in the thickness map. The reason is that may be less sediment succession from the shore to the inner part of the Persian Gulf.

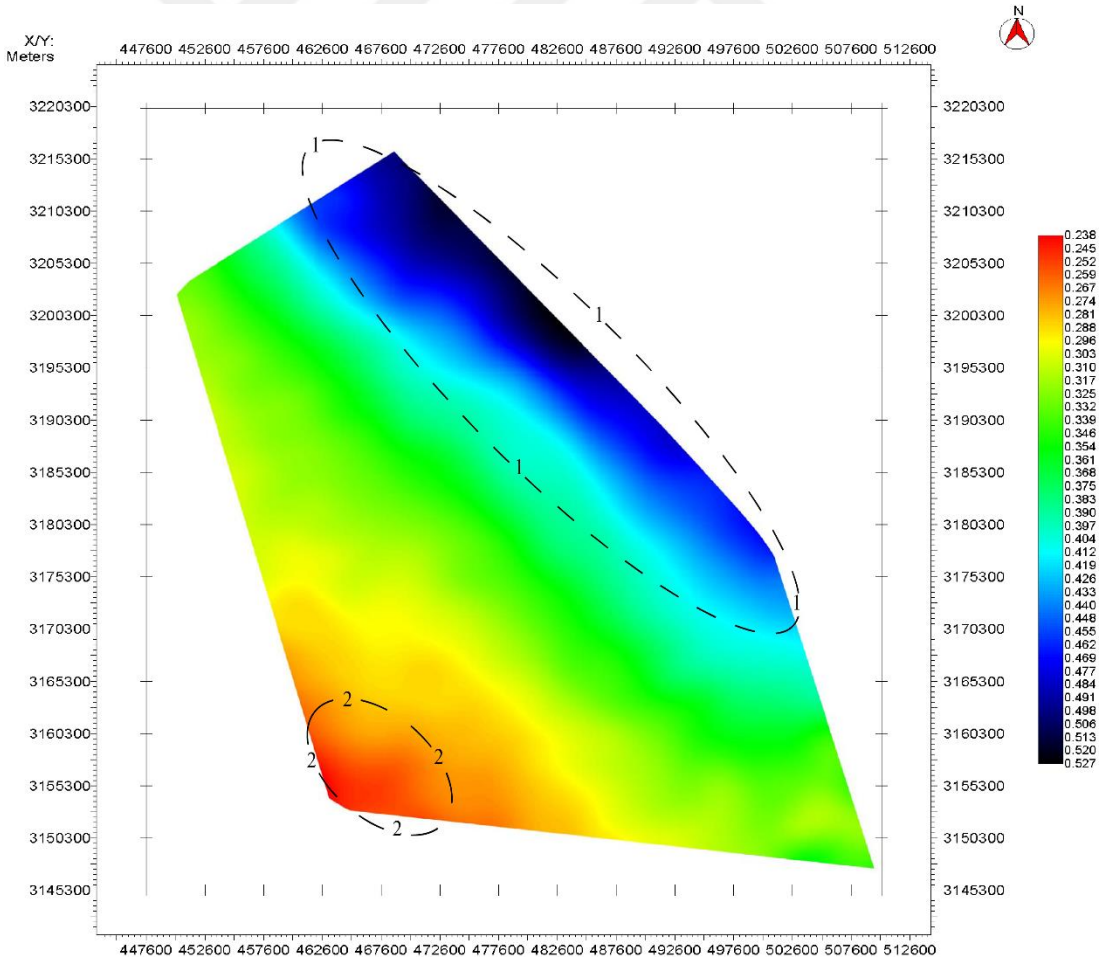

Figure 23 : The Thickness Map Between Horizon-2 and Horizon-3.

4.4.4 The Thickness Map Between Horizon-3 and Horizon-4

Thickness changes between horizon-3 and horizon-4 are shown in Figure 24. The corresponding geological unit is the Mishan Formation.

Thickness map that the thickest fields are shown in bluish-blue colors, middle thick parts are illustrated in green and light blue colors, and the thinnest areas are red.

The rectangle area which is marked by arrow 1, shows the thickest parts of the Mishan Formation. The thinnest area is 0.11 km and the thickest area is 0.33 km. The thickest part of this geological unit is at the Bushehr anticline area (dark blue). Thinner place, is in the elliptical shape and marked by two, is settled in the southeast. However, another red field is placed at the southeast corner. The area may indicate wrong data coverage.

It is clear that thickness rate is dropped from northeast to southwest direction in the thickness map. The reason for this may be less sediment transition from the onshore to the offshore.

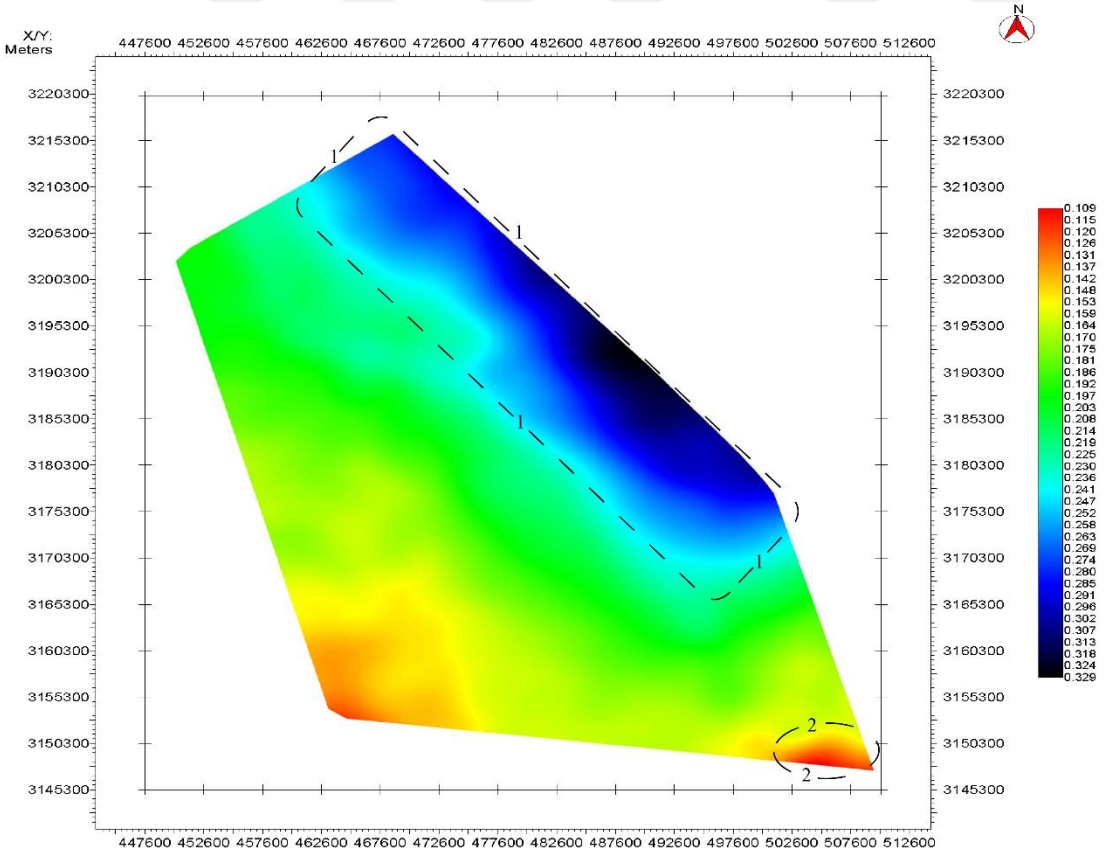

Figure 24 : The Thickness Map Between Horizon-3 and Horizon-4.

4.4.5 The Thickness Map Between Horizon-4 and Horizon-5

The thickness map (Figure 25) shows thickness differences between horizon-4 and horizon-5. The geological unit which is named the Guri member, is the smallest recognizable stratigraphic unit of the Gachsaran formation.

As shown on the thickness map that the thinnest areas are demonstrated with red, middle thick parts are illustrated in green and light blue colors, and the thickest fields are shown in bluish-blue colors. The thinnest area is 0.43 km and the thickest area is 0.77 km.

The thinner part of the formation, is marked by arrow 1, is settled in the northwest wing of the thickness map. The thicker parts are indicated by arrow 2 and dashed lines. The thickest domain is situated in the north to northeast.

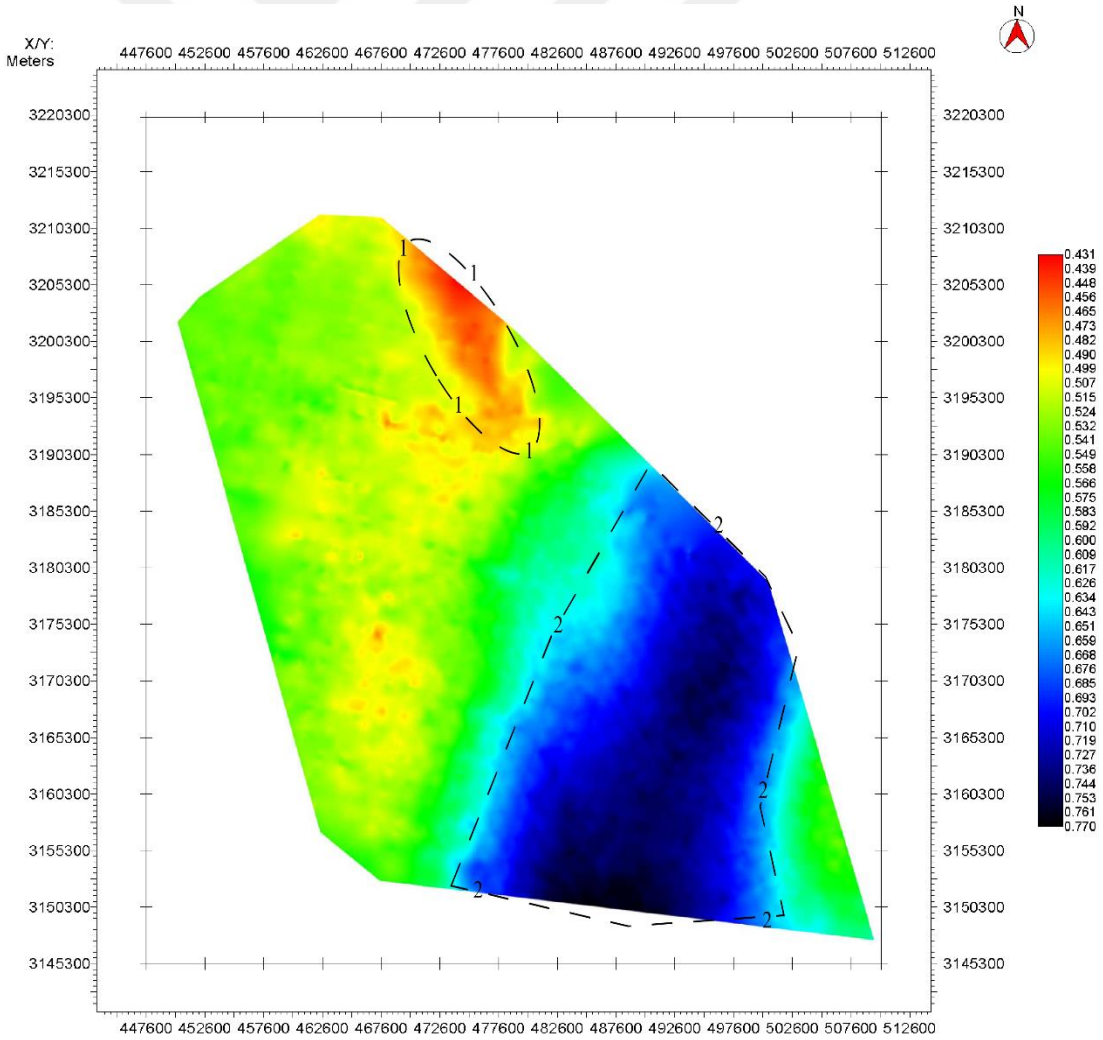

Figure 25 : The Thickness Map Between Horizon-4 and Horizon-5.

4.4.6 The Thickness Map Between Horizon-5 and Horizon-6

As shown in Figure 26, thickness changes between horizon-5 and horizon-6 are illustrated. The geological unit is named as Gachsaran formation.

As can be seen from the thickness map that the thickest fields are shown in bluish-blue colors and middle thick parts are illustrated in green and light blue colors. Excluding the area with high thickness which is in the ellipse-shaped region and marked by arrow 1, middle thick areas largely cover the grid. Yellow, orange and red colors probably show incorrect or erroneous data coverage due to lack of proper interpretation in the Kingdom program. The thinnest area is 0.35 km and the thickest area is 0.55 km.

It is clear that the thickness of the Gachsaran Formation is pretty much constant over the study area. Considering with grid-5 and grid-6, thick area, covers the growing syncline region, may largely have filled by sediments.

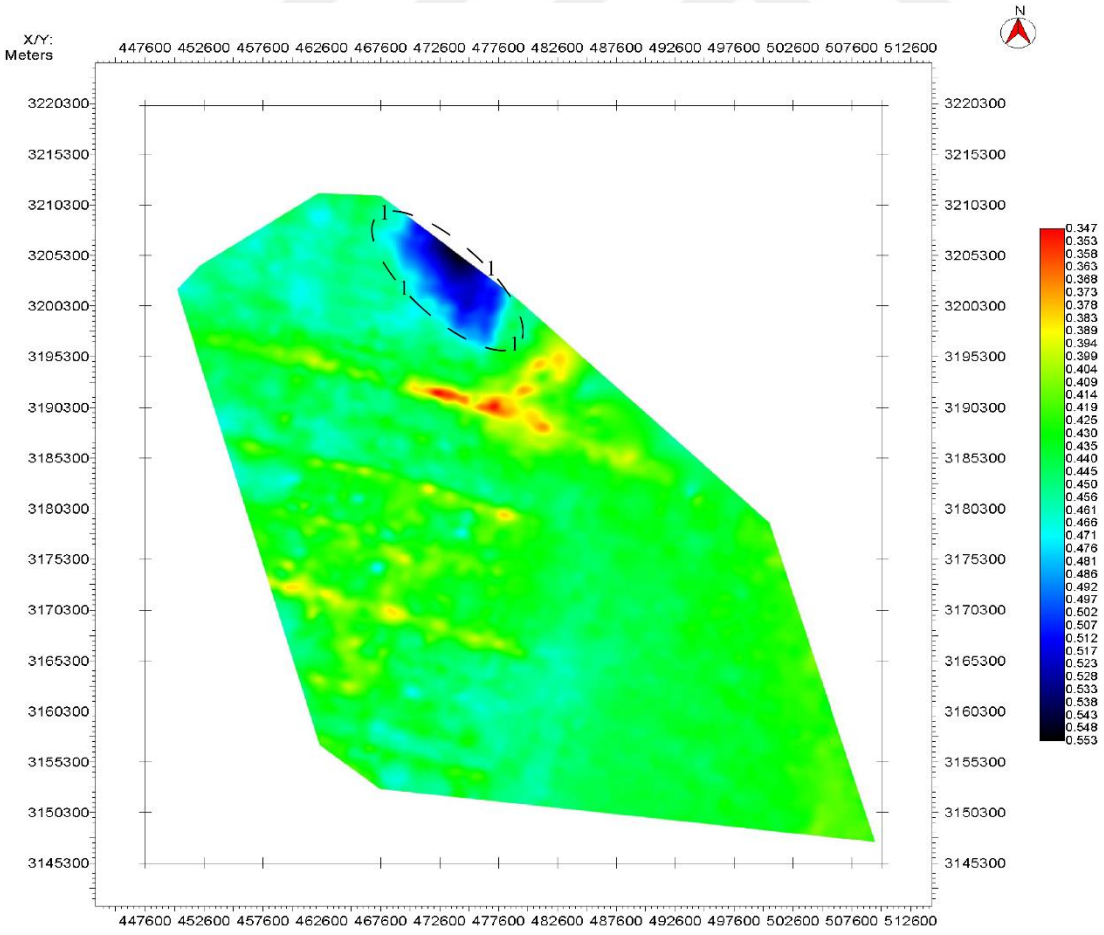

Figure 26 : The Thickness Map Between Horizon-5 and Horizon-6.

4.4.7 The Thickness Map Between Horizon-6 and Horizon-7

The thickness map (Figure 27) shows thickness differences between horizon-6 and horizon-7. The Geological Unit is appointed/assigned as the Asmari Jahrum Formation.

As shown on the thickness map, the thickest fields are shown in bluish-blue colors and middle thick parts are illustrated in green and light blue colors. The thicker part is indicated by arrow 1 and dashed lines. The thickest domain is shown in dark blue color and is situated in the east of the thickness map. Orange and red areas, are marked by arrow 2, probably show erroneous data coverage due to lack of incomplete interpretation in the Kingdom program. The thinnest area is 0.22 km and the thickest area is 0.38 km.

It is obvious that deposition of sediments took place completely different in the offshore domain. Therefore, the Asmari Jahrum formation was distributed in various direction.

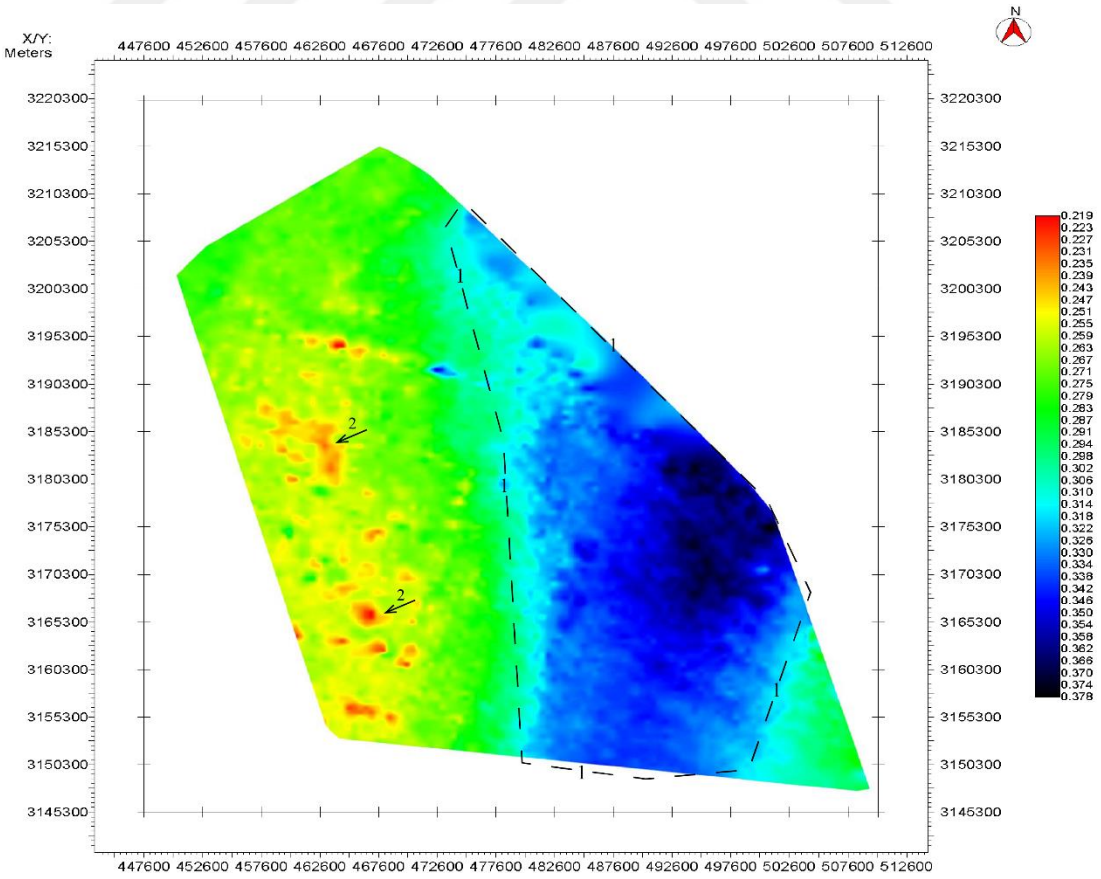

Figure 27 : The Thickness Map Between Horizon-6 and Horizon-7.

4.5 Summary of Thickness Map Section Interpretation

Based on the thickness maps, we see a dynamic development of depocenter of the study area. From old to young, initially the Asmari Jahrum Formation (Figure 27) was deposited in the eastern offshore part of the study area in a N-S oriented depo center. This depo center was active until the development of horizon 4, and also comprises the Gachsaran Formation (Figure 25). Subsequently a NW-SE oriented, elongate depocenter (lateral extend > ca. 50km; width ca. 10km) developed at the eastern (landward) edge of the offshore study area (Mishan Formation) (Figure 24). Then, another NW-SE oriented depocenter started to develop ca. 40km basinward at the western edge of the offshore study area (Figure 23), containing the Agha Jari Formation. A final step in the tectono-sedimentary development of the study area is the development of a NNW-SSE oriented, elongate depocenter at the SE edge of the study area (Figure 21, 22), coinciding with the development of an elongate structural high ca. 20km to the north.

4.6 2D/2D Cross Section Restorations

4.6.1 The Joined Onshore & Offshore Section

The Move 2016.1 program was used to create one interpreted onshore-offshore section. In order to pick up a seismic line from the offshore side of the study area, the cross section A-A' starting point was defined in ArcGIS. The point matched with the seismic line X at the coast, and the offshore cross-section was mapped along this line.

The offshore and onshore areas horizons were matched based on with their depths. In the present study, H1, H2, H3, H4, H5 and H7 were picked from the onshore data, and the matched horizons were selected at equal depths from the offshore part of the study area. Moreover, other horizons (H8, H9, H10, H11, H12 and H13) in the onshore area are included in figure 28. A salt diapir and mountain frontal faults are additionally illustrated in the figure.

In the 2D cross section, the horizons cover ca. 102km horizontal distance and a depth (b.s.l) of ca. 8,2km. Contractional faults angle in Figure 28 may actually differ.

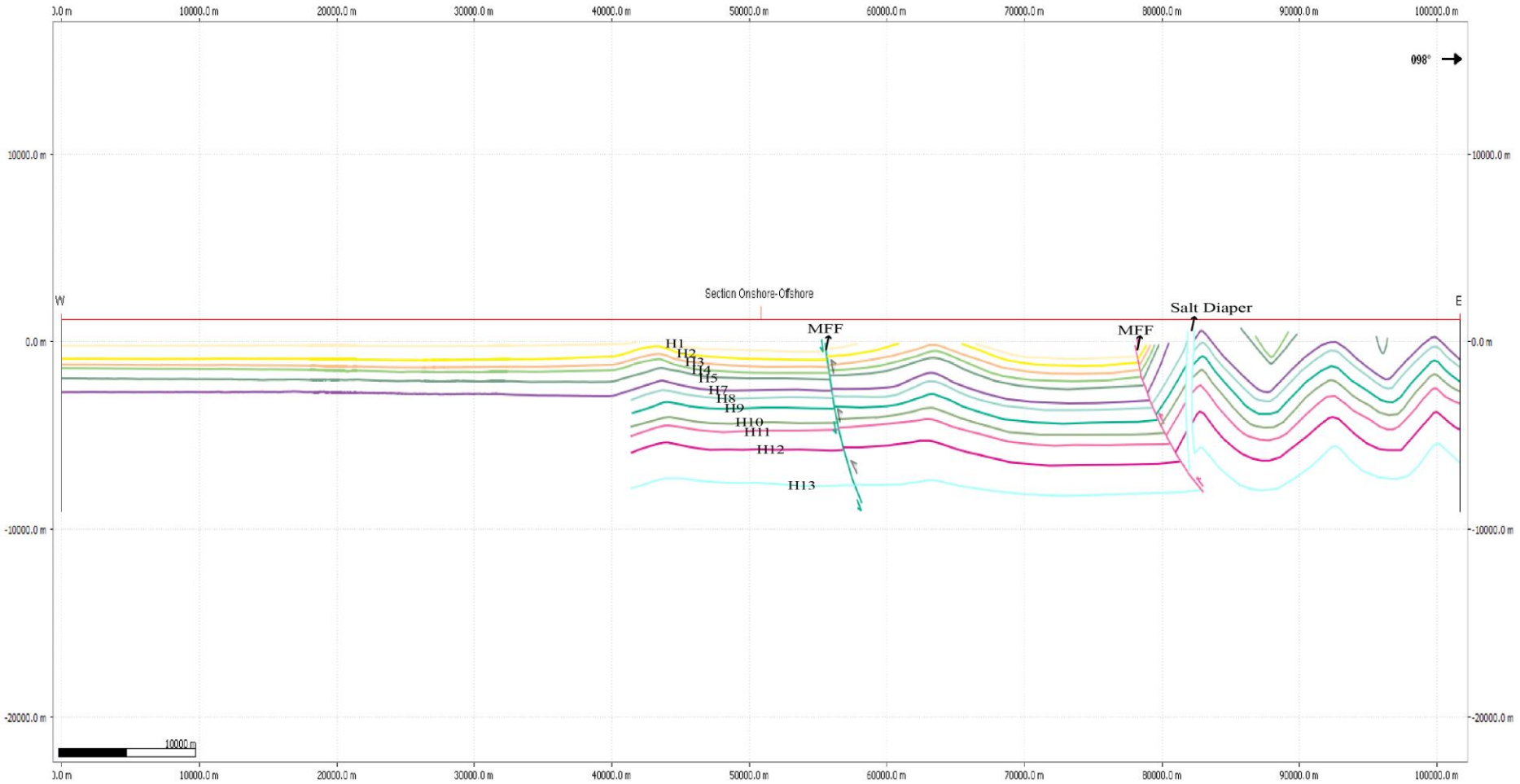

Figure 28 : Offshore - Onshore Intersection (Line X - Cross Section A-A') (angles of contractional faults may vary in reality).

4.6.2 Restoration of the Onshore & Offshore Section

4.6.2.1 Fault Restorations

The mountain frontal faults (MFF) are reverse faults (Figures 28 & 29). These faults were active and displaced the horizons in the study area. In order to get accurate results for the study, a fault restoration process was undertaken.

Arrow 1 (Figure 29) shows the young mountain frontal fault after the first fault restoration. Horizons were restored in accordance with their previous level. It should be noted that the angle of the reverse fault might differ due to the lack of land seismic data.

Arrow 2 (Figure 29) illustrates an old MFF. Horizons, which are situated around the old MFF, were also restored according to their former geometry.

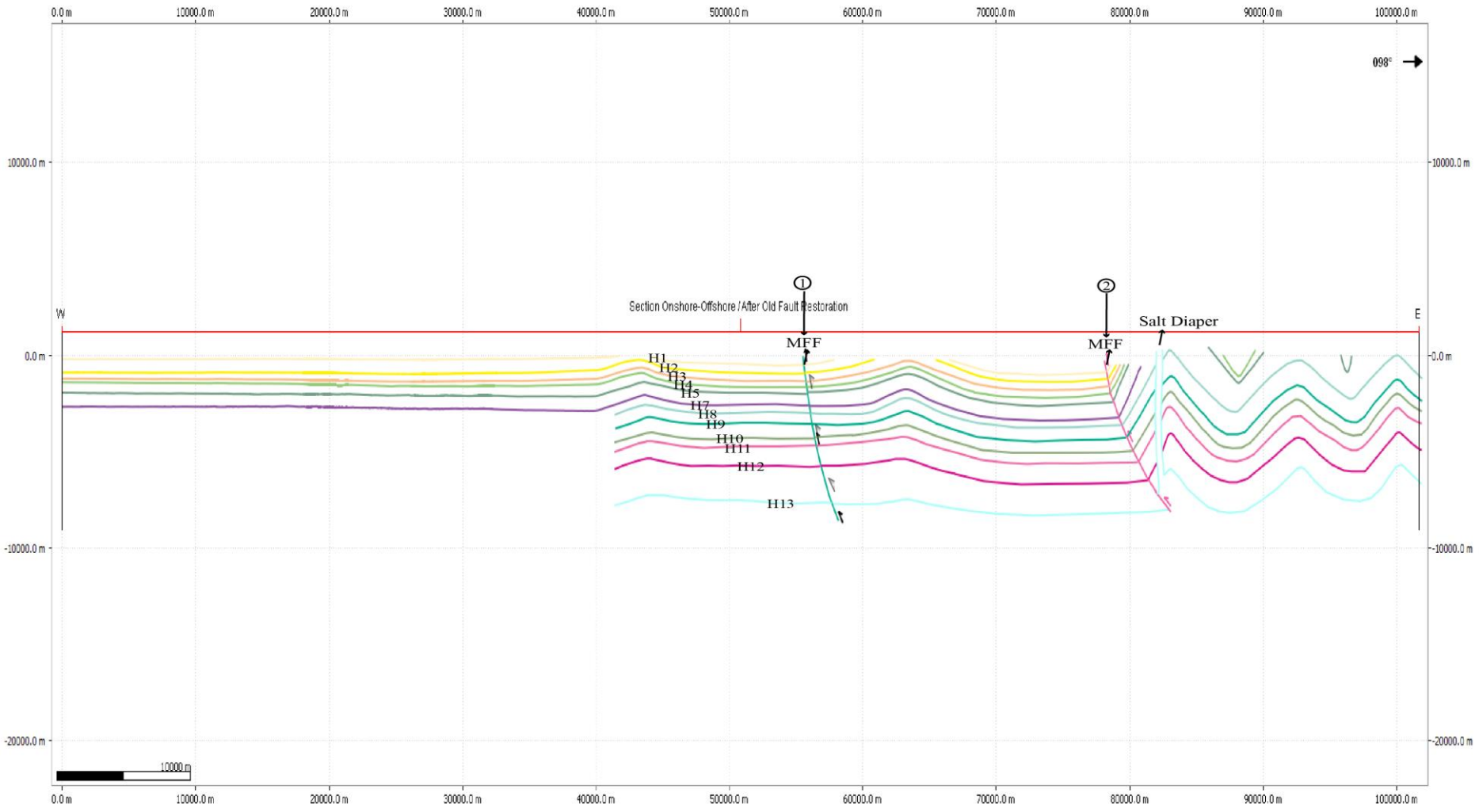

Figure 29 : View of Restored Fault (angles of contractional faults may vary in reality).

4.6.2.2 Unfolding

Unfolding was done in two approaches, a simple (1) and a complex (2) approach.

4.6.2.2.1 Simple Approach

The simple unfolding approach (figure 30) determined of the actual elongations of the folded structures. In the study, contractional faults were mainly taken into account obtaining accurate results. Furthermore, the simple unfolding method started in the area of the young reverse fault, and continued in the area of the older reverse fault. The simple shear method was used two times for the unfolding process.

Firstly, the younger MFF, in the centre of figure 30 was selected for horizon unfolding of the strata around. Horizons are placed at the footwall of young MFF were defined as passive objects and horizons on the hanging wall side of the fault were appointed as active objects. Additionally, hanging-wall horizons were limited to the area between the young MFF and the old MFF.

Secondly, strata around the older MFF were picked to carry out a second unfolding. Horizons in the footwall of the old MFF were selected as passive objects, and the horizons on the hanging-wall side of the fault were picked as active objects.

Figure 30 shows that the first run was quite effective to unfold the horizons. It is clear that the extensions of horizons can be viewed on the footwall of the old MFF. The second run showed a moderate success to unfold entire horizons. The result of the runs is 5,7km that can be seen in the east part of the figure 30.

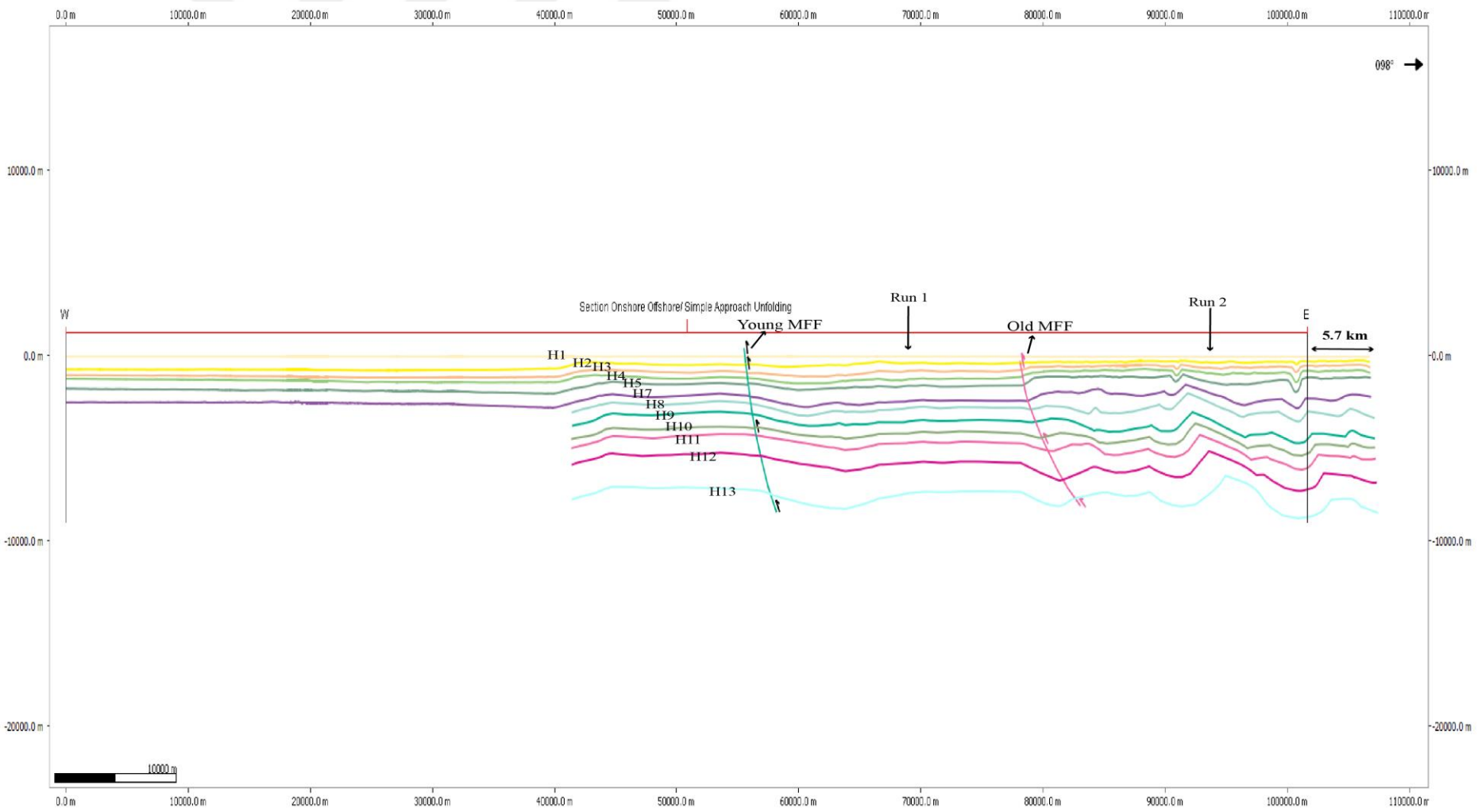

Figure 30 : Simple Approach Unfolding (angles of contractional faults may vary in reality).

4.6.2.2.2 Complex Approach

The complex unfolding approach also determined the extension of folded structures. The method implementation first began from the young reverse fault in the center of the section and proceeded with the older, eastern reverse fault. The simple shear method was supplied eleven times used for the unfolding processes.

The younger MFF and its footwall / hanging-wall were not selected for the unfolding process. As it is mentioned in the previous section, after the simple approach, the area covered almost accurate date due to that unfolding process was applied in the eastern part of the study area. Horizons that were in the footwall of the old MFF were chosen as passive objects. The horizons on the hanging wall side were not used as active objects.

H1 and the old MFF were picked as active objects and a first unfolding run was made. Then, H1 was taken of the system and H2 and the old MFF was selected as active. Then second run has proceeded. These processes were continued and eleven run were made in total. Figure 31 illustrates the unfolding measurement for H4 after the third run. The unfolding results of the entire horizons are shown in the table four.

Table 4. Unfolding Results for the Entire Horizons.

Horizons	Unfolding Measurement Results (km)
Horizon-2 (H2)	5.15
Horizon-3 (H3)	5.44
Horizon-4 (H4)	5.90
Horizon-5 (H5)	6.50
Horizon-7 (H7)	6.92
Horizon-8 (H8)	7.84
Horizon-9 (H9)	8.55
Horizon-10 (H10)	9.10
Horizon-11 (H11)	9.62
Horizon-12 (H12)	9.41
Horizon-13 (H13)	9.38
Mean	7.62

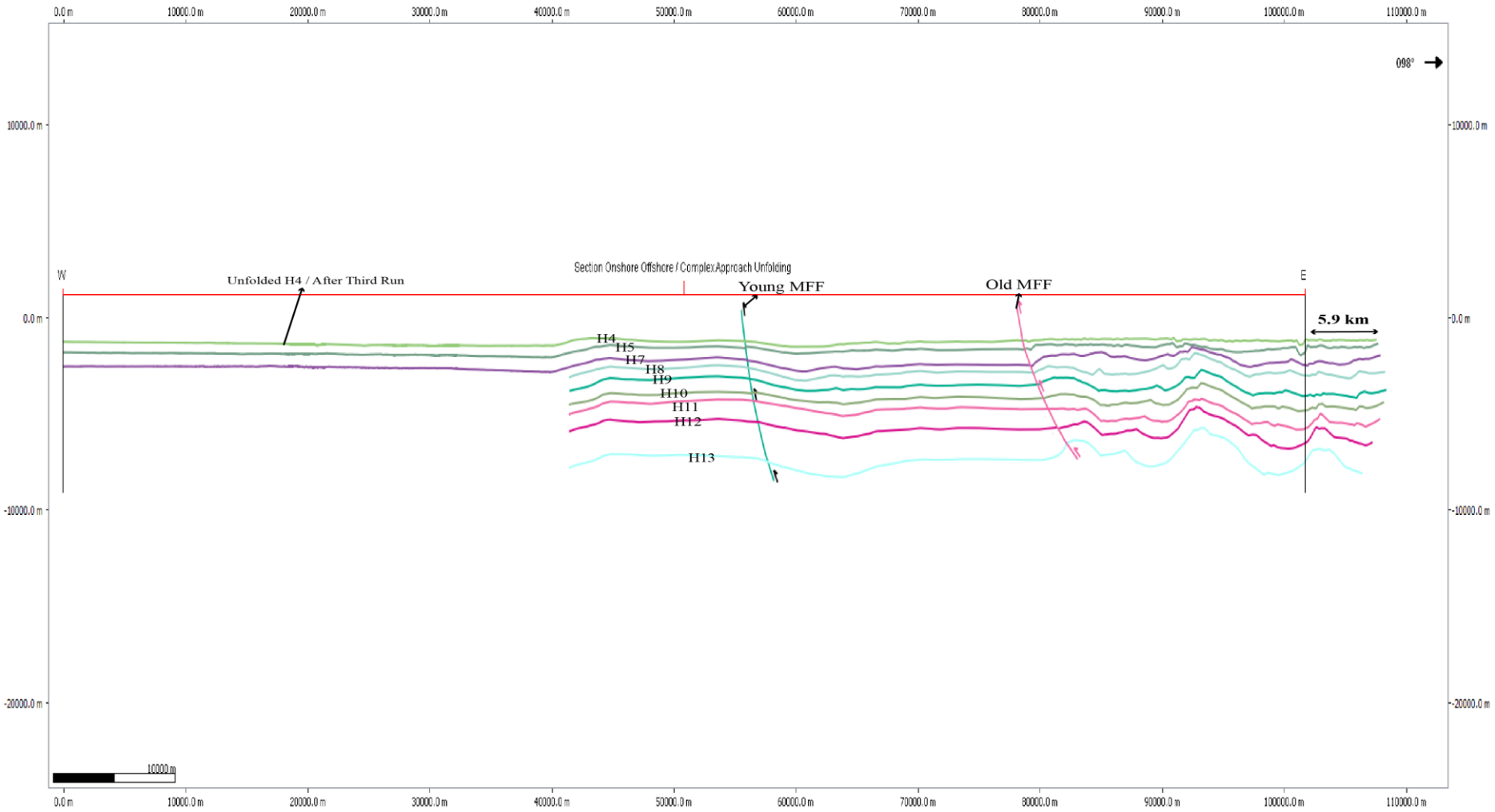

Figure 31 : Complex Approach Unfolding for Horizon 4 (After Third Run) (Angles of contractional faults may vary in reality).

4.7 3D Combined Onshore & Offshore Model

The Move 2016.1 Program used to create a 3D Model. The reason to choose the program is that it is a relevant/suitable program for 3D structural modelling.

The top part of the model is forward by a DEM. 6 pieces of Aster Global DEMs were downloaded from the USGS website and adjusted in accordance with the study area.

In order to create 3D surfaces in the offshore part of the area, grids were exported from the Kingdom project. For the study, seven grids (grid 1, grid 2, grid 3, grid 4, grid 5, grid 6 and grid 7) were selected and loaded into the 3D model.

Surfaces in the onshore part were created from 4 cross sections (profiles; A-A', B-B', C-C', D-D') uploaded in Move. Identical names were assigned/appointed for horizons, faults and a salt diapir in these cross sections.

Lastly, the surface menu from the model-building panel in Move was used to create surfaces from grids and horizons. According to their match, seven different surfaces were built (Figure 32).

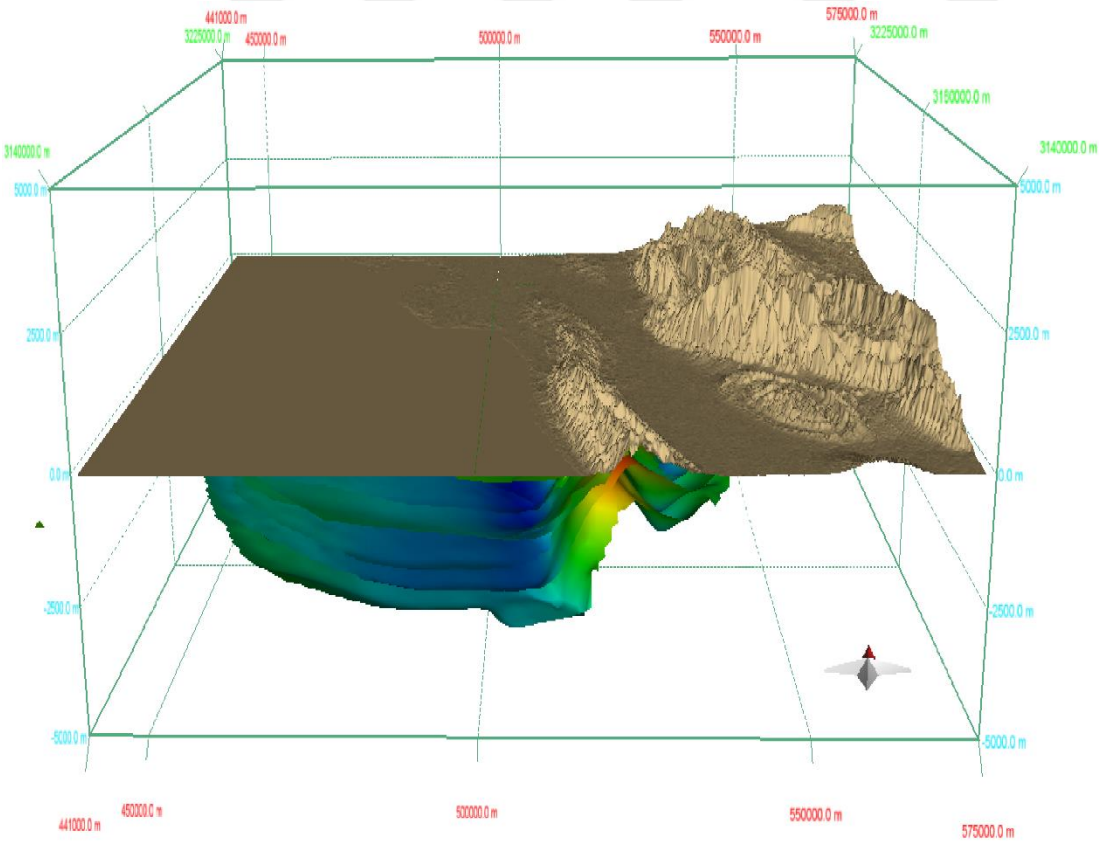

Figure 32 : Entire 3D-Surfaces were constructed from balanced cross sections and seismic grids.

4.8 3D Retrodeforming

4.8.1 Surface-1

Surface-1 (Figure 33) was created from grid-1 and H1. Figure 33 comprises a north arrow, the bounding box with XYZ coordinates, a color bar and surface-1.The color bar, which is placed below the bounding box of figure 33, indicates significant elevation differences in the surface. Reddish and pink areas show high elevation and blue to bluish places show low elevation. Although anticline structures are difficult to see, some syncline structures can partly be identified.

Arrow 1 shows one syncline between the Mand Anticline and the Chah Pir Anticline. Surface 1 defines the base of the Bakhtyari Formation and top of the Lahbari member. As it is mentioned in the section 4.4.2, the Lahbari member is smallest recognizable stratigraphic unit of Agha Jari Formation. It is obvious that some parts of Lahbari member are missing. There may have been erosion that may have affected entire surface.

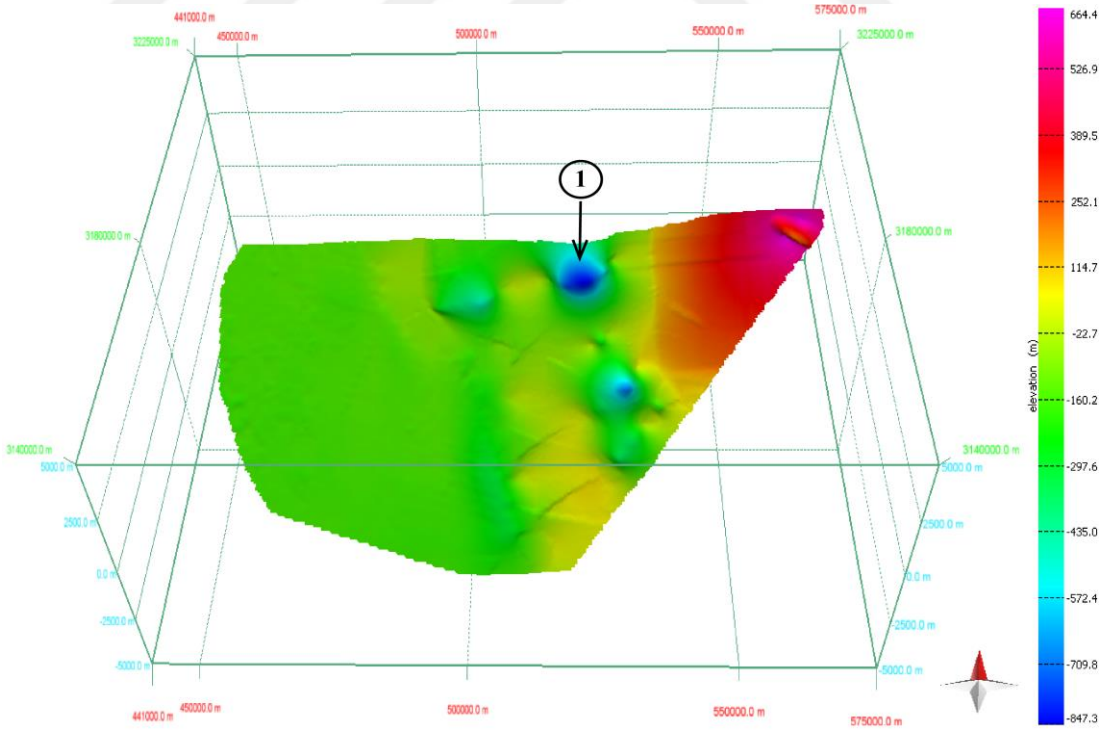

Figure 33 : Surface-1 was constructed from balanced cross sections and grid-1.

4.8.2 Surface-2

Surface-2 (Figure 34) was formed from grid-2 and H2. Figure 34 comprises a north arrow, the bounding box with XYZ coordinates, a color bar and surface-2. Red and reddish colors show high elevation and blue places show low elevation. Anticline structures are more clear than on surface-1. For instance, the Mand Anticline and the Bushehr Anticline are observable. Arrow 1 shows a syncline structure. Arrow 2 also shows a syncline that was situated between the Mand Anticline and the Khurmuj Anticline. Another syncline (Arrow 3) between the Mand anticline and the Bushehr anticline is also visible.

The surface shows base of the Lahbari member and top of the Agha Jari Formation. The high Zagros Mountains are situated in the east and north-east part of the study area. It is clear that the anticline structures of this area are not visible in this part, since adjacent to the study area.

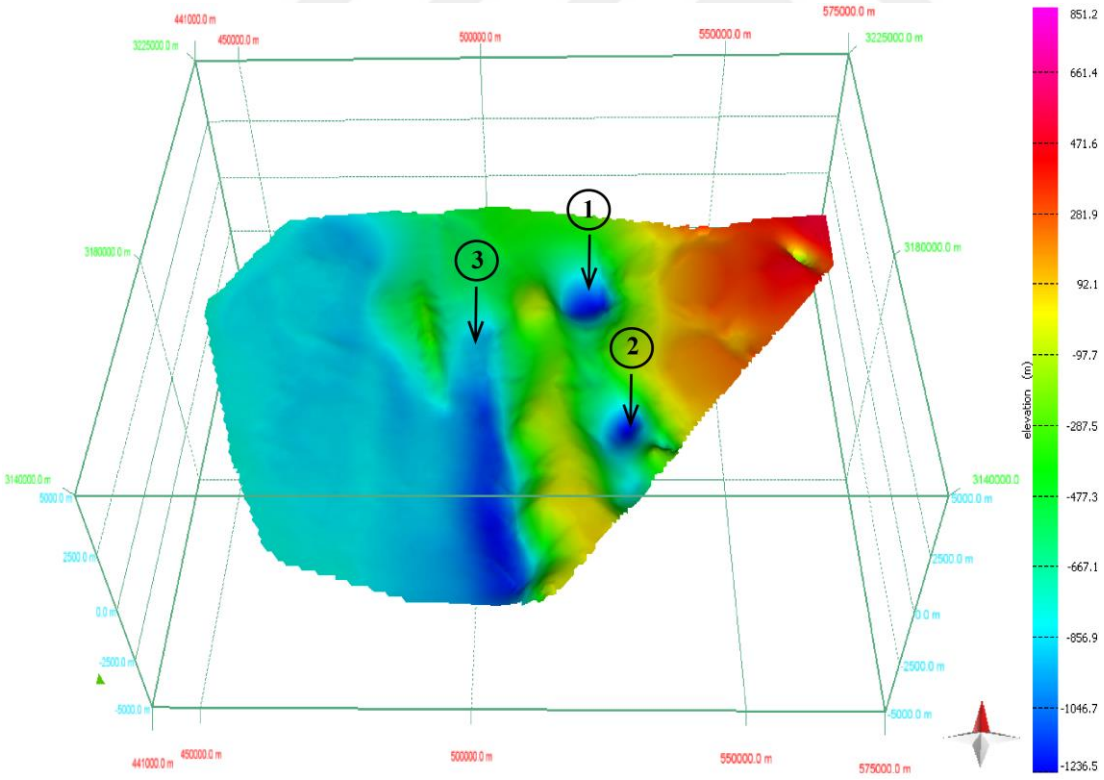

Figure 34 : Surface-2 was constructed from balanced cross sections and grid-2.

4.8.3 Surface-3

Surface-3 (Figure 35) was created from grid-3 and H3. Figure 35 comprises a north arrow, the bounding box with XYZ coordinates, a color bar and surface-3. Reddish and red colors show high elevation and blue to light blue areas show low elevation. Anticline structures on the surface are, compared with surface-1 and surface-2, more clear. For example, the Khurmuj Anticline (Arrow 1), the Bushehr Anticline (Arrow 2), the Mand Anticline (Arrow 3) and a part of the Khaki Anticline (Arrow 4) are present. Synclines show in comparison with surface-2, no distinct changes.

Arrow 1 shows the Khurmuj Anticline and the area partially balanced and reshaped due to cut by surface-2. The surface corresponds to the base of the Agha Jari formation and the top of the Mishan Formation.

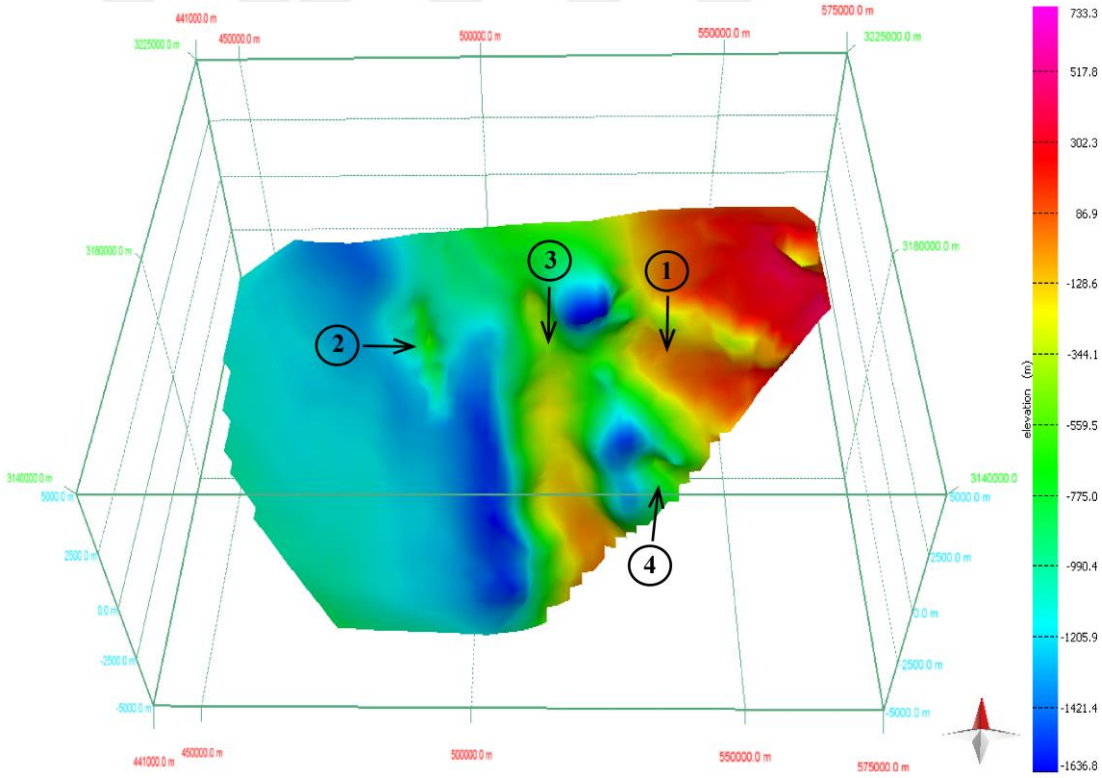

Figure 35 : Surface-3 was constructed from balanced cross sections and grid-3.

4.8.4 Surface-4

Surface-4 (Figure 36) was created from grid-4 and H4. Figure 36 comprises a north arrow, the bounding box with XYZ coordinates, a color bar and surface-4. Blue colors show low elevation and reddish colors show high elevation. The anticline structures of the surface show, if compared with surface-3, no distinct changes. Only, the Chah Pir Anticline (Arrow 1) can be additionally seen. One of the syncline (Arrow 2), which is settled between the Khurmuj Anticline and the Chah Pir Anticline, is more visible.

Surface-4 corresponds to the base of the Mishan Formation and top of the Guri Member. As it is stated in the section 4.4.5, the Guri Member is smallest recognizable stratigraphic unit of the Gachsaran formation.

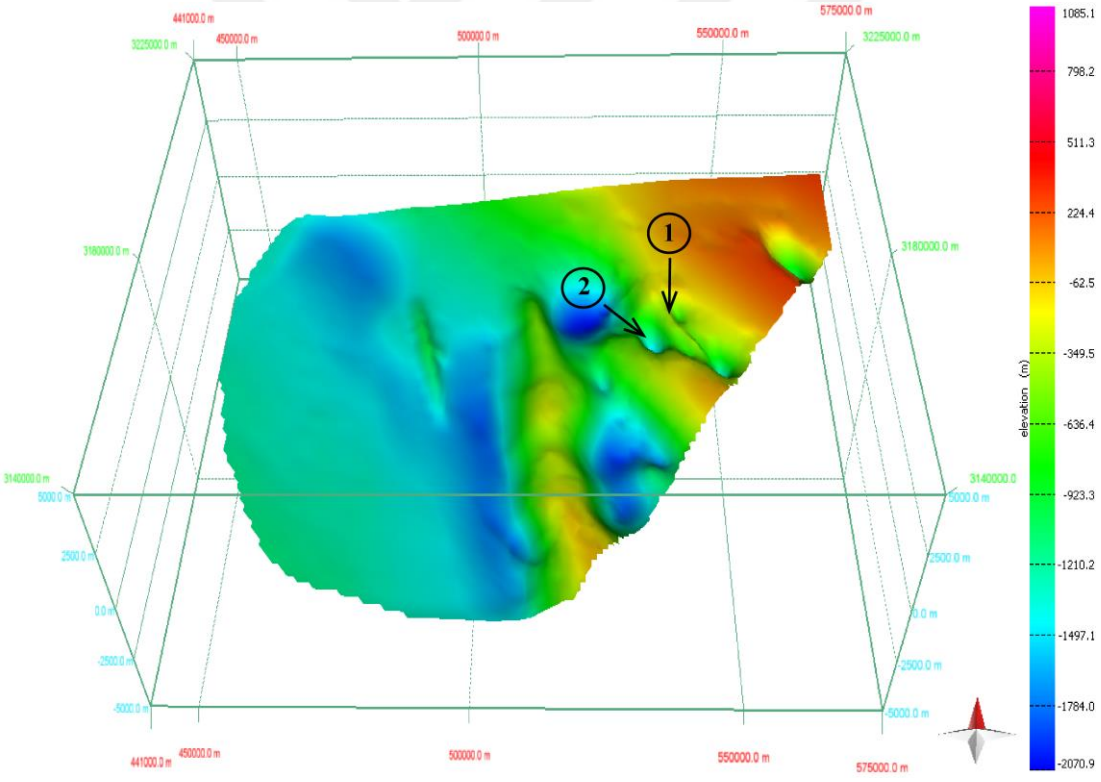

Figure 36 : Surface-4 was constructed from balanced cross sections and grid-4.

4.8.5 Surface-5

Surface-5 (Figure 37) was created from grid-5 and H5. Figure 37 shows a north arrow, the bounding box with XYZ coordinates, a color bar and surface-5. Areas with dark blue, blue and light blue colors show low elevation. Dark red and red colors show high elevation. The anticline structures of surface-5 show, when compared with surface-4, changes. The Khurmuj Anticline is oriented NW-SE. However, a part of the anticline (Arrow 1) is curved in N-S direction. In the north-eastern part of the study area, the Siah Anticline (Arrow 2) and the Gisakan Anticline (Arrow 3) are visible. The surface corresponds to the base of the Guri Member and top of the Gachsaran Formation.

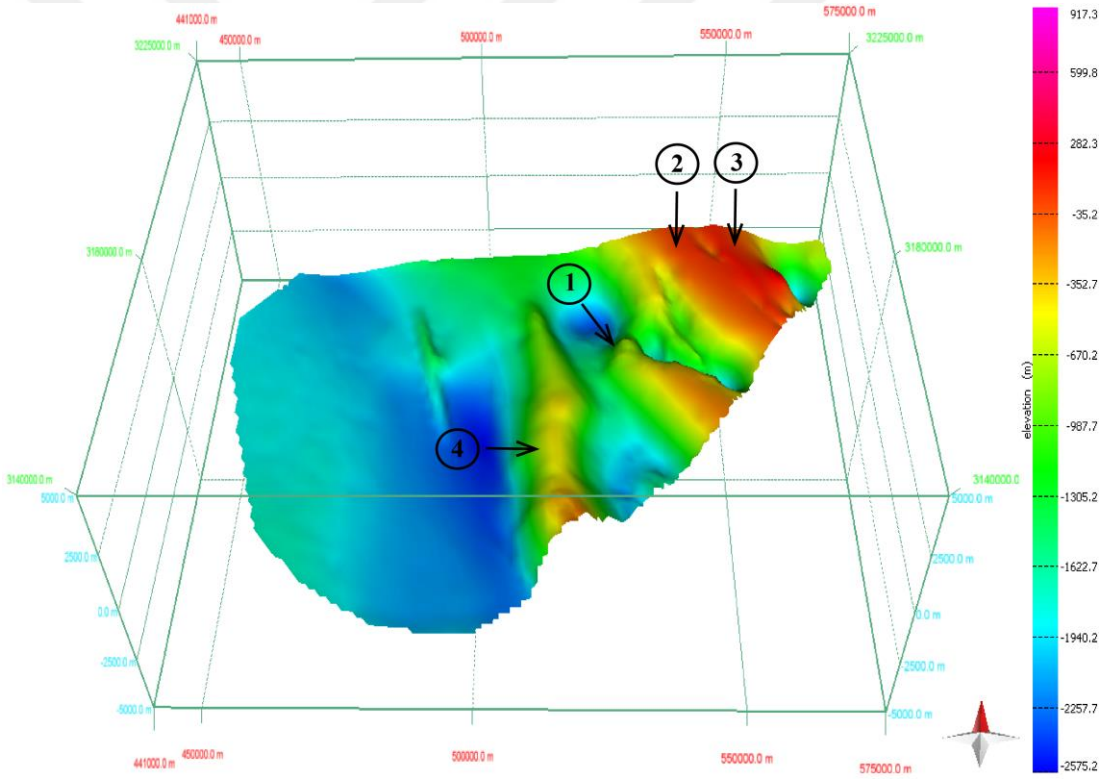

Figure 37 : Surface-5 was constructed from balanced cross sections and grid-5.

4.8.6 Surface-6

Surface-6 (Figure 38) was created from grid-6 and H6. Figure 38 shows a north arrow, the bounding box with XYZ coordinates, a color bar and surface-6.

The blue areas show low elevation and red places show high elevation. Anticline structures show, if compared with surface-5, some changes. The Gisakan Anticline and the Siah Anticline structures are more pronounced. A part of the Mand Anticline, the Gisakan anticline and the Chah Pir Anticline were partially reshaped due to intosection by a lower surface. Furthermore, a syncline (Arrow 1) rectified because of its incorrect geometry. The surface shows base of the Gachsaran Formation and top of the Asmari Jahrum Formations.

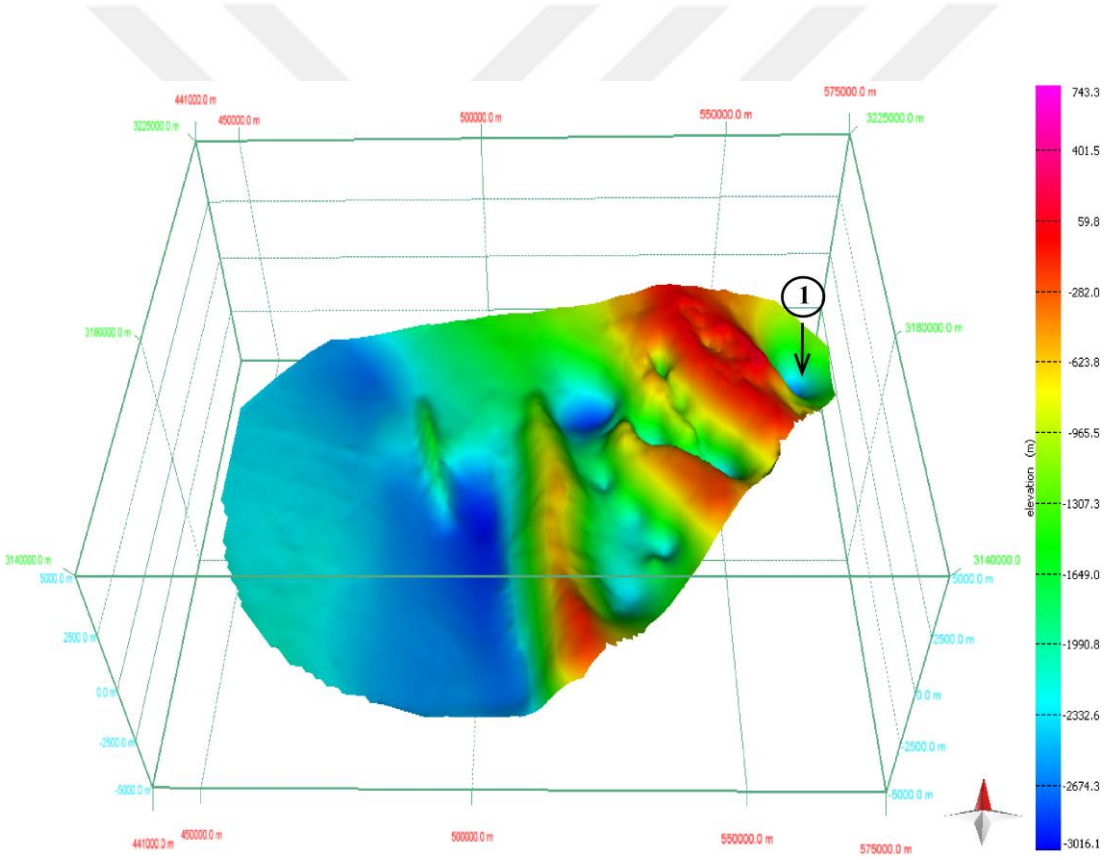

Figure 38 : Surface-6 was constructed from balanced cross sections and grid-6.

4.8.7 Surface-7

Surface-7 (Figure 39) was created from grid-7 and H7. Figure 39 shows a north arrow, the bounding box with XYZ coordinates, a color bar and surface-7. Red and reddish colors show high elevation and blue and light blue places show low elevation. Anticline and syncline structures of the surface compared with entire surfaces represent distinct changes. All anticline and synclines on surface-7 are clearly defined. The surface shows base of the Asmari Jahrum Formations and top of the Pabdeh Gurpi Formation.

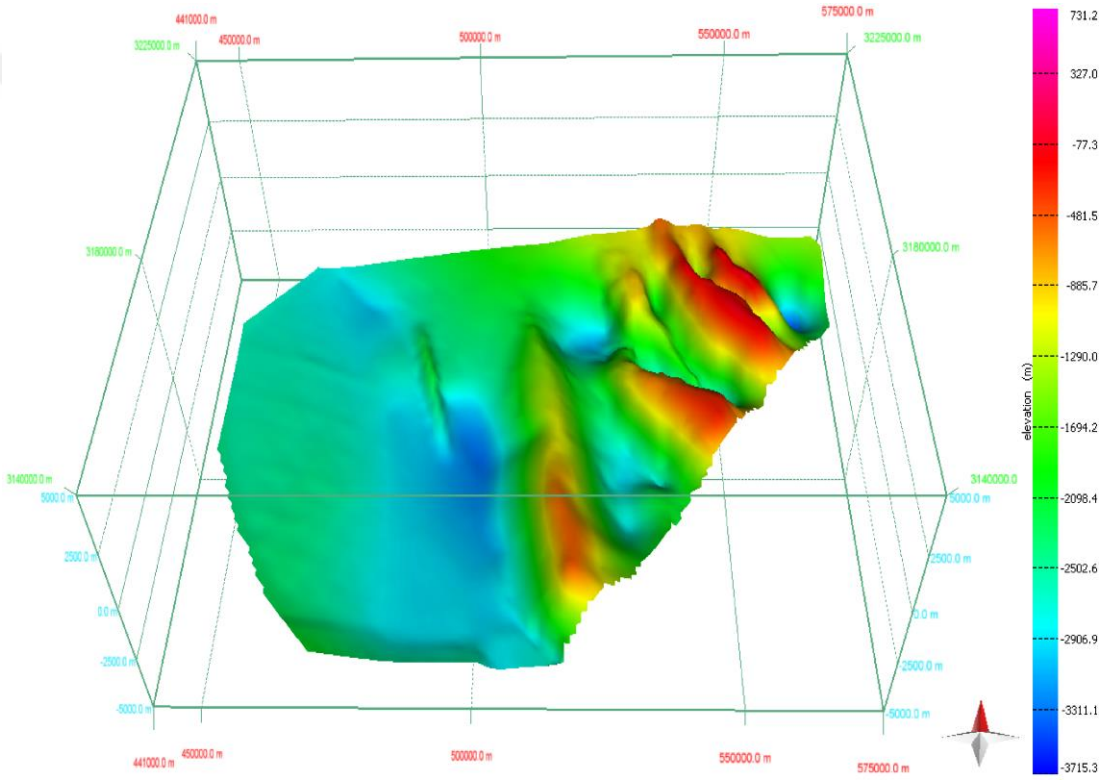

Figure 39 : Surface-7 was constructed from balanced cross sections and grid-7.

Result of entire 3D surfaces indicate that onshore domain demonstrates intense folding areas. In spite of this, offshore region shows slightly folded fields. This part of the study area is inside of the foreland basin. However, I could not observe any contarctional fault and salt diapirs in the offshore part, which can be reasons to fold the lithological units intensely.

5. DISCUSSION

Figure 40, which is drawn based on the thickness map between horizon-4 and horizon-7, shows the depocenter of the Asmari Jahrum Formation, the Gachsaran Formation and the Guri Member. The Asmari Jahrum Formation deposited from the middle Eocene to the early Miocene, the Gachsaran Formation settled in the middle Miocene, and the Guri member of the Mishan Formation subsided in the late Miocene. The color bar demonstrates thickness changes from the middle Eocene to late Miocene in the offshore domain. The thinnest area is 1,15 km and the thickest area is 1,55 km. The figure also includes profile 1, which is orientated NNE - SSW, was drawn to represent the depocenter elongation.

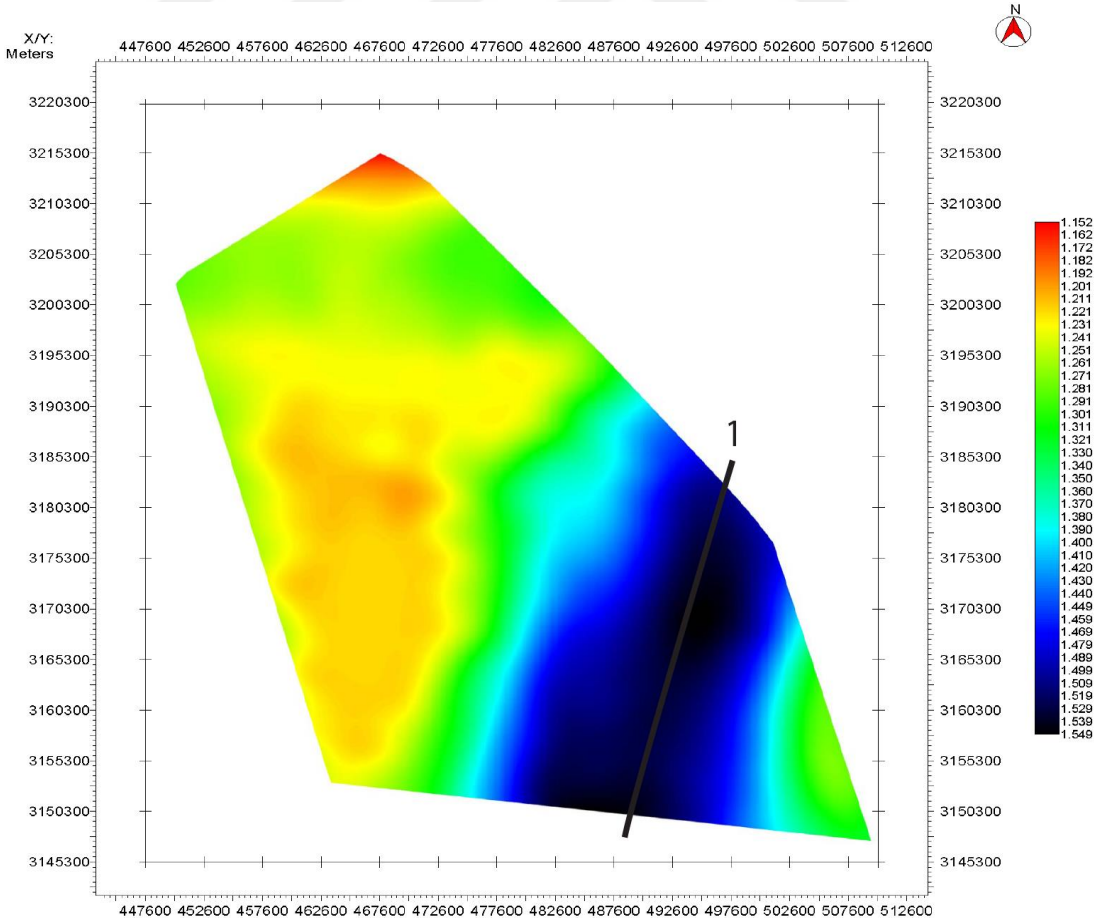

Figure 40 : The thickness map between horizon-4 and horizon-7.

Figure 41, which is drawn based on the thickness map between horizon-2 and horizon-4, shows the depocenter of the Mishan Formation and the Agha Jari Formation. The Mishan Formation subsided in the late Miocene and the Agha Jari Formation deposited from the late Miocene to the Pliocene. The color bar demonstrates thickness changes from the late Miocene to the Pliocene in the offshore domain. The thinnest area is 0.36 km and the thickest area is 0.82 km. The figure also includes profile 2, which is orientated NW - SE, was drawn to represent the depocenter elongation.

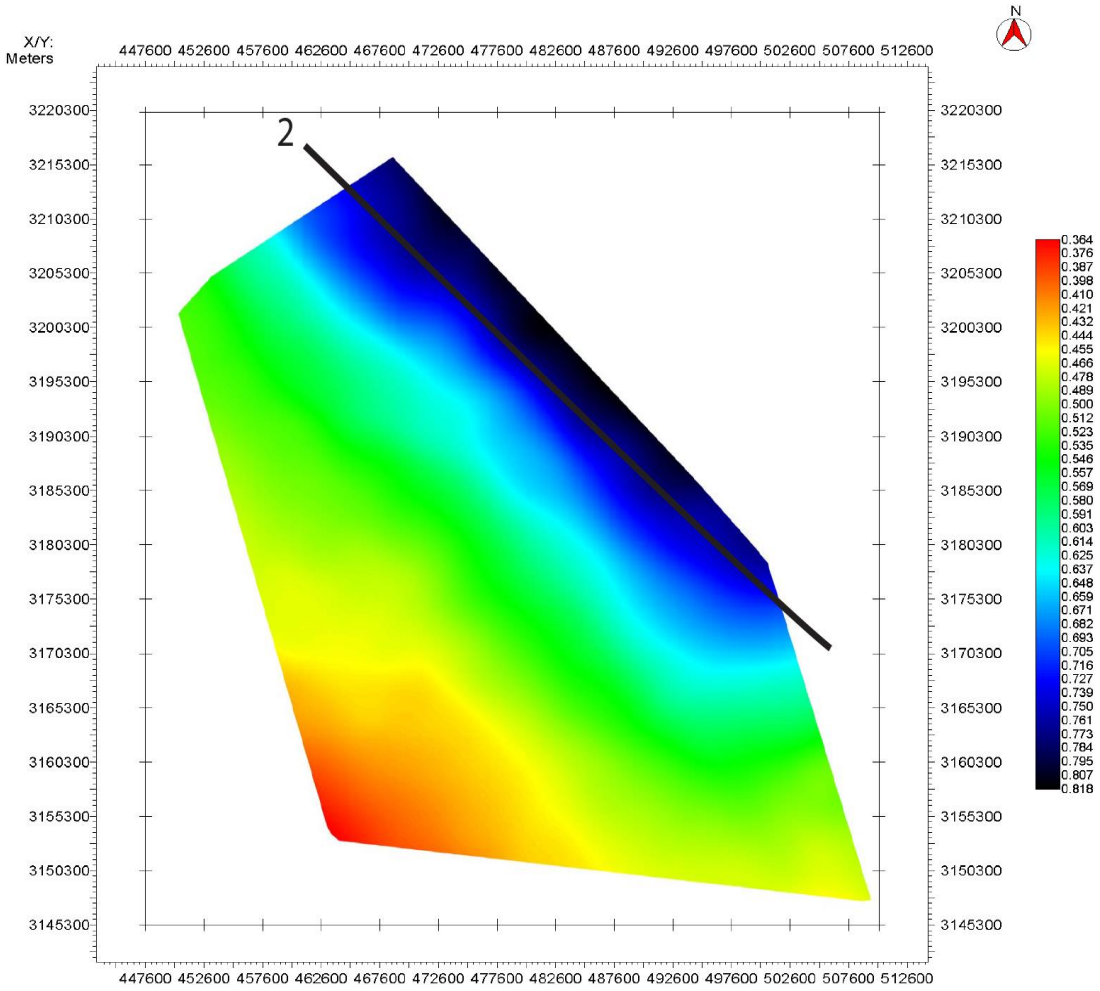

Figure 41 : The thickness map between horizon-2 and horizon-4.

Figure 42, which is drawn based on the seafloor thickness map and horizon-2, shows the depocenter of the Lahbari Member and the Bakhtyari Formation. The Lahbari Member of Agha Jari Formation settled in the Pliocene and the Bakhtyari Formation subsided in the upper Pliocene. The color bar demonstrates thickness changes from

the Pliocene to the upper Pliocene in the offshore domain. The thinnest area is 0.55 km and the thickest area is 1.19 km. The figure also includes profile 3, which is orientated NNW - SSE, was drawn to represent the depocenter elongation.

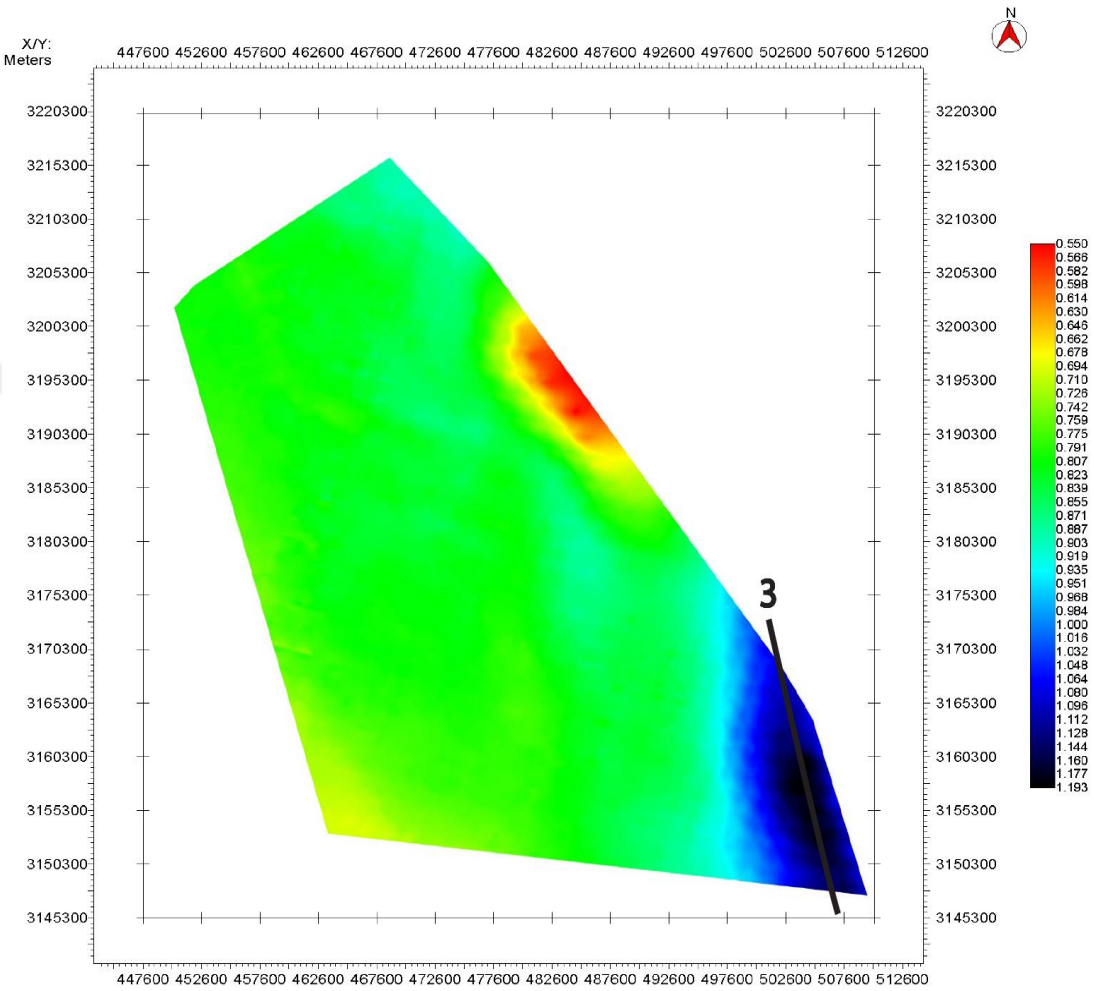

Figure 42 : The thickness map between Seafloor and horizon-2.

Figure 43 demonstrates 3 different profiles in the offshore part of the study area which were drawn according to the depocenter extensions. As it is shown in the figure, profile 1 demonstrates NNE-SSW elongation and profile 3 illustrates NNW-SSE elongation. There are not much orientation differences between profile 1 and profile 3. What it differs is Profile 2. Roughly, 0.36 to 0.82 km thick sedimentary pile was loaded to the area and it is oriented NW-SE direction apart from other profile directions.

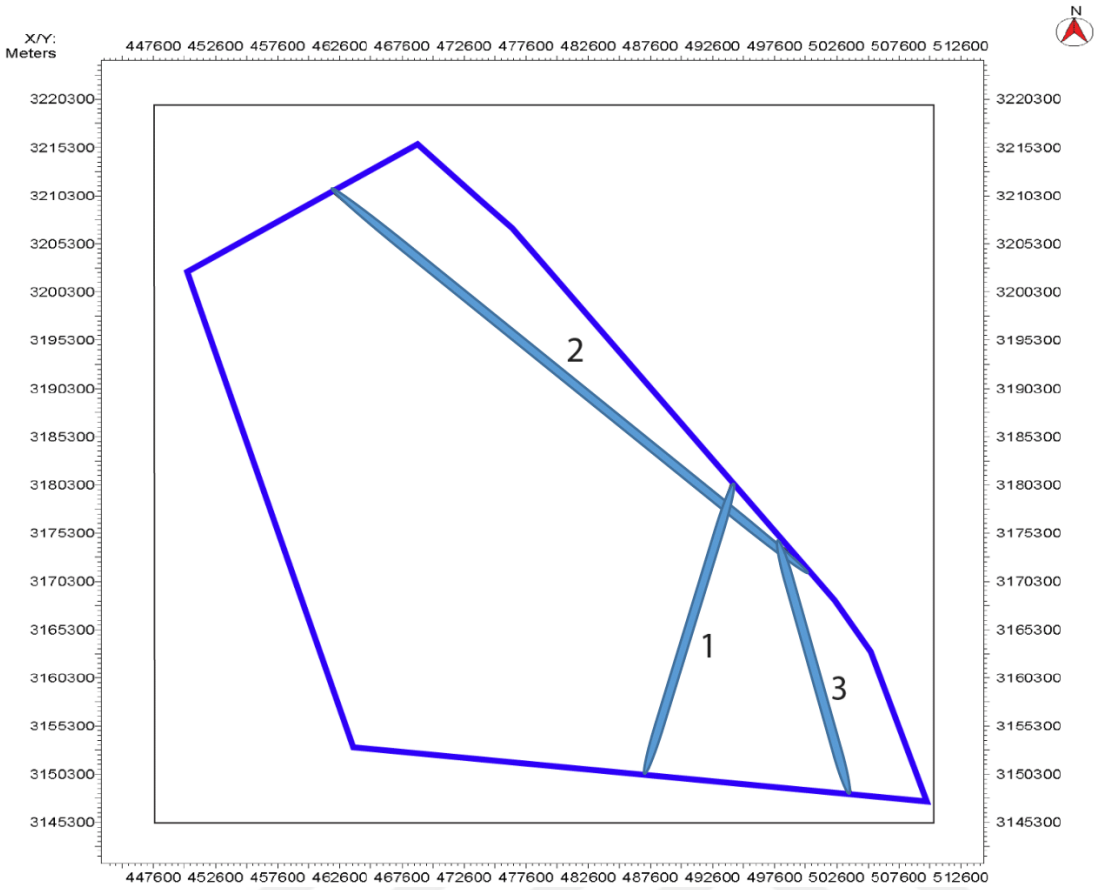

Figure 43 : Orientations of the depocenters in the offshore part of the study area; Profile 1 (NNE-SSW), Profile 2 (NW-SE) and Profile 3 (NNW-SSE).

In the onshore part of the study area, the Zagros Foredeep Fault (right-lateral, oblique-slip fault), which was placed between the coastline and the Mand Anticline, strikes NNW-SSE. The Borazjan Fault (right-lateral strike-slip fault), which was situated ca. 24km away from the shore, strikes N-S. The Borazjan Fault is also a segment of Kazerun Fault. Kazerun fault is active since the late Miocene. According to Tavakoli et al., 2008, strike-slip motion of the Borazjan segment is not active anymore. From my point of view, these 2 faults may have been active for distribution of the Mishan Formation and the Agha Jari Formation (Profile2), and they may have played a role to orientate the depocenter.

6. CONCLUSIONS AND RECOMMENDATIONS

This thesis covers a detailed study of seismic reflection data along from offshore Iran and a comprehensive analysis of combined offshore/onshore geological cross sections in the foreland of the Zagros Simply Folded Belt. Combiened 3D surface models were generated/created from the onshore and offshore data. In the offshore domain, anticline and syncline structures are smoothly visualized with grids (section 4.3). The main structural finding is; a syncline area (plunging northwest direction) is located in the western part of the Mand anticline. Another sycline is located in the northwest of the Bushsehr anticline, which is shown in grid-3, grid-4, grid-6 and grid-7. Additionally, an anticline, which has a large axial length, was discovered in the SW of the study area. In addition to these structural elements, the depth of the seabed, which covers an area of approximatelly 2600 km^2, was revealed by the Grid-Seafloor (section 4.3.1). In the onshore area, faults, a salt diapir and other structural features were investigated with geological cross sections. Various studies indicate that the erosion rate is generally high in the study area. The Bakhtyari Formation (Upper Pliocene), the Lahbari member (Pliocene) and the Agha Jari Formation (Late Miocene-Pliocene), which are younger units, cannot be seen on the top of some anticline structures. It is clear that, while the study area was uplifting, anticlines structures may have eroded; the erosion rates seen to have generally increased towards to the Zagros Mountains.

Thickness maps in the offshore area shows a dynamic growth of depocenters. The offshore interpretation section of this thesis can be used for further the tectono-sedimentary development studies of the inner and costal sides of the NE Persian Gulf.

The Zagros Foredeep Fault (right-lateral, oblique-slip fault) and the Borazjan Fault (right-lateral strike-slip fault) may have been active for distribution of the Mishan Formation (late Miocene) and the Agha Jari Formation (late Miocene - Pliocene), and they may have played a role to orientate the depocenter.

The total shortening amount in the ZSFB were measured in the study set in relation for other approaches by several researchers including Molinaro et al. (2005): 45km; Sherkati et al. (2005): 50km; and McQuarrie (2004): 67km. Their studies consist of onshore domains from the shore toward to the Zagros Mountains. In this master thesis, calculations cover the combination of the offshore and onshore areas at a distance of 101km. Horizons were unfolded, and simple and complex methods were applied. Simple method showed 5,7km shortening rate and complex method illustrated several values from 5,15km to 9,38km. The structural interpretational part (section 4.6.2.2) of the thesis is open for prospective shortening rate studies for wide distances in the ZSFB.

This thesis study includes a 3D surface modelling part. Combined offshore-onshore 3D surfaces illustrate the complex structure of the entire study area, which is discussed with respect to tectonic and geomorphological analysis.

On one hand, 3D surface modelling results presented can be used to find potential hydrocarbon-bearing fields in the south-west part of Iran. On the other hand, the study shows structural changes from Early Eocene to the present, which provides a new perspective for tectonic and geomorphologic research.

REFERENCES

Alavi, M. (1994). Tectonics of the Zagros orogenic belt of Iran: new data and interpretations. *Tectonophysics 229, 211-238*.

Agard, P., Omrani, J., Jolivet, L., and Mouthereau, F. (2005). Convergence history across Zagros (Iran): Constraints from collisional and earlier deformation. *International Journal of Earth Sciences, 94(3), 401-419.*

Agard, P., Omrani, J., Jolivet, L., Whitechurch, H., Vrielynck, B., Spakman, W., Monie, P., Meyer, B., and Wortel, R. (2011). Zagros orogeny: A subduction-dominated process. *Geological Magazine, 148(5-6), 692-725*.

Bahroudi, A., and Koyi, H. A. (2003). Effect of spatial distribution of Hormuz salt on deformation style in the Zagros fold and thrust belt: An analogue modelling approach. *Journal of the Geological Society London, 160, 719-733.*

Berberian, M., and King, G.C.P. (1981). Towards a paleogeography and tectonic evolution of Iran. *Canadian Journal of Earth Sciences, 18(2), 210-265*.

Berberian, M. (1995). Master "blind" thrust faults hidden under the Zagros folds: active basement tectonics and surface morphotectonics. *Tectonophysics, 241, 193-224.*

Bordenave, M.L. (2004). Petroleum Systems and Distribution of the Oil and Gas Fields in the Iranian Part of the Tethyan Region. *Edition: Memoir 106, Chapter: 14, Publisher: The American Association of Petroleum Geologists, Editors: L. Marlow, C. Kendall, L. Yose, 505-540.*

Bushehr Geological Quadrangle Map. (1980). Sheet No: 20514, Scale 1:250,000. *National Iranian Oil Company*.

City Population, Province and Counties of Iran, https://www.citypopulation.de/php/iran-admin.php, date taken: 07 November 2018.

Edgell, H. S. (1996). Salt tectonism in the Persian Gulf Basin, in Salt Tectonics, edited by Alsop G. I., Blundel D. J., and Davison I. *Geological Society of London, 129-151*.

Elliott, J.R., Bergman, E.A., Copley, A.C., Ghods, A.R., Nissen, E.K., Oveisi, B., Tatar, M., Walters, R.J. and Yamini-Fard, F. (2015). The 2013 Mw 6.2 Khaki-Shonbe (Iran) Earthquake: Insights into seismic and aseismic shortening of the Zagros sedimentary cover. *Earth and Space Science*, *2*(11), *pp.435-471*.

Ellouz-Zimmermann, N., Lallemant, S. J., Castilla, R., Mouchot, N., Leturmy, P., Battani, A., Buret, C., Cherel, L., Desaubliaux, G., Deville, E., Ferrand, J., Lügcke, A., Mahieux, G., Mascle, G., Mühr, P., Pierson-Wickmann, A.C., Robion, P., Schmitz, J., Danish, M., Hasany, S., Shahzad, A., and Tabreez, A. (2007). Offshore Frontal Part of the Makran Accretionary Prism: The Chamak Survey (Pakistan). *In Thrust Belts and Foreland Basins; from fold kinematics to hydrocarbon systems.*

Esri, ArcGIS software suite, https://www.esri.com/en-us/home, date taken: 01 August 2017.

Fakhari, M.D., Axen, G.J., Horton, B.K., Hassanzadeh, J., and Amini, A. (2008). Revised age of proximal deposits in the Zagros foreland basin and implications for Cenozoic evolution of the High Zagros. *Tectonophysics, 451, 170-85.*

Hamshahri Online, The Provinces of the County, http://www.hamshahrionline.ir/news/263382, date taken: 07 November 2018.

Hassanzadeh, J., Stockli, D.F., Horton, B.K., Axen, G.J., Stockli, L.D., Grove, M., Schmitt, A.K., and Walker J.D. (1974). U-Pb zircon geochronology of late Neoproterozoic–Early Cambrian granitoids in Iran: Implications for paleogeography, magmatism, and exhumation history of Iranian basement. *Tectonophysics, 451, 71-96.*

Husing, S.K., Zachariasse, W.J., Hinsbergen, D.J.J., Krijgsman, W., Inceoz, M., Harzhauser, M., Mandic, O., and Kroh, A. (2009). Oligocene–Miocene basin evolution in SE Anatolia, Turkey: constraints on the closure of the eastern Tethys gateway. *Geological Society of London, Special Publications, 311, 107-132*.

Hessami, K., Koyi, H.A., Talbot, C.J., Tabasi, H., and Shabanian, E. (2001). Progressive unconformities within an evolving foreland fold-thrust belt, Zagros Mountains. *Journal of the Geological Society London, 598(158), 969-981*.

Hessami, K., Jamali, F., and Tabassi, H. (2003). Major active faults map of Iran. 1:2,500,000 scale. *International Institute of Earthquake Engineering and Seismology (IIEES)*.

Husseini, M.I. (1988). The Arabian lnfracambrian extensional system. *Tectonophysics, 148, 93-103*.

Jahani, S., Hassanpour, J., Firouz, S., Letouzey, J., Lamotte, D., Alavi, S., and Soleimany B., (2017). Salt tectonics and tear faulting in the central part of the Zagros Fold-Thrust Belt, Iran. *Marine and Petroleum Geology, 86 (2017), 426-446*.

Jolivet, L., and Faccenna, C. (2000). Mediterranean extension and the Africa-Eurasia collision. *Tectonics, 19(6), 1095-1106*.

Kent, P.E. (1970). The salt plugs of the Persian Gulf region. *Leicester Literary and Philosophical Society, 64, 56-88.*

Kharg-Ganaveh-Kazerun Geological Quadrangle Map. (1975). Sheet No: 20512, Scale 1:250,000. *Oil Service Company of Iran*.

Khormoj Geological Quadrangle Map. (1980). Sheet No: 20515, Scale 1:250,000. *National Iranian Oil Company*.

Kingdom, Seismic and Geological Interpretation Software, IHS Markit, https://ihsmarkit.com/products/kingdom-seismic-geological-interpretation-software.html, date taken: 07 November 2018.

Konert, G., Al-Afifi, A.M., and Al-Hajri, S.A. (2001). Paleozoic stratigraphy and hydrocarbon habitat of the Arabian Plate. *GeoArabia, vol 6, no: 3, 407-442*.

Konyuhov, A.I., and Maleki, B. (2007). The Persian Gulf Basin: Geological History, Sedimentary Formations, and Petroleum Potential. *Lithology and Mineral Resources, Vol. 41, No. 4, 344-361*.

McQuarrie, N. (2004). Crustal scale geometry of the Zagros fold–thrust belt, Iran. *Journal of Structural Geology, 26 (2004), 519-535.*

Molinaro, M., Leturmy, P., Guezou, J.C., de Lamotte D.F., and Eshraghi, S.A. (2005). The structure and kinematics of the southeastern Zagros fold-thrust belt, Iran: From thin-skinned to thick-skinned tectonics. *Tectonics, 24, TC3007, doi: 10.1029/2004TC001633.*

Motiei, H. (1994). Stratigraphy of Zagros. *Geological Survey of Iran Publications* (In Farsi).

Motiei, H. (1995). Petroleum geology of Zagros. *Geological Survey of Iran Publications* (In Farsi).

Mouthereau, F., Lacombe, O., and Meyer, B. (2006). The Zagros folded belt (Fars, Iran): Constraints from topography and critical wedge modelling. *Geophysical Journal International, 165(1), 336-356.*

Mouthereau, F., Lacombe, O., and Verges, J. (2012). Building the Zagros collisional orogen: Timing, strain distribution and the dynamics of Arabia/Eurasia plate convergence. *Tectonophysics, 532, 27-60.*

Move, Geologic modelling software, Midland Valley, https://www.mve.com/software/move, date taken: 07 November 2018.

Nehlig, P., Genna, A., Asirfane, F. (2002). A review of the Pan-African evolution of the Arabian Shield. *GeoArabia, 7, 103-124.*

Oveisi, B., Lave, J., and Beek, P. (2007). Rates and Processes of Active Folding Evidenced by Pleistocene Terraces at the Central Zagros Front (Iran). *In: Lacombe O., Roure F., Lavé J., Vergés J. (eds) Thrust Belts and Foreland Basins. Frontiers in Earth Sciences. Springer, Berlin, Heidelberg.*

Oveisi, B., Lave, J., Beek, P., Carcaillet, J., Benedetti, L., and Aubourg, C. (2008). Thick- and thin-skinned deformation rates in the central Zagros simple folded zone (Iran) indicated by displacement of geomorphic surfaces. *Geophysical Journal International, doi: 10.1111/j.1365-246X.2008.04002.x.*

Paul, A., Hatzfeld, D., Kaviani, A., Tatar, M., and Pequegnat, C. (2010). Seismic imaging of the lithospheric structure of the Zagros mountain belt (Iran), in Tectonic and Stratigraphic Evolution of Zagros and Makran During the Mesozoic-Cenozoic, edited by Leturmy P., and Robin C. *Geological Society of London, 5-18.*

Pirouz, M., Simpson, G., Bahroudi, A., and Azhdari A. (2011). Neogene sediments and modern depositional environments of the Zagros foreland basin system. *Geological Magazine, 148(5-6), 838-853.*

Regard, V., Bellier, O., Thomas, J.C., Abbassi, M., Mercier, J., Shabanian, E., Feghhi, K., and Soleymani, S. (2004). Accomodation of Arabia-Eurasia convergence in the Zagros-Makran transfer zone, SE Iran: A transition between collision and subduction through a young deformation system. *Tectonics 23, TC4007, doi:10.1029/2003TC00 1599.*

Regard, V., Hatzfeld, D., Molinaro, M., Aubourg, C., Bayer, R., Bellier, O., Yamini-Fard, F., Peyret, M., and Abbassi, M. (2010). The transition between Makran subduction and the Zagros collision: recent advances in its structure and active deformation. In Tectonic and Stratigraphic Evolution of Zagros and Makran during the Mesozoic-Cenozoic. *Geological Society of London, Special Publication no. 330.*

Ricou, L.E. (1971). Le croissant ophiolitique péri-arabe, une ceinture de nappes mise en place au crétacé supérieur. *Revue deGéographie Physique et de Géologie Dynamique 13, 327-50*.

Ruh J.B., Hirt, A.M., Burg, J.P., and Mohammadi, A. (2014). Forward propagation of the Zagros Simply Folded Belt constrained from magneto-stratigraphy of growth strata. *American Geophysical Union, 10.1002/2013TC003465*.

Sengor, A.M.C., and Yilmaz, Y. (1981). Tethyan evolution of Turkey: A plate tectonic approach. *Tectonophysics, 75, 181-241*.

Sepehr, M., and Cosgrove, J.W. (2004). Structural framework of the Zagros Fold-Thrust Belt, Iran. *Marine and Petroleum Geology 21, 829-43*.

Sherkati, S., and Letouzey, J. (2004). Variation of structural style and basin evolution in the central Zagros (Izeh zone and Dezful Embayment). *Marine and Petroleum Geology, Iran, 21(5), 535-554.*

Sherkati, S., Molinaro, M., de Lamotte D.F., and Letouzey, J. (2005). Detachment folding in the Central and Eastern Zagros fold-belt (Iran): Salt mobility, multiple detachments and late basement control. *Journal of Structural Geology, 27(9), 1680-1696.*

Sherkati, S., Letouzey, J., and de Lamotte D.F. (2006). Central Zagros fold-thrust belt (Iran): New insights from seismic data, field observation, and sandbox modeling. *Tectonics, 25, TC4007, doi:10.1029/2004TC00 1766.*

Stern, R.J., and Johnson, P. (2010). Continental lithosphere of the Arabian Plate: A geologic, petrologic, and geophysical synthesis. *Earth-Science Reviews, 101, 29-67.*

Stocklin, J. (1968). Structural history and tectonics of Iran: A review. *The American Association of Petroleum Geologists Bulletin, 52, 1223-1258.*

Stoneley, R. (1981). The geology of the Kuh-e Dalneshin area of southern Iran, and its bearing on the evolution of southern Tethys. *Journal of the Geological Society, 138, 509-526.*

Talbot, C.J., and Alavi, M. (1996). The past of a future syntaxis across the Zagros. *Geological Society of London, Special Publications, 100, 89-109.*

Tavakoli, F., Walpersdorf, A., Authemayou, C., Nankali, H.R., Hatzfeld, D., Tatar, M., Djamour, Y., Nilforoushan, F., and Cotte, N. (2008). Distribution of the right-lateral strike–slip motion from the Main Recent Fault to the Kazerun Fault System (Zagros, Iran): Evidence from present-day GPS velocities. *Earth and Planetary Science Letters, doi:10.1016/j.epsl.2008.08.030.*

Vernant, P., Nilforoushan, F., Hatzfeld, D., Abbasi, M.R., Vigny, C., Masson, F., Nankali, H., Martinod, J., Ashtiani, A., Bayer, R., Tavakoli, F., and Chery, J. (2004). Present-day crustal deformation and plate kinematics in the Middle East constrained by GPS measurements in Iran and northern Oman. *Geophysical Journal International 157, 381-98.*

Ziegler, M.A. (2001). Late Permian to Holocene Paleofacies Evolution of the Arabian Plate and its Hydrocarbon Occurrences. *GeoArabia, Vol. 6, No:3.*

CURRICULUM VITAE

Name Surname : Hasan Özge Gezgin

Place and Date of Birth : Acipayam / 25.11.1989

E-Mail : gezginha@itu.edu.tr

EDUCATION :

- **B.Sc.** : 2011, Suleyman Demirel University, Engineering and Architecture Faculty, Department of Geological Engineering.

PROFESSIONAL EXPERIENCE:

- 03/2016 - 11/2016: Pozitif Drilling Company.
- 03/2014 - 04/2015: Geolog International B.V.

PUBLICATIONS, PRESENTATIONS AND PATENTS ON THE THESIS:

- **Gezgin, H.O., Akyuz, H.S., Back, S., and Reicherter, K.** 2018: "Zagros Simply Folded Belt" in Batı Kıyı Kesiminin Sismik Yansıma Verileri Yardımıyla Morfotektonik Analizi, GB İran. Aktif Tektonik Araştırma Grubu 22. Çalıştayı (ATAG 22), November 01-03, 2018 Canakkale, Turkey.